CHALMERS
UNIVERSITY OF TECHNOLOGY

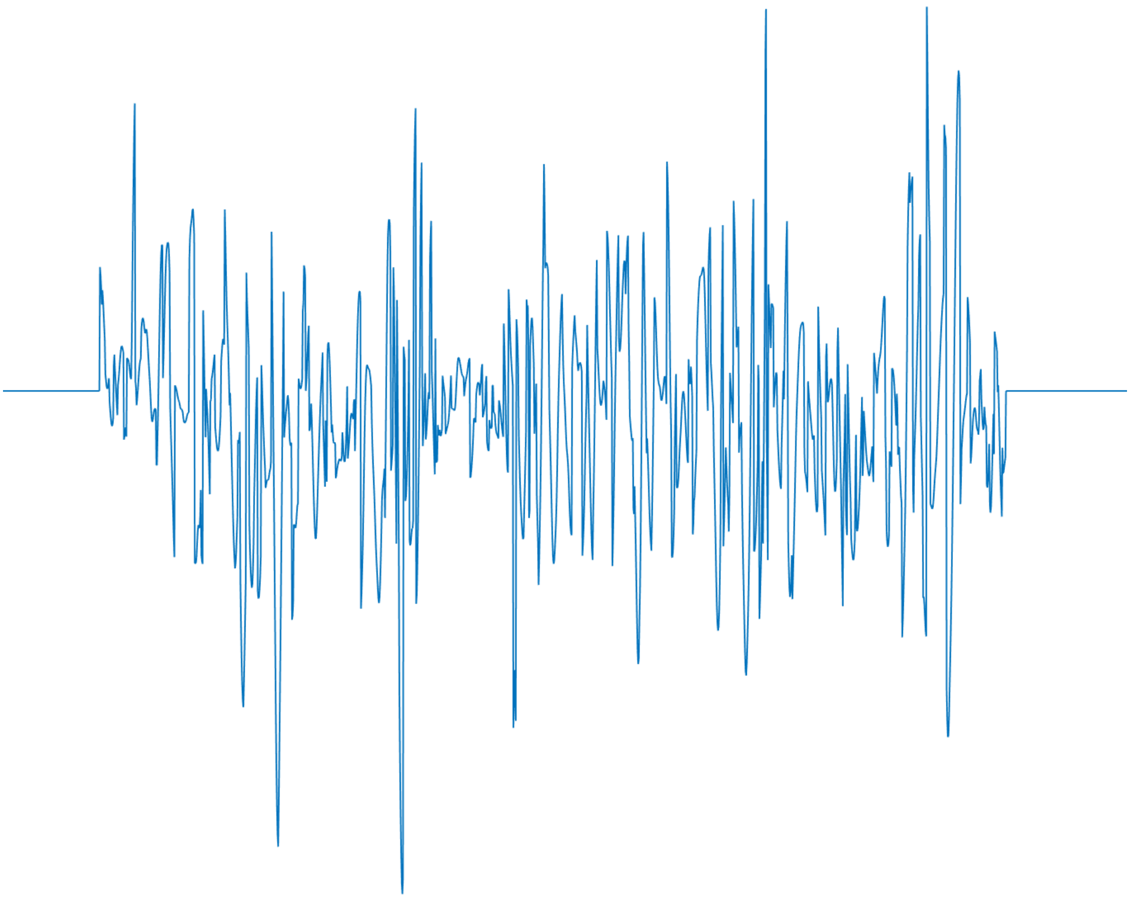

Developing a load case for analysis of Squeak and Rattle events in passenger cars

Master's thesis in Product Development

RASMUS BLOM
JONATAN NILSSON

Department of Industrial and Materials Science
CHALMERS UNIVERSITY OF TECHNOLOGY
Gothenburg, Sweden 2020

Master's thesis 2020

Developing a load case for analysis of Squeak and Rattle events in passenger cars

Developing a load case signal for virtual analysis and physical verification of Squeak and Rattle events in passenger cars, by screening out important parts from longer excitation signals. In collaboration with Volvo Cars.

Rasmus Blom
Jonatan Nilsson

Department of Industrial and Materials Science
Division of Product Development
Chalmers University of Technology
Gothenburg, Sweden 2020

Developing a load case for analysis of Squeak and Rattle events in passenger cars
Developing a load case signal for virtual analysis and physical verification of Squeak and Rattle events in passenger cars, by screening out important parts from longer excitation signals. In collaboration with Volvo Cars.
RASMUS BLOM
JONATAN NILSSON

Supervisor: Mohsen Baynani, Volvo Cars, Solidity Department
Examiner: Lars Lindkvist, Chalmers, Department of Industrial and Materials Science

Master's Thesis 2020
Department of Industrial and Materials Science
Division of Product Development
Chalmers University of Technology
SE-412 96 Gothenburg
Telephone +46 31 772 1000

Cover: Spindle accelerations left rear wheel, concept C9.

Typeset in LaTeX
Printed by Chalmers Reproservice
Gothenburg, Sweden 2020

Developing a load case for analysis of Squeak and Rattle events in passenger cars
Developing a load case signal for virtual analysis and physical verification of Squeak and Rattle events in passenger cars, by screening out important parts from longer excitation signals. In collaboration with Volvo Cars.

RASMUS BLOM
JONATAN NILSSON
Department of Industrial and Materials Science
Chalmers University of Technology

Abstract

A part of Volvo Cars strategy is shifting engineering activities to the early phases of the product development, without the need for complete vehicle prototypes. An important early phase activity in the product development of passenger cars is to evaluate Squeak & Rattle emitted from subsystems in the car. The subsystem studied in this project is the instrument panel (IP). Today's excitation signals applied onto the IP is longer than necessary and not optimized for Squeak & Rattle evaluation. The aim of this thesis is consequently to develop effective excitation signals and provide the method of how this is achieved for further improvements and the possibility to develop new excitation signals for future product development of passenger cars.

The thesis describes the process of recording excitation- and response signals, for the car as a whole and the IP subsystem. Nine different road tracks are recorded for two cars. A methodology for creating shortened excitation signals is explained, with crucial steps of identifying Squeak & Rattle events, grouping these into parts and concatenating them sequentially in time domain. The frequency content of the shortened excitation signals is examined to avoid significant deviations from the unshortened excitation signals.

Eleven different concepts for the development of an excitation signal is created. The synthesized signals performance is verified with two test rigs. With regards to the Squeak & Rattle causing properties of the signal and the time compression ability, an optimal concept is presented. This concept proved to have favourable characteristics although further optimization could generate an even better concept. The methodology is not flawless, whilst nevertheless having the capability to compress the total excitation signal time by up to 95% and maintaining decent quality. Possible error sources and further methodology improvements is finally discussed.

Keywords: squeak, rattle, excitation signal, signal compression, product development, relative displacement, instrument panel, FFT, testing, accelerometers, CAE, optimization.

Acknowledgements

This project would not have been what it is without the continuous and clever support from our supervisor Mohsen Bayani, a big thank you from us for guiding us through this project. We would also like to thank our co-supervisor Anneli Rosell, and everyone else in the Solidity department at Volvo Cars for their help when we needed it. Further, we would like to mention the support we have recieved from the engineers at the test rigs that has been used, much appriciated! Finally, we would like to thank our examiner Lars Lindkvist, for academic support and supervision of this last project on our journey to getting our degree.

Rasmus Blom, Jonatan Nilsson, Gothenburg, June 2020

Abbreviations

CAE	Computer-Aided Engineering
E-Line	Evaluation-Line
EP	E-Point; Evaluation-Point
FFT	Fast Fourier Transform
FP-rig	Four-poster rig
IFFT	Inverse Fast Fourier Transform
IP	Instrument Panel
IP-rig	Instrument Panel test-rig
MAD	Mean Absolute Deviation
S&R	Squeak & Rattle

Contents

List of Figures

List of Tables

1
Introduction

This Master's Thesis is done in collaboration with Volvo Cars, in the Solidity group. Solidity, an important attribute within the Craftsmanship and Durability Centre at Volvo Cars, is responsible for Squeak & Rattle (S&R) sounds and solid feeling in the car. Squeak & Rattle are non-stationary sounds that occur when adjacent parts are in contact, either by impacting or sliding. These sounds downgrade the perceived quality of the car, and in overall impairs the experience of driving in a passenger car. It is of high priority to reduce this problem, as high quality is in great demand for passenger cars, especially in the premium segment.

1.1 Background

With the current focus on electrification of passenger cars, non-stationary, annoying noises in the car cabin will draw the attention of passengers and be perceived as quality deficient. Squeak & Rattle are the non-stationary annoying noises, that is targeted in this project. A part of Volvo Cars strategy is shifting engineering activities to the early phases of the product development, without the need for complete vehicle prototypes. An important early phase activity in the product development of passenger cars is to evaluate Squeak & Rattle emitted from subsystems in the car. A practical approach to address this challenge is to use virtual and physical test rigs, both at subsystem and complete system levels. The subsystem studied in this project is the instrument panel (IP).

Today, excitation signals for Squeak & Rattle simulation and tests are the measured vibrations from driving cars on special road profiles at a proving ground. However, the length of some of these signals are unnecessarily long and the content is not completely relevant for Squeak & Rattle evaluation. This makes the simulation time unnecessarily long. Therefore, the task is to create a method for generation of new shorter signals that include a similar frequency content of the reference signals, whilst the redundant parts are excluded. Both the method and the final signals are considered as project deliverables, where the signal is a way of verifying that the developed method work.

1.2 Purpose and aim

This thesis work is part of and contributes to a larger project with the aim of improving methods and tools for Squeak & Rattle prediction during the development of new cars at Volvo Cars. The excitation signals are parts of the tools used in the product development phases from design to physical verification phases. The aim of this project is to reduce the time spent simulating Squeak & Rattle by reducing the signal length without significantly reducing the quality of the result.

1.3 Objectives

The main objective of the work is to develop Squeak & Rattle specific excitation signals for virtual and physical simulation and testing, as well as developing a functional method for doing so. The first task towards reaching the main objective, is to gather excitation signals from relevant road tracks that would be used in the project. The next task is to identify critical sections in the excitation signals. These relevant sections is separated from the signal and merged together with a developed method, which is a third task. The final task is to verify that the new signal works, by confirming that the Squeak & Rattle response is comparable to the original, whereas it is shorter in time. This is achieved using virtual simulations and physical tests in two different test rigs.

1.4 Limitations

The project is limited to only fulfilling the subjective desires stated in Section 3.7.1, as was given by Volvo Cars. This was interpreted as the given task and therefore no further requirements or desires have been created. As several physical tests are required to carry out this project, the availability of Volvo Cars test rigs is a limitation on the projects scope. This includes the number of cars, number of road tracks, number of concepts and number of iteration loops that can be performed in the testing and verification phases. The projects time scope is delimited to 20 weeks full-time work.

2
Theory

This section provides a brief introduction of some fundamental theory, necessary to carry out this project. The information is primarily based on published literature, although project specific details are here and there described to put the theory into context.

2.1 Squeak & Rattle theory

Squeak & Rattle are undesirable sounds that can appear when two adjacent components move relative to each other, commonly measured as relative displacement. Rattle can occur when the relative displacement is in normal direction and the components repeatedly come in contact. Squeak can occur when the components are in contact and there is relative displacement in planar direction.

2.1.1 Rattle

Rattle might occur when the relative displacement of one part compared to the other is equal to the gap between them in the direction towards the other part. The nominal gap is the designed distance between the two components. Tolerances may be considered to account for manufacturing variations, temperature variations or material ageing. The impact velocity affects the severity of the rattle events. To calculate whether rattle is occurring, gap measurements are needed. These measurements are done on a virtual model for this project.

2.1.2 Squeak

To find out how prone materials are to cause squeak, when in contact with each other, measurements of material combinations are done. At Volvo Cars, a stick slip machine is used for assessment of stick-slip phenomenon of a material pair. According to ZIEGLER-Instruments (2016), one material is attached to a carrier where the velocity can be adjusted. The other material in the pair is mounted on a spring, where normal force is applied and the friction force is measured. In this project, the desired output parameter from the stick slip test is the impulse rate, which is the number of pulses per millimeter relative displacement. The inverse of impulse rate is defined as the stick distance. This essentially means the distance the two parts stick to each other before starting to slip in a relative movement. If the relative planar displacement is larger than this stick distance, then there might be squeak. Also, if the relative planar displacement is lower than the stick distance, there is no risk for squeak.

2.1.3 S&R relevant measured data

The method in this work assesses the risk of Squeak & Rattle generation, and is evaluated for the new signal relative to the old signal. The absolute values of the calculated metrics do not necessarily denote the actual occurrences of S&R, although a higher number shows more of an altered risk generation tendency of S&R compared to the original recording. This implies that the method is not very sensitive to minor errors in the accuracy of the data. Moreover, the same data is used for all signals, meaning that the error in this data is the same for all evaluations, which reduces the need for precise measurements. The data used in this project is classified and cannot be presented. This applies to both gap distances and impulse rates. However, it is still used in the calculations to get a somewhat realistic estimate of the Squeak & Rattle events.

2.2 Fast Fourier Transform

The Fourier transform decomposes a time domain signal into its constituent frequencies. Ling. (2007) claims the continuous Fourier transform can mathematically be described according to Eq. 2.1, where x is the signal in time domain, X corresponds to the frequency domain representation, ω is the angular frequency and t is time.

$$X(\omega) = \int_{-\infty}^{+\infty} x(t)e^{-j\omega t}dt \tag{2.1}$$

To convert a signal in frequency domain back to time domain, the continuous inverse Fourier transform is used and is mathematically defined in Eq. 2.2.

$$x(t) = \frac{1}{2\pi}\int_{-\infty}^{+\infty} X(\omega)e^{j\omega t}d\omega \tag{2.2}$$

Sundararajan (2001) asserts a signal is continuous if it is defined at all time instances. If the signal is defined at only discrete instances, the signal is referred as a discrete signal. Since the recorded signals are registering values at a set sampling frequency, the signal is discrete and a discrete Fourier transform is the proper method of transforming a time signal into frequency domain.

Fast Fourier transform or FFT is an algorithm that allows a fast way of computing a discrete Fourier transform of a sequence. It allows a reduction of number of computations from N^2 to $N * log(N)$ which may be hundreds of times faster, where N is the number of sample points (Cooley & Tukey, 1965). This algorithm is used in this project as a way of transforming a signal from time domain to frequency domain. Working with a signal in frequency domain allow for analysis of its content without influence of time. Specific important frequencies may be identified and it gives input to what type of filters may be applied. FFT is used for many spectrum analyzers used in Squeak & Rattle assessments as it produces an approximation of the spectral content of a sampled signal (Feng & Hobelsberger, 1999). An obvious requirement on the signal is that it must fulfill the Nyquist-Shannon theorem, meaning that the sampling frequency must be at least twice the highest frequency of interest in the recorded event.

2.3 Omega Arithmetics

Accelerometers were used to measure instrument panel (IP) responses. To acquire the displacements of a certain E-point as a function of time, this can be done by double-integration. In practice, recorded signals often have some level of noise. After double-integrating a signal with noise, a drift of the displacement signal will occur. Drift is meaning that the starting position of the E-point will not be the same as the ending position of the E-point, even if the IP is attached to a fixture in a rig, see Figure 3.20 for drift visualized. According to Mercer (2006), the displacement signal can be obtained without double-integrating the acceleration signal. This is done by applying omega arithmetics, which includes simple multiplication and division operations with the angular velocity, ω, when in the frequency domain. A simple sine wave displacement can be described as in Equation 2.3 and with its first and second derivative according to Equations 2.4 and 2.5.

$$x = A \sin \omega t \tag{2.3}$$

$$\dot{x} = -\omega A \cos \omega t \tag{2.4}$$

$$\ddot{x} = -A\omega^2 \sin \omega t \tag{2.5}$$

From these equations it is possible to derive $\ddot{x} = -\omega^2 x$, $\dot{x} = i\omega x$, $\ddot{x} = i\omega \dot{x}$ and the following transformation operations as ordered in Table 2.1.

Table 2.1: Omega arithmetic transformation operations

Output	**Input**		
	$X(f)$	$\dot{X}(f)$	$\ddot{X}(f)$
$X(f)$	1	$1/i\omega$	$-1/\omega^2$
$\dot{X}(f)$	$i\omega$	1	$1/i\omega$
$\ddot{X}(f)$	$-\omega^2$	$i\omega$	1

2.4 Coordinate systems and rotation matrices

The global coordinate system convention for cars in this report have been according to Figure 2.1. This means X-direction is in the driving direction, Y-direction is to the drivers left side, and Z-direction is upwards from the driver.

Figure 2.1: Global coordinate system

The convention used for Squeak & Rattle direction is, squeak always acts in the local X-, and Y-direction (planar) while rattle acts in the local Z-direction (normal to the plane). This local Squeak & Rattle coordinate system will therefore be dependent on the E-points geometrical interface.

On the IP, accelerometers were placed on two sides of an E-Point, with the intention of having their local coordinate system aligned with the cars global coordinate system. For some E-Points, the accelerometers could not be placed orthogonal to the cars coordinate system. Besides, to calculate the accelerometers relative displacement, the coordinate systems need to be aligned. For calculating the accelerometers translation in squeak and rattle direction, it was also necessary to rotate the initial coordinate system of the accelerometer. To achieve this rotation, the local coordinate system of one accelerometer were transformed with a combination of rotation matrices. According to Evans (2001), three-dimensional rotation around X-, Y-, and Z-axis is done with the transformation matrices below:

$$R_x(\Phi) = \begin{bmatrix} 1 & 0 & 0 \\ 0 & \cos\Phi & -\sin\Phi \\ 0 & \sin\Phi & \cos\Phi \end{bmatrix}$$

$$R_y(\Phi) = \begin{bmatrix} \cos\Phi & 0 & \sin\Phi \\ 0 & 1 & 0 \\ -\sin\Phi & 0 & \cos\Phi \end{bmatrix}$$

$$R_z(\Phi) = \begin{bmatrix} \cos\Phi & -\sin\Phi & 0 \\ \sin\Phi & \cos\Phi & 0 \\ 0 & 0 & 1 \end{bmatrix}$$

These three-dimensional rotational transformation matrices can be combined together to enable rotation around any axis. The order of multiplication by these matrices is crucial for the final rotation output. It is common to either use XYZ-rotation or ZYX rotation (XYZ-rotations is mainly used in this project). A XYZ-rotation is calculated according to Eq. 2.6, while a ZYX rotation is calculated in the order written in Eq. 2.7.

$$R_{XYZ} = R_x(\alpha)R_y(\beta)R_z(\gamma) \tag{2.6}$$

$$R_{ZYX} = R_z(\alpha)R_y(\beta)R_x(\gamma) \tag{2.7}$$

2.5 Statistical measures

Several statistical measures have been used to get an overview of the recorded signal data. Key measures are explained below. The sampling frequency multiplied by the total signal time will be the length of each data subset used for calculating the statistical measures. For example, a sampling frequency of 1 000 and signal time of 33 seconds implies that the length of the data subset vector contains 33 000 elements.

2.5.1 Mean

Mean, also referred to as the arithmetic mean is the average of a set of numbers, and is a measure of central tendency. The arithmetic mean is calculated by adding all numbers in a data set and dividing by the total count of those numbers.

2.5.2 Mean absolute deviation

According to Cortinhas & Black (2012), mean absolute deviation (MAD) is a measure of variability and is the average of the absolute values of the deviations around the mean for a specified set of numbers. Hence, MAD is calculated according to Eq. 2.8, where μ is the average value of a data set, N is the number of values in the data set and i is the indexing of each individual data set value x.

$$MAD = \frac{\sum_{i=1}^{N} |x_i - \mu|}{N} \tag{2.8}$$

2.5.3 Percentile

The percentile is measuring the central tendency by dividing a data set into 100 parts. It is calculated by ordering all numbers in an ascending array, thereafter the index of the nth percentile is located. The value of this index-location is thus the nth percentile. Additionally, for the nth percentile, at least n percent of the numbers in the data set must be below the percentile value and at most $(100 - n)$ percent are above that value (Cortinhas & Black, 2012).

2.5.4 Standard deviation

Standard deviation, denoted as σ, is a measure of variation and calculated as the square root of the variance as in Eq. 2.9.

$$\sigma = \sqrt{\frac{\sum_{i=1}^{N}(x_i - \mu)^2}{N}} \tag{2.9}$$

An important feature of the standard deviation compared to the variance is that the unit is the same as the sampled raw data. For a normally distributed data set, approximately 68% of the data is within one standard deviation from the mean. For two standard deviations from the mean, about 95% of all data is within this range. Data within three standard deviations from the mean covers approximately 99.7% of all analyzed data (Cortinhas & Black, 2012).

3
Method

3.1 Measurements

The desired test signals were decided in an early phase of the project. Not all of these signals had been recorded in a way that fit how they would be used in this project. This led to the need of recording the road tracks *Pave TT* and *Washboard* as excitation signals. Further, recordings of vibrations in the IP were needed as that is what was used as an indicator on whether the shortened excitation signal functions properly. This is an important tool in the development of such a shortened signal.

The final purpose of physical testing is to verify that the developed signals functions as intended. The shaker rig is firstly used to find the relative performance of developed concepts. The best concepts are taken to the FP-rig for final verification.

Every time a test is carried out in a test rig or test track, the exact same car have been used to avoid variations in the instrument panel or other subsystems of the car. This has imposed a limitation on when a test can be performed since the cars must be booked in advance. Consequently, all testing has been done for Car A and Car B, and these have been represented by the exact same cars throughout the project. The IP-model used in the IP-rig have always been the same between testing and verification, although not the same IP as used in the cars. This is to reduce the risk of errors.

3.1.1 Recorded road tracks

Together with experienced engineers, a few road patterns with the most relevance for this project was selected along with relevant velocities. In Figure 3.1, is the recorded tracks shown with respective accelerations. The plotted signals are recorded at the front left spindle, meaning that the surface of the road is basically recorded, with the difference being the dampening from the tyre. Recordings were done for Car A and Car B. The plotted signals are from Car B and highly similar to the signals recorded on Car A, as they are measured on the wheel hub spindle. The road track Washboard was divided into two parts, *Washboard 1st part* and *Washboard 2nd part*. The reason for this is that the 1st parts road pattern caused the car to oscillate in a markedly lower frequency than the 2nd part of Washboard. In Figure 3.1h, there is a spike at the end of the signal. This is the beginning of the second part of washboard. It is there since the signal is cut only when the rear wheels is on the second part.

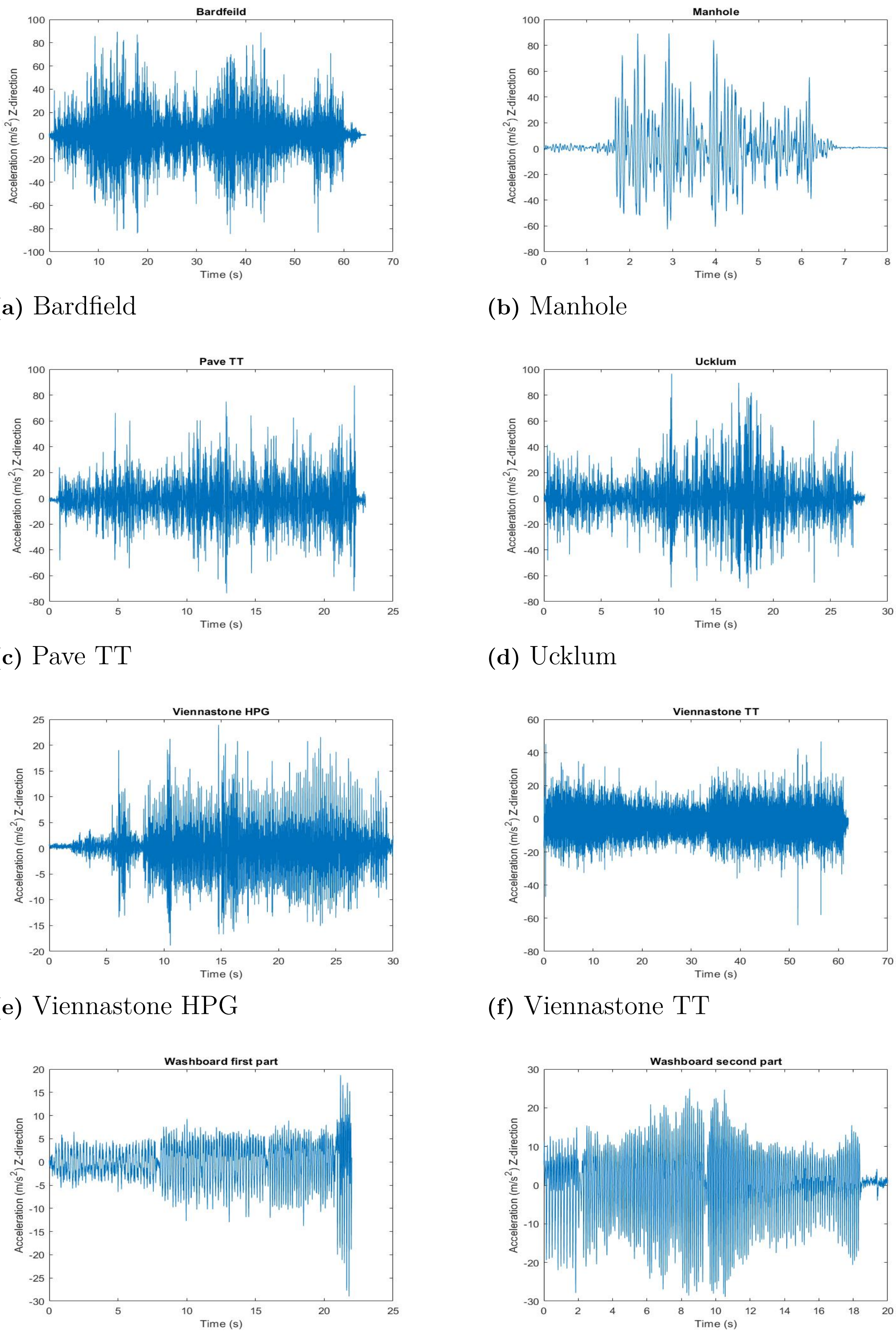

(a) Bardfield **(b)** Manhole

(c) Pave TT **(d)** Ucklum

(e) Viennastone HPG **(f)** Viennastone TT

(g) Washboard first part **(h)** Washboard second part

Figure 3.1: Recorded tracks, front left wheel hub, Car B, IPEtronix accelerometers

3.1.2 Accelerometers and measurement devices

For recording the accelerations at the wheel hubs and vibrations of the IP, two accelerometer systems were used. The accelerations at the wheel hubs were recorded with the IPEtronix system, consisting of 2 modules with the capacity to record 16 channels simultaneously (see Figure 3.2). The accelerometers used for measuring the spindle accelerations with the IPEtronix system were designed for measuring accelerations up to 100 G. The signals were recorded with a sampling rate of 200 Hz.

(a) Triaxial accelerometer **(b)** Recording modules

Figure 3.2: Equipment used for the IPEtronix system

For measuring the vibrations of the IP, the SQuadriga system were used, consisting of 2 modules, with the possibility to record 12 channels simultaneously (see Figure 3.3). For the SQuadriga system, the modules are manufactured by HEAD acoustics, and triaxial accelerometers from Brüel & Kjær were used. Compared to the accelerometers used for the IPEtronix system, these from Brüel & Kjær had a better accuracy and possibility of higher sampling rate although not capable of recording very high accelerations as is common in the wheels hub positions. The recording sampling rate were set to 12000 Hz.

Six channels were used for recording seat rail accelerations and another six channels were used for recording the accelerations of the IP attachment points at the A-pillar. Ideally, all three X-, Y- and Z-directions per accelerometer should have been recorded on the IP. Two accelerometers were needed to be able to record relative displacement in an E-Point. Since the SQuadriga system only could record 12 channels simultaneously, multiple recording repetitions were necessary to capture all desired acceleration signals. However, some directions were not regarded as necessary for later work. To reduce the number of recording repetitions needed, some E-Point directions were not captured in the recordings. Finally, 42 different channels were captured distributed on four different recording repetitions. By, dividing the recordings in four different recordings, the signals required to be synchronized for later Squeak & Rattle evaluation to be valid.

(a) Triaxial accelerometer from Brüel & Kjær

(b) SQuadriga II, recording modules from HEAD acoustics

Figure 3.3: Equipment used for the SQuadriga system

Both recording systems required calibration before use. Accompanying data sheets with sensitivity values were inserted during calibration of the SQuadriga system. In addition, calibrating the range needed to be done during an actual vibration environment, similar in roughness as used in recording of the accelerations. For the IPEtronix system, the calibration was performed by engineers at Volvo Cars.

3.1.3 IP-rig

Part of the testing have been carried out in a shaker rig that can excite various components with the purpose of studying noise and vibrations. In this project an instrument panel has been used. Measurements at the instrument panels A-pillar attachments that were recorded at the FP-rig and test tracks are applied as excitation signals for the IP-rig. IP vibrations, also referred to as responses, are measured in different positions. The recorded acceleration responses in this rig are used for a comparison between original and compressed signal responses. The responses in the seat rail position and IP A-pillar attachments from this rig is further used in CAE simulations for further testing.

3.1.4 FP-rig

A method for replicating vibrations from the test tracks in a controlled environment is by using a FP-rig. A car is placed in a chamber with a piston under each wheel that can vibrate in a way that mimics the recorded signals from the test track. Each wheel has its own vibrations, hence the need to record at each wheel hub with the accelerometers. The pistons can only replicate vibrations up to 50 Hz, although this is sufficient for capturing the most critical frequencies. The recorded vibrations at the instrument panel will nevertheless reach higher frequencies than 50Hz in the responses. The rig was initially used to get response signals for Car A and Car B, and later for testing and verification of the synthesised new signal concepts.

After accelerations are recorded at each wheel hub at a test track, the car can be driven into the rig with the accelerometers still attached. The rig can start vibrating and after some iterations learn to match the readings from the accelerometers to the previously recorded accelerations from the test track. This is done to the project specific developed signal to verify the signal functionality.

3.1.5 E-points

The E-line method is a method for measuring and simulating Squeak & Rattle along an interface between two parts. It consists of several measurement points along the interface of interest. Accelerometers used in physical tests give acceleration responses that can be transformed into displacement. This result may also be represented by CAE simulations. Relative displacement is usually the main parameter of interest. This is measured in a local coordinate system and can be compared to the distance between two parts in an interface (gap) to estimate the risk of Squeak & Rattle (Weber et al., 2013).

In this project, this method is one of the main tools when analysing recorded data and simulations. However, it was in this project sufficient with only one measurement point per E-line, making it an E-point.

The accelerometers were placed along interfaces where the instrument panel had issues with Squeak & Rattle. The specific positions were decided in collaboration with experienced engineers, based on a CAD-check analysis and previous project documentation. In each E-Point, the most interesting acceleration directions have been measured, depending on location and orientation of parts. The positioning of the E-points is presented by the red circles in Figure 3.4.

Figure 3.4: Position of E-points, red circles, from IP-rig.

When the accelerometers were positioned at E-point one, it was impossible to close the door to the car, hence it needed to be open slightly when it was driven in the test track and in the FP-rig. It is likely that this has compromised the quality of that measurement, due to induced extra vibrations. This means that also measurements from E-point three might be unreliable or of poor quality, as E-point one and three were measured simultaneously. There is two E-points with the number six since the right air-vent was missing in the IP-rig, while the right one was used for the first tests at the test tracks and in the FP-rig

Figure 3.5 displays an example of how an E-point is placed in an interesting E-line. In Figure 3.6, the coordinate systems are approximately the same as the accelerometers have when doing physical tests. The *200* coordinate system is located between the parts and have the Z-direction from part one towards part two in the normal rattle direction. This is defined as rattle direction in the future calculations.

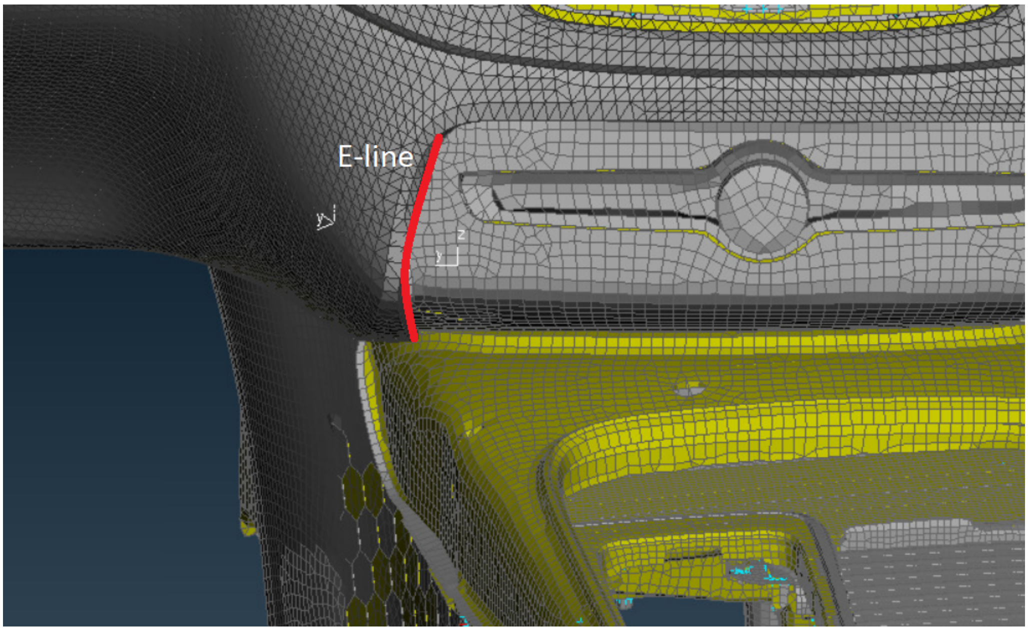

Figure 3.5: E-line approximated by E-point 2

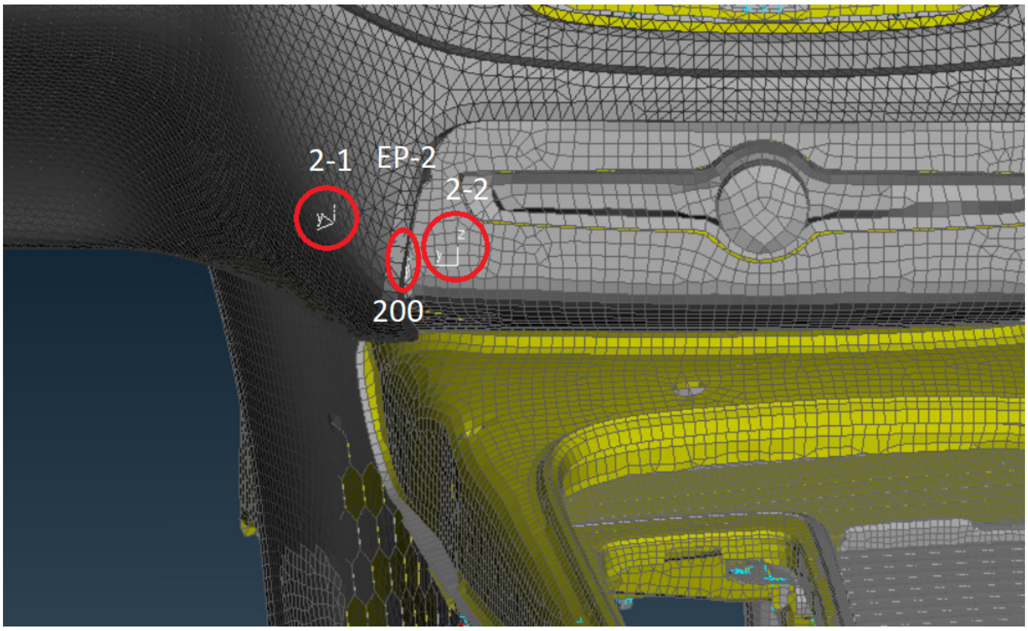

Figure 3.6: E-point 2, accelerometer coordinate system and position, as well as rattle direction coordinate system.

3.1.5.1 Description of each E-point

Each E-point has an orientation and specified rattle direction. The rattle direction is specified as the normal direction of impacts between two parts in an assembly, with the positive direction being from part one towards part two. Generally accelerometer one is placed to the left or above and accelerometer two is placed to the right or below. Due to limitations in the measuring devices, it was not possible to measure all E-points simultaneously. This is a source of error as each measurement session might have been slightly different from the last one, especially when driving on tracks. And it also led to manual synchronization of the signals afterwards. More about errors in Section 5.4. In Figure 3.7, 3.8 and 3.9, the E-points that were measured together are presented.

(a) E-point 1 **(b)** E-point 3

Figure 3.7: E-point 1 and 3

The orientation in 3.7 is left to right, for both. The accelerometers for E-point one made it impossible to close the door, hence some disturbances have been introduced from this, both in E-point one and three.

(a) E-point 2 **(b)** E-point 4

Figure 3.8: E-point 2 and 4

In Figure 3.8, E-point two have number one to the left and E-point four have number one above. These two points have proven to have the best correlation between CAE simulations and physical measurements.

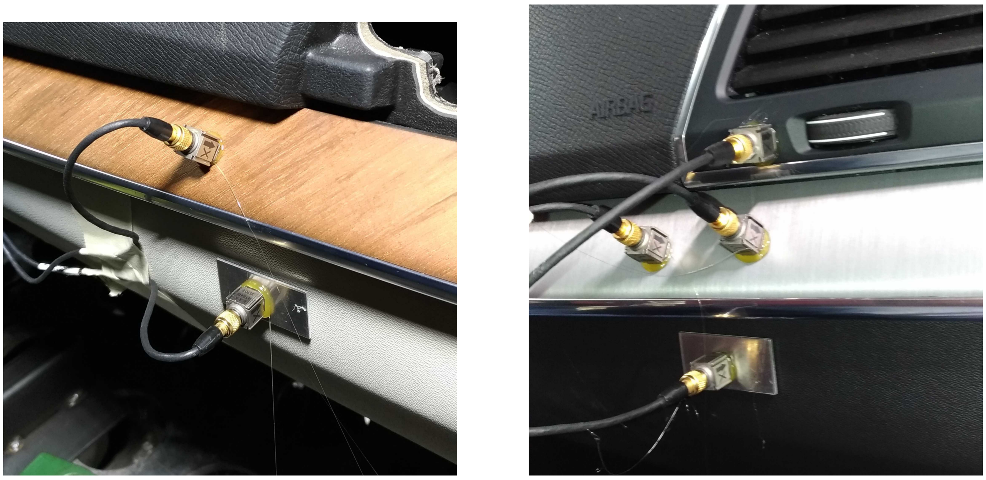

(a) E-point 5

(b) E-point 5 and 6, compare other picture.

Figure 3.9: E-point 5 and 6

E-point five and six both have number one above. When measuring in the cars, E-point six was on the passenger side air-vent. However this was missing in the instrument panel used in the IP-rig so the measurement had to be done on the driver side air-vent. Figure 3.9 (a) is from the IP-rig, Figure 3.9 (b) is from the car when tested in the FP-rig.

Due to limitations in the channel capacity of the SQuadriga modules, certain EP directions were disregarded, as explained in section 3.1.2. The recorded accelerometer directions were selected as in Table 3.1. By, recording in only two directions, it imposes restrictions in the possibility to rotate the directions freely in three dimensions in the post-processing of the acceleration signals. This resulted in EP2 not having any normal (in rattle direction) translation in the local Squeak & Rattle coordinate system. Without normal translation, it is impossible to calculate the rattle event severity. Even the squeak event severity can not be calculated since it is dependent upon the normal translation, see Eq. 3.3 and Eq. 3.5. In retrospect, it would have been desirable to have recorded all three translation directions, especially for EP2, to not lose this E-Point's contribution.

Table 3.1: The measured accelerometer directions for each E-Point

E-Point	**Measured directions**
EP1	Y and Z
EP2	Y and Z
EP3	X, Y and Z
EP4	X, Y and Z
EP5	X and Z
EP6	X, Y and Z

3.1.6 Other Measurements

Both a IPEtronix and a SQuadriga accelerometer were put on the A-pillar behind the side cover on the IP-panel. The purpose of this was to gather excitation signals for the IP-rig, as well as a comparison between the accuracy of the IPEtronix and SQuadriga. The IPEtronix measurements were also used for verifying the excitation signals of the SQuadriga measurements. In Figure 3.10, the mounting of accelerometers at the A-pillar position is displayed.

(a) A-pillar Left

(b) A-pillar Right

Figure 3.10: A-pillar accelerometer positions

Measurements on the inner seat rail on the right and left side were also done. In Figure 3.11, the position of the accelerometers is shown. In the IP-rig, measurements at similar corresponding places were done. These signals were used to excite the model in CAE.

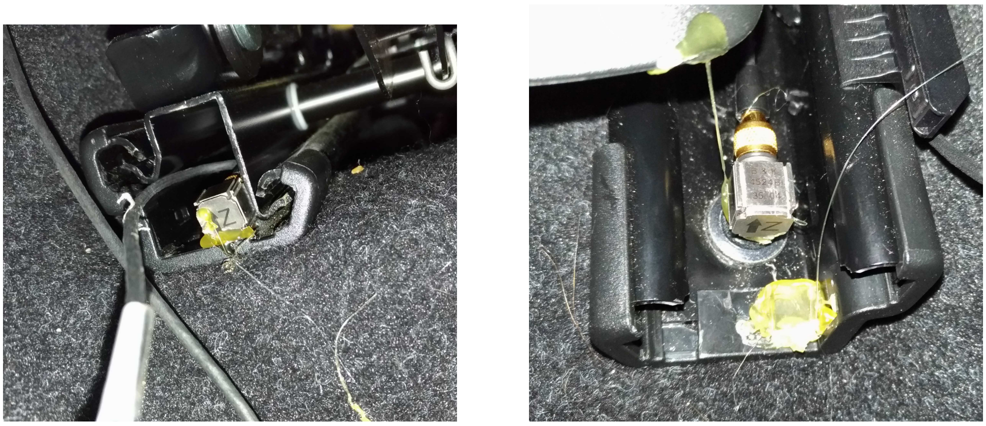

(a) Seat-Rail Left (inner) (b) Seat-Rail Right (inner)

Figure 3.11: Seat rail accelerometer positions

The positions on the IP-rig corresponding to the seat rails is presented in Figure 3.12. This is on the fasteners, used to mount the tunnel. The tunnel is the console between the driver seat and the passenger seat. The same measurements were done on both sides.

Figure 3.12: Position of accelerometers in IP-rig corresponding to seat rails

IPEtronix accelerometers were mounted on the spindle close to the wheel to provide measurements of the accelerations there, caused by the uneven road track. This effectively means that the road surface was measured, nonetheless with slightly decreased amplitude, since the only dampening between the road and the accelerometer was the tyre. The location of the accelerometers can be seen in Figure 3.13. The main reason for recording at all four wheel hubs was to make it possible to replicate the excitations in the FP-rig.

(a) Left front wheel

(b) Right front wheel

(c) Left rear wheel

(d) Right rear wheel

Figure 3.13: Position of IPEtronix accelerometers, all spindles

3.2 Statistical data about recordings

Several statistical data were calculated in each track case and in each position. This makes it possible to judge the relative importance between the different tracks. If the developed method is used to create new signals after this project, these statistical data may be used to screen out a few important signals rather than using them all. This would lead to an even shorter synthesized signal time as there is less input. As all signals are used in the result of this project, these plots now serves as a basis for comparing the original signals and the synthesized final concept signal.

The plots in this section are mainly created from data from the IP-rig, since all tracks are available there which allow for a better comparison between them all. Due to confidentiality, the Y-axis of the plots is normalized. Figure 3.14, 3.15, 3.16 and 3.17 present data from the IP-rig, with a normalized Y-axis. Moreover, in Figure 3.18, the spindle accelerations is included. They are however not included in the other figures as the measurements in the IP-rig can not capture spindle accelerations. Additionally, the higher amplitude of the spindle accelerations make it difficult to differentiate the other signal statistics.

Legend explanations:

- IP-mag means the average magnitude of the accelerations for the left and right A-pillar position (resultant of X-, Y- and Z-directions).
- IP-Z means the average magnitude of the accelerations, only in Z-direction for the left and right A-pillar position.
- Wheels means the average magnitude of the accelerations, in Z-direction for the four wheel hub spindle positions.
- EP-squeak means the average magnitude of the accelerations in local X- and Y-direction for all E-Points.
- EP-rattle means the average magnitude of the accelerations in only local Z-direction for all E-Points.

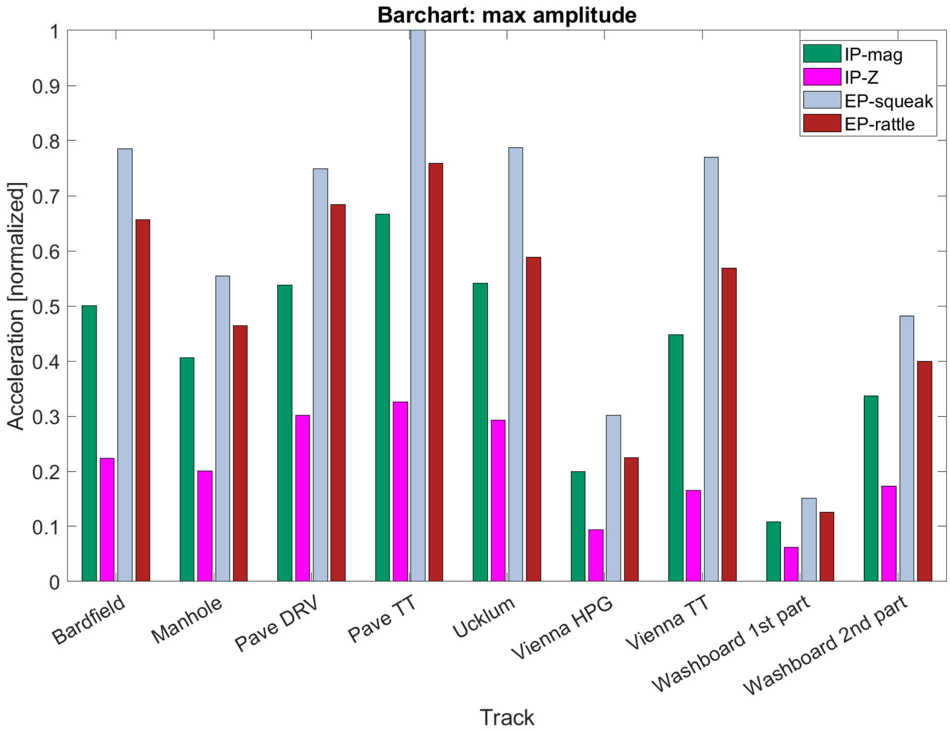

Figure 3.14: Max amplitude for each track in Car A, from IP-rig. Normalized Y-axis.

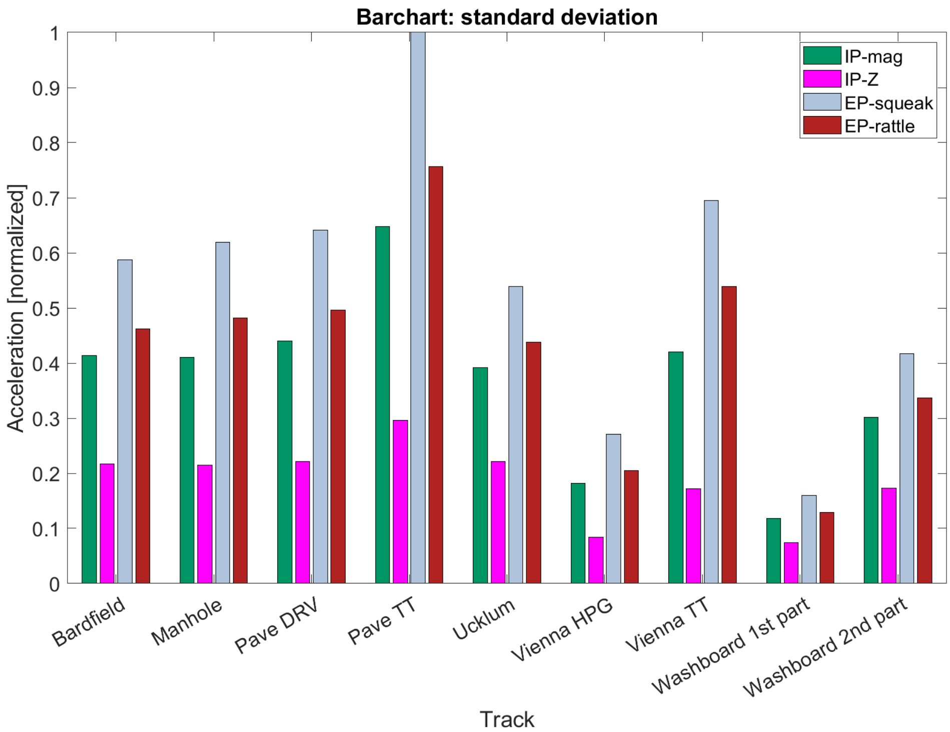

Figure 3.15: Standard deviation for each track in Car A, from IP-rig. Normalized Y-axis.

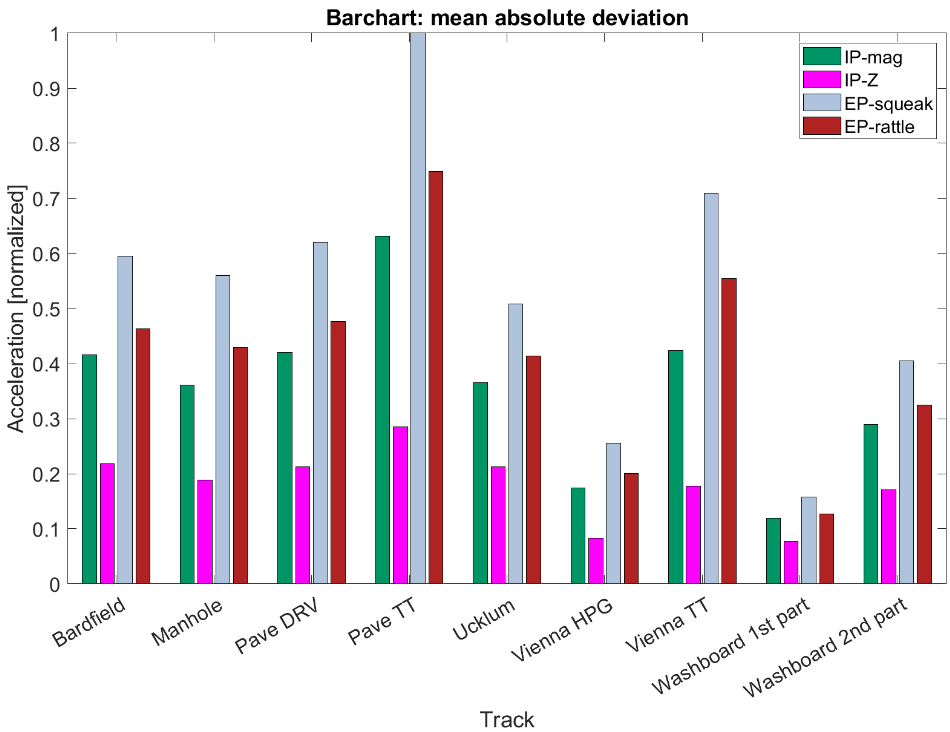

Figure 3.16: Mean absolute deviation for each track in Car A, from IP-rig. Normalized Y-axis.

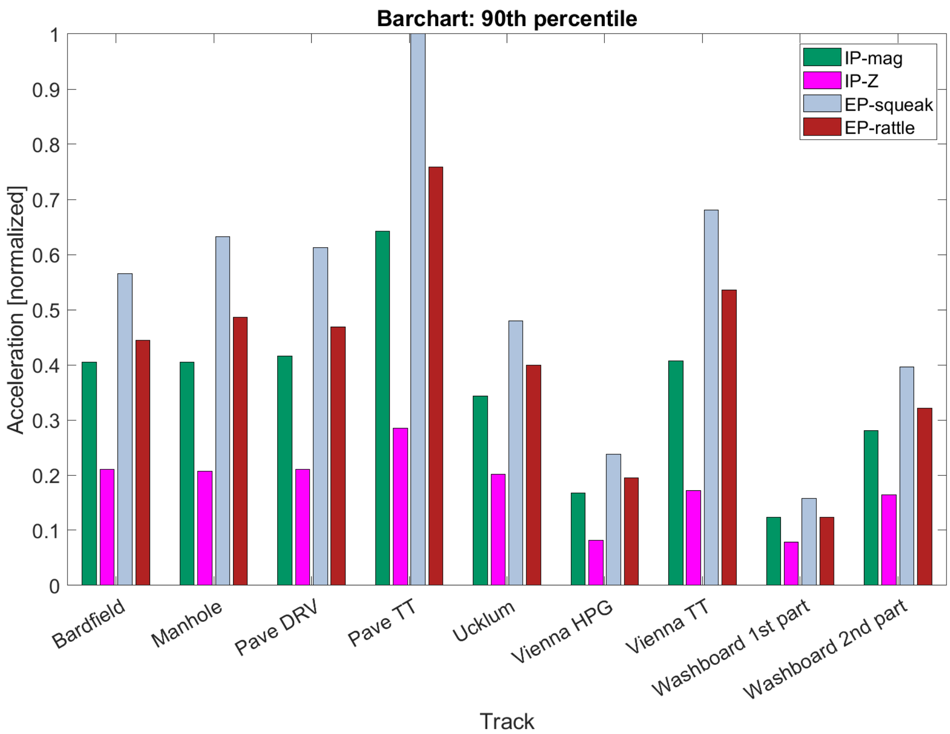

Figure 3.17: 90th percentile for each track in Car A, from IP-rig. Normalized Y-axis.

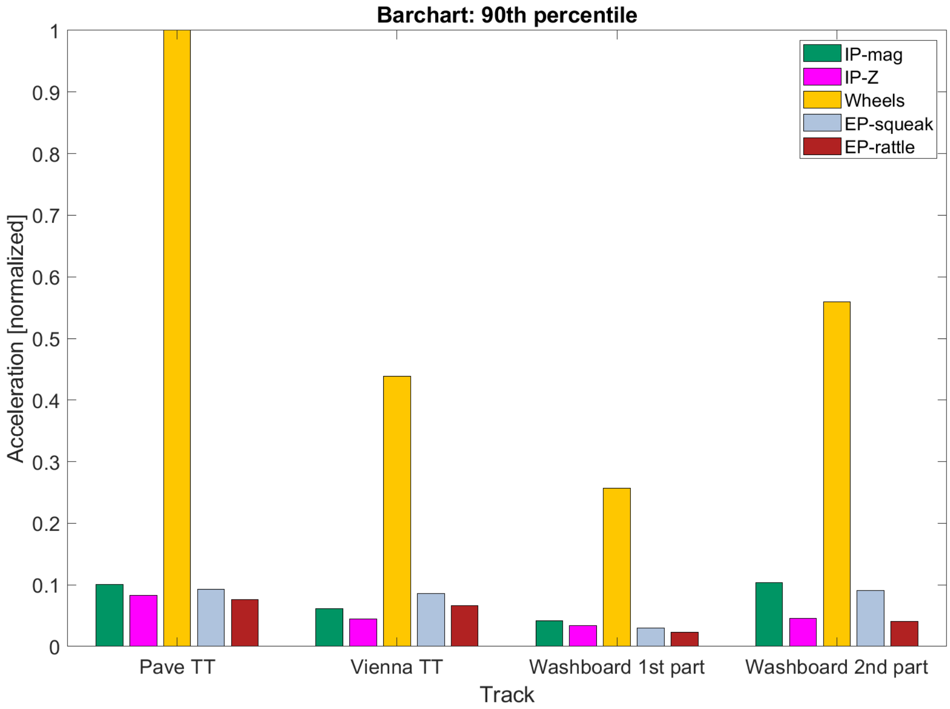

Figure 3.18: 90th percentile for each track in Car A, from TT track, including wheel hub accelerations. Normalized Y-axis.

3.3 Filtering

From the recorded acceleration signals it was possible to obtain velocity- and displacement signals by applying omega arithmetics, described in section 2.3. This was performed on all acceleration signals, with an example shown for EP52 in Z-dir, on track Ucklum in the FP-rig with Car A, as in Figure 3.19.

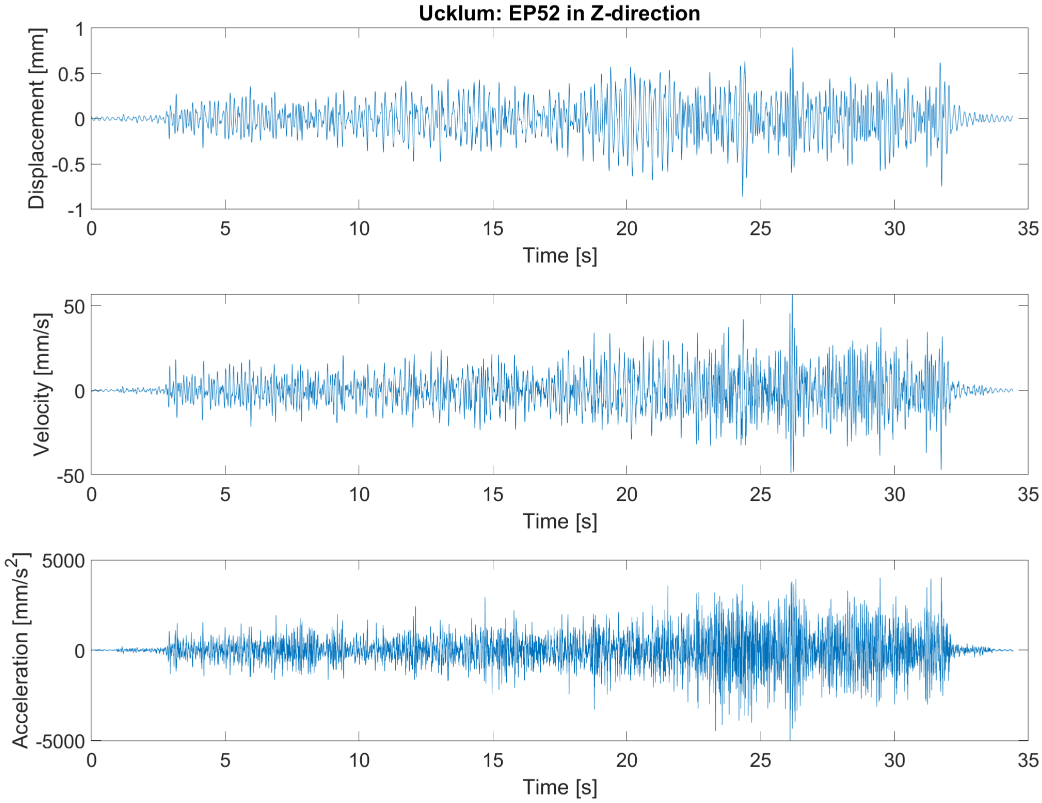

Figure 3.19: Time domain representation of acceleration, velocity and displacement of EP52 in Z-dir, on track Ucklum in the FP-rig, with Car A.

The time domain signals have furthermore been transformed into frequency domain with FFT. The purpose of this transformation is to analyse the frequency composition of the signals and have been used in the development and verification of these signals. All signals have been filtered with a high pass filter at 5Hz. The reason for this is to remove drift of the displacement- and velocity signal, caused by noise in the signal recordings. See Figure 3.20 and 3.21, for examples of drift of the unfiltered signals. High-pass filtering at higher frequencies will result in less drift, with the risk of removing necessary signal components, while high-pass filtering at lower frequencies will result in more drift with more signal components retained. By testing various filtering frequencies for all recorded signals and finding at what frequency the displacement converge, a filtering frequency was set to 5Hz. For the FP-rig, the maximum displacement for high pass filtering frequencies ranging from 0-7 Hz are summarized in Table 3.2, and for the TT-track in Table 3.3. The maximum displacement is including all E-points, IP-attachments and Seat-Rail positions for all available X-, Y- and Z-directions.
If the unfiltered maximum displacement is above the filtered maximum displacement, it is due to signal drift. The unfiltered signals show an obvious drift, since the unfiltered maximum displacement exceeds 1000 mm at most in Figure 3.20, which is far above the filtered maximum displacement.
By applying higher filtering frequencies, the maximum displacement is lowered.

There is however a risk of removing valuable signal information by filtering at too high frequencies. When the maximum displacement has converged, it is a suitable filtering frequency. For the FP-rig and the TT-track, the maximum displacement had converged at around 5 Hz, which therefore was set as an appropriate filtering frequency for future signal processing. A necessary factor in contributing to this filtering frequency was the limitations of the IP-rig, which could not handle a filter at a lower frequency than 5 Hz for our specific signals, due to risk of colliding parts. Filtering at 7 Hz or higher also removed necessary signal frequencies of the road track $Washboard\_1st\_part$. An example of frequency domain representation of the signals is shown in Figure 3.22.

Table 3.2: Maximum displacement [mm] of signals in the FP-rig for Car A.

Maximum displacement [mm] for a given high-pass filter					
Roadtrack	**Unfiltered**	**1 Hz**	**3 Hz**	**5 Hz**	**7 Hz**
Bardfield	72.7	14.5	2.6	1.5	1
Manhole	8.5	7.3	2.4	1.1	0.8
Pave	1205.2	14.8	3.2	1.6	1.1
Ucklum	125.2	14.1	2.7	1.5	1.2
Viennastone	19.2	6.1	1.5	0.6	0.4
Max of all roadtracks	**1205.2**	**14.8**	**3.2**	**1.6**	**1.2**

Table 3.3: Maximum displacement [mm] of signals in the TT track for Car A.

Maximum displacement [mm] for a given high-pass filter					
Roadtrack	**Unfiltered**	**1 Hz**	**3 Hz**	**5 Hz**	**7 Hz**
Pave	884.2	13.0	3.8	1.3	1.1
Washboard1	29.8	3.8	1.4	1.1	0.7
Washboard2	23.9	8.4	1.4	1.6	1.4
Viennastone	881.7	7.6	1.2	0.7	0.6
Max of all roadtracks	**884.2**	**13.0**	**3.8**	**1.4**	**1.4**

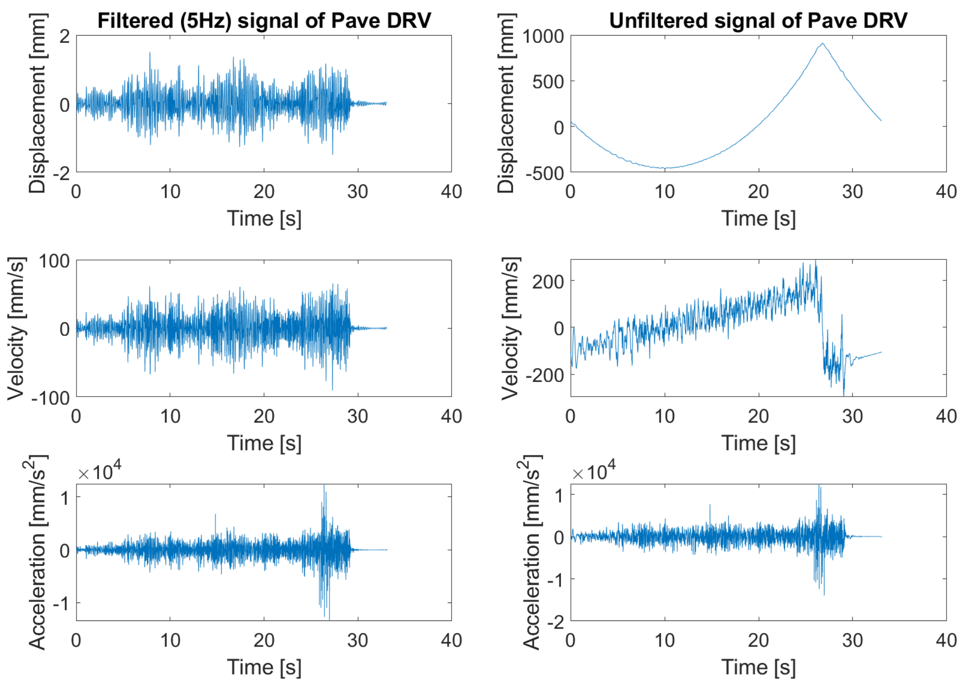

Figure 3.20: Drift for the moderately rough case of Pave DRV. Comparison of unfiltered and filtered acceleration-, velocity- and displacement signals. IP-attachment left, Z-direction. FP-rig Car A.

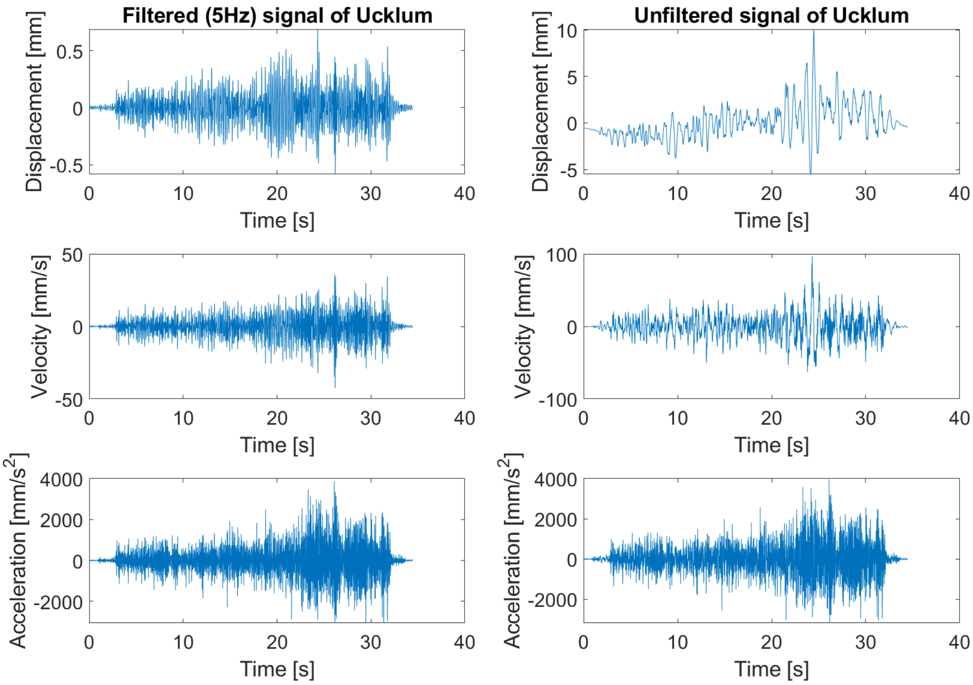

Figure 3.21: Drift for track Ucklum. Comparison of unfiltered and filtered acceleration-, velocity- and displacement signals. EP52, Z-direction. FP-rig Car A.

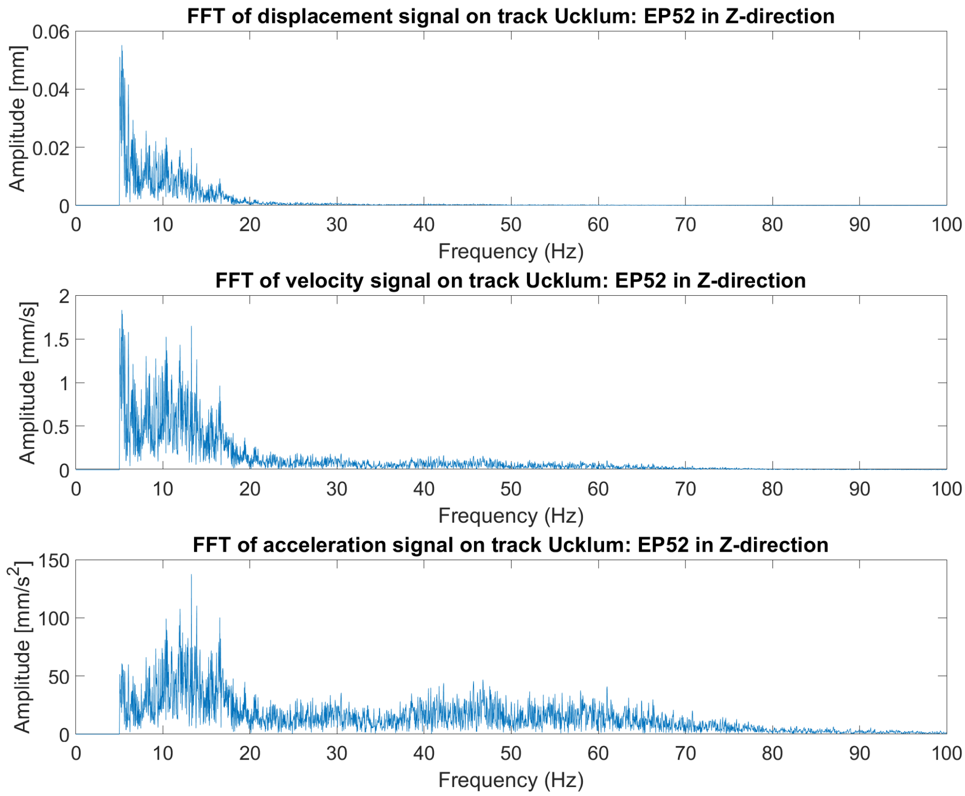

Figure 3.22: Frequency domain representation of acceleration, velocity and displacement of EP52 in Z-dir, on track Ucklum in the FP-rig with Car A

An essential part of developing the shortened, synthesized signals have been to calculate relative displacement, velocity and acceleration as a function of time. The calculation procedure is simply to subtract the displacement of one side of the E-point from the other side of the E-point, given that the two coordinate systems are aligned. An example of the relative acceleration-, velocity- and displacement signals is visualized in Figure 3.23.

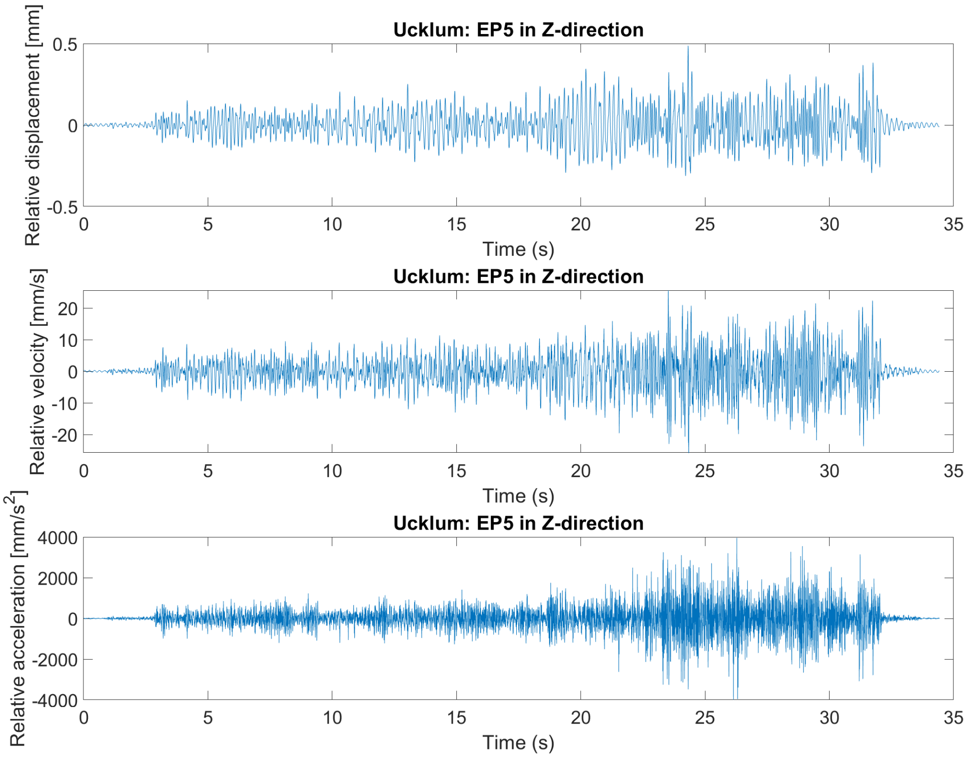

Figure 3.23: Relative acceleration-, velocity- and displacement signals of EP5 in Z-dir, on track Ucklum in FP-rig with Car A.

When the signals are run in the IP-rig, a low pass filter is applied at 100Hz, and in the FP-rig, a 50 Hz low pass filter is applied. This is because the rigs cannot handle higher frequencies.

3.4 CAE

A virtual geometric model of Car A instrument panel has been used to develop the shortening method. Recorded acceleration signals have been applied to positions in the model corresponding to where they were measured in the physical tests. ANSA (BETA CAE, 2020a) has been used as a pre-processor, NASTRAN (MSC Software, 2020) as processor and META (BETA CAE, 2020b) as post-processor. SOL 103 is used for modal analysis and SOL 112 for enforced acceleration analysis in NASTRAN. In Figure 3.24, the model can be seen with the positions where accelerations are applied. No additional boundary conditions are applied apart from the excitation signals.

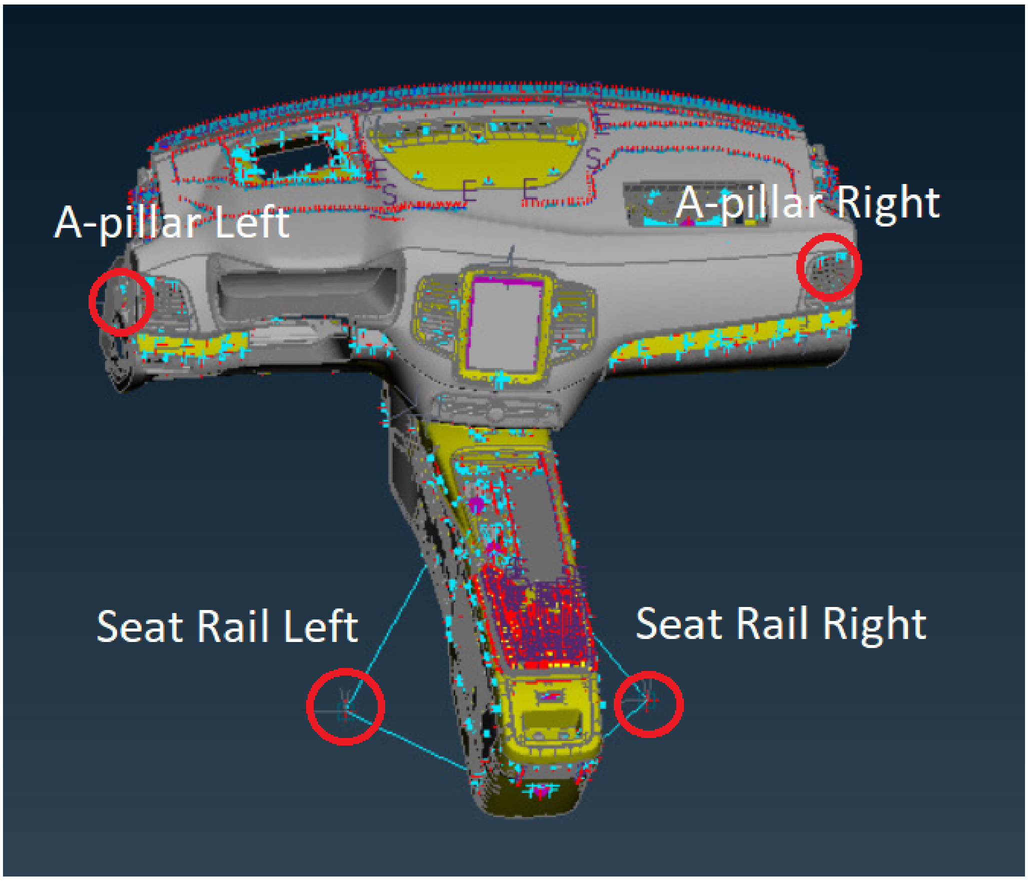

Figure 3.24: ANSA model with marked excitation points.

The accuracy of the result compared to the measurements vary greatly from E-point to E-point. A comparison between simulation and measurement in one of the best positions and directions can be seen in Figure 3.25 and Figure 3.26. A comparison in a poor position can be seen in Figure 3.27 and Figure 3.28.

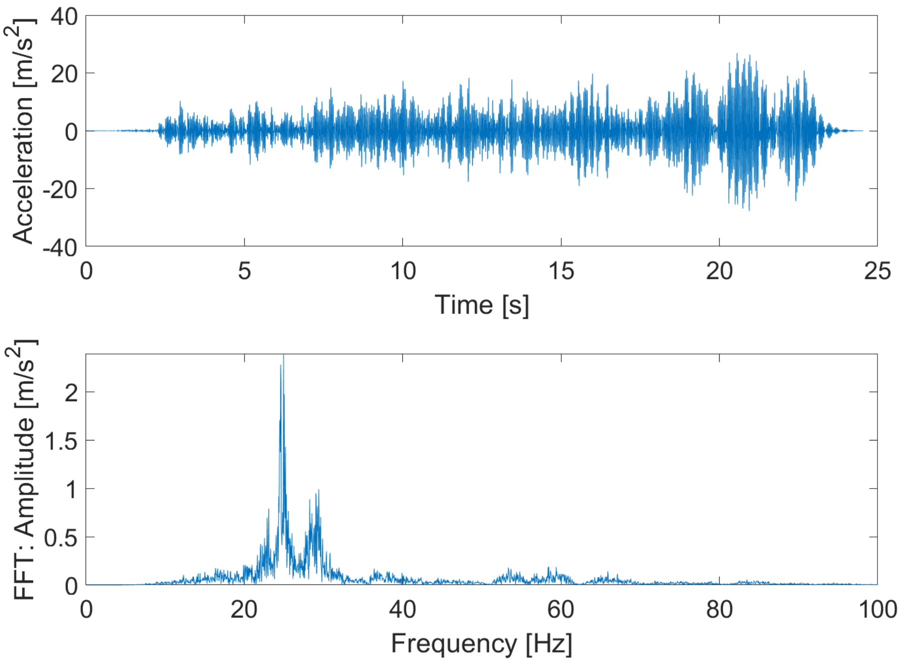

Figure 3.25: Accelerometer on EP42, direction Z, CAE. Track Pave TT

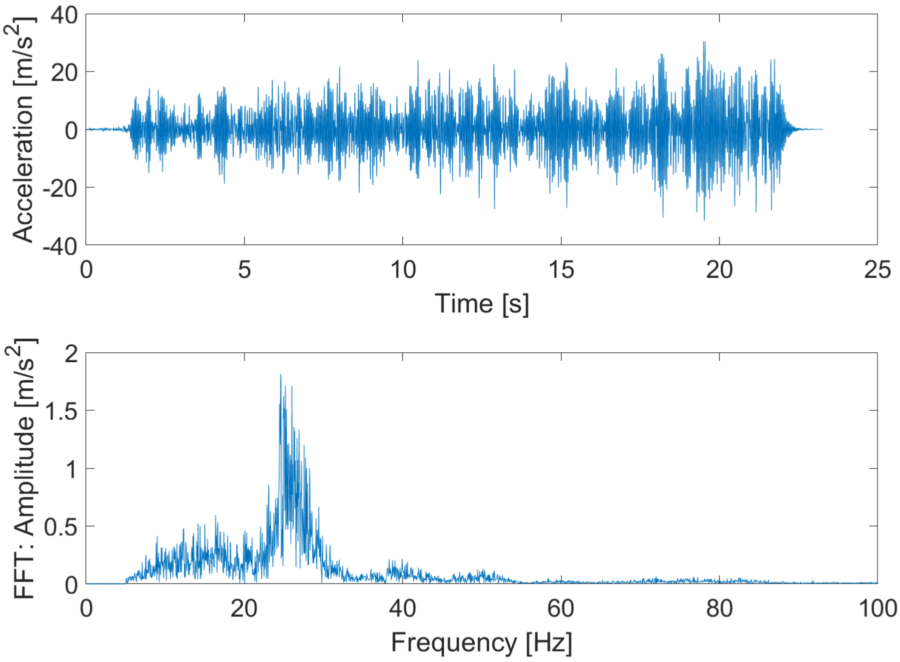

Figure 3.26: Accelerometer on EP42, direction Z, measured

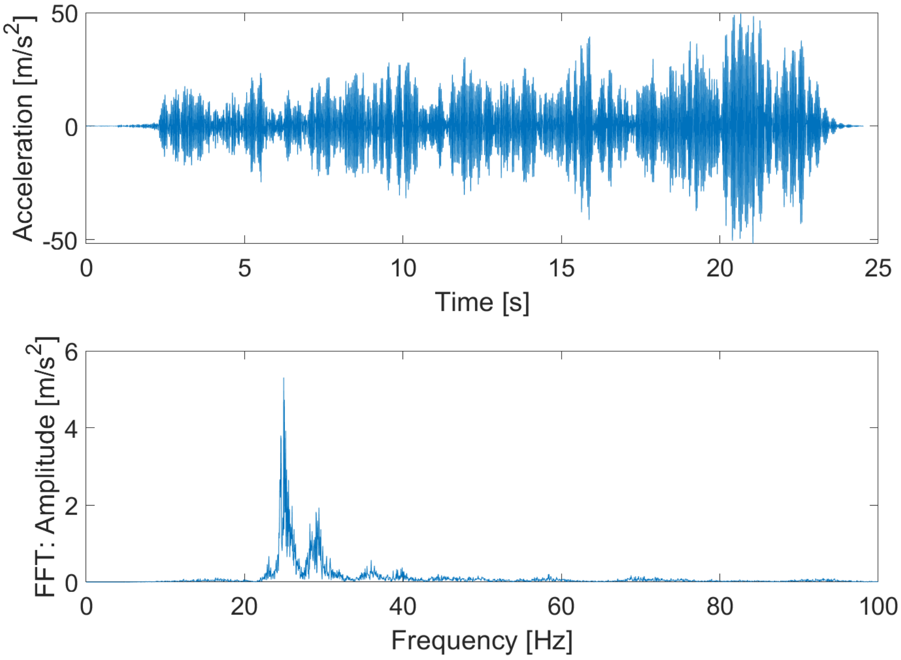

Figure 3.27: Accelerometer on EP31, direction Z, CAE. Track Pave TT

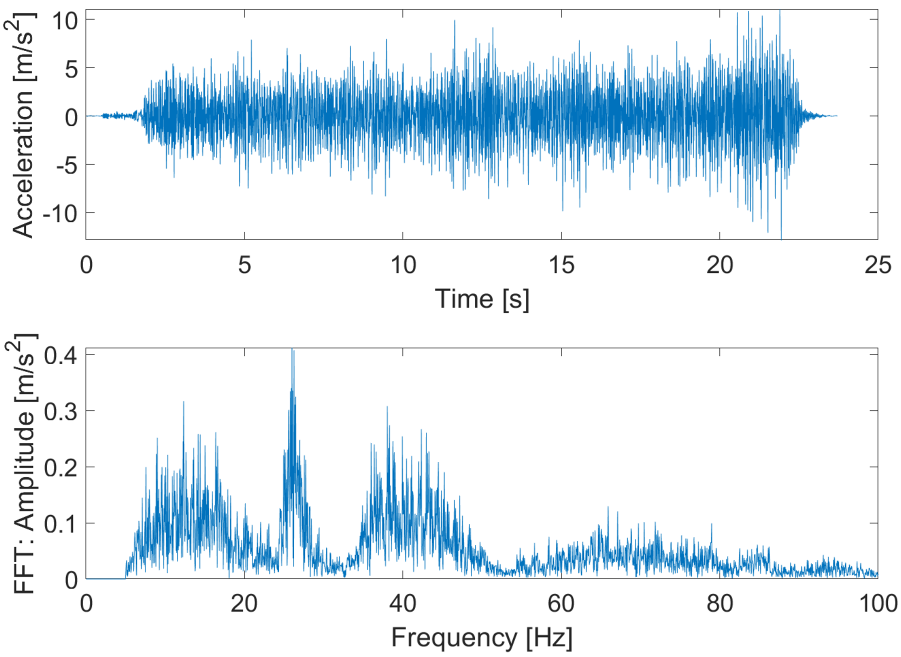

Figure 3.28: Accelerometer on EP31, direction Z, measured

3.4.1 Modal Analysis

A simple modal analysis was done in NASTRAN (SOL103) to see that the model was somewhat well defined and to find what the lowest eigenfrequency was. This value was around 23 Hz and was later used to define pause duration when merging decomposed signal sections together. Some parts were removed from the model that caused very unrealistic modal movements and were far away from E-points.

3.4.2 Comparing CAE to physical measurements

There is no doubt that the virtual model needs to be of very high quality if similar results are to be expected from the CAE results as from the physical measurements. There is however not as clear correlation between how this difference would affect the new signal if the cutting is based on the responses from these two different versions. In Figure 3.29, the shorter cut version of the excitation signals is plotted, both in time domain and in frequency domain. In this signal, all road tracks is concatenated after each other in time sequence. The shortening parameters used are based on concept three, further explained in Section 3.7.

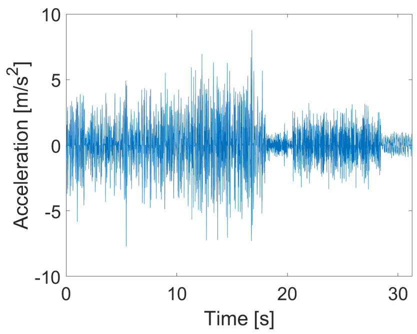

(a) Time domain, CAE based new signal. Concept 3

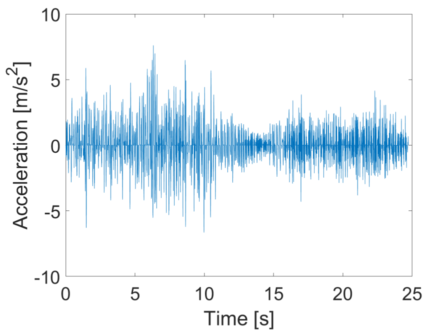

(b) Time domain, IP-rig based new signal. Concept 3

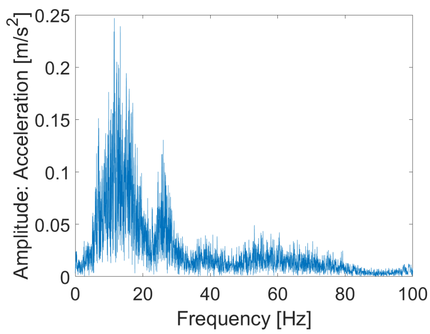

(c) Frequency domain, CAE based new signal. Concept 3

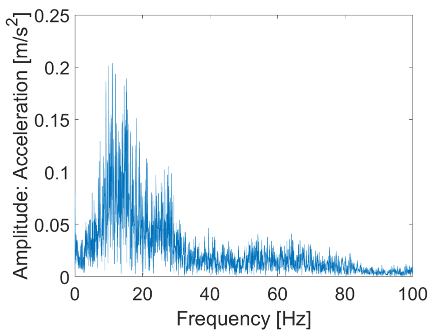

(d) Frequency domain, IP-rig based new signal. Concept 3

Figure 3.29: CAE response based shortened excitation signal versus IP response based shortened excitation signal, frequency domain and time domain.

3.5 Squeak & Rattle assessment

To assess whether a signal part is potent within Squeak & Rattle or not, a factor is formed for setting a numerical value on this. A factor is created for both squeak and rattle separately. This value is used for deciding what parts of a signal should be kept and what should not. They are assessed by mathematically quite simple methods, although requiring precise data in order to get reliable and good results. This section describes how these evaluation factors are designed. The formulation and theory for these metrics was given by Volvo Cars.

3.5.1 Squeak assessment

Parallel translational displacement of two points on two adjacent surfaces as well as stick-slip material data is needed to assess the risk of squeak in a signal. The translations is easily accessed from the accelerometer measurements. From the stick-slip data, a specific parameter called impulse rate is of interest. Impulse rate can be described as a counting of how many slips occurs in one millimeter when two materials are pressed together with a spring of a certain force and they slide against each other. A slip is happening when static friction is overcome and turns into dynamic friction, which has a lower value than static friction. In this squeak assessment, the test case most prone of causing squeak has been selected. There was to a degree insufficient testing data, meaning that not all desired material combinations had been tested. Data from similar materials were accepted as sufficient for this project, as there were no possibility to test the exactly correct materials. Both choosing the most sensitive case and using only similar materials might not be the best representation of reality, although it is sufficient in this project as only the risk of Squeak & Rattle is assessed in the signals, not prediction of actual Squeak & Rattle events. This means that as long as all signals are evaluated based on the same data, they will be equally evaluated, even if the data is slightly incorrect.

The squeak slip is calculated according to Eq. 3.1, where relative displacement is defined as the resultant from relative displacements in the planar direction. So, $rel.disp_{planar}$ will always be positive for squeak events, while $Squeak.slip$ always will be negative for squeak events.

$$Squeak.slip = stick.distance - rel.disp_{planar} \tag{3.1}$$

The calculations are done for each time index by finding if the displacement is larger than the inverse of the impulse rate. This means finding if the accelerometers have a relative planar displacement larger than what the materials can translate while in contact without slipping against each other and creating a risk of squeak.

By strictly using the calculation of actual squeak, several of the E-Points will not have any squeak (caused by slip) at all. For evaluation purposes, it is more effective if all E-Points are assigned a value of squeak occurrences. The alternative method used in this thesis for the squeak assessment has been to find a percentile of the relative displacement, where exceeding this will count as squeak event. Using the percentile method of squeak assessment further downplays the importance of obtaining exactly the correct material data and tolerance variations. For deciding an adequate percentile limit, varying percentile limits in the range 60th-99th percenile were compared to actual squeak criteria. A precision of 5th percentile for finding an optimal limit were regarded as sufficient. The optimal limit were obtained by iterating through all recorded signals and calculating the deviation from the actual squeak criteria, see Table 3.4. This is a minimization problem were a mean deviation of 0 indicates a perfect match between actual rattle-penetration plus squeak-slip occurrences and of the model based on a percentile of the relative displacement. The percentile optimization is agnostic whether the percentile based model under-predicts or over-predicts the event occurrences. Considering this, implies it is more conservative to use a lower percentile limit, and thereby including more penetration and slip events. The minimal model error is at the 95th percentile. However, the 90th percentile is close behind in the error size estimation. By setting the percentile at the 90th percentile, it will include more events and can be regarded as safer since crucial penetration and slip events might otherwise be disregarded by setting the percentile at a higher value. Thus, the 90th percentile of relative displacement will be chosen as the limit for future Squeak & Rattle assessments.

Table 3.4: Percentile optimization. For each percentile, the mean deviation from the actual penetration and slip occurrences is calculated. 0 implies perfect match with the actual penetration and slip occurrences.

Mean model error/deviation for S&R - percentile based							
Percentile	**60th**	**70th**	**80th**	**85th**	**90th**	**95th**	**99th**
Squeak dev.	≈ 368	≈ 298	≈ 229	≈ 194	≈ 168	≈ 166	≈ 192
Rattle dev.	≈ 237	≈ 198	≈ 140	≈ 113	≈ 91	≈ 87	≈ 117
Sum S&R dev.	≈ 605	≈ 496	≈ 369	≈ 307	≈ 259	≈ 253	≈ 309

To assess the severity of squeak, Eq. 3.3 was provided by Volvo Cars as a way to calculate the severity of squeak. The equation have similarities with the calculation of momentum equation $p = mv$ and Newton's second law $F = ma$. $F = ma$ can be re-written and inserted into $p = mv$ to get Eq. 3.2.

$$p = Fv\frac{1}{a} \tag{3.2}$$

Eq. 3.3 is not the same as Eq. 3.2, although parallels can be made. The $rel.disp_{planar}$ and $rel.disp_{normal}$ part represents the force exerted in planar and normal direction. $rel.vel_{planar}$ corresponds to the velocity part in Eq. 3.2. $(1 - rel.acc_{planar}/g)$ is an unitless scaling factor to account for the $1/a$ part. Hence, the squeak severity for each event will amount to $Factor_{squeak}$.

$$Factor_{squeak} = (rel.disp_{normal})(rel.disp_{planar})abs(rel.vel_{planar})(1 - rel.acc_{planar}/g) \tag{3.3}$$

The squeak metric was calculated as the mean value of $Factor_{squeak}$ for all events where both the percentile value were exceeded for normal and planar displacement. This requirement was set since the two components must be in contact to cause squeak (secured by checking percentile value in normal direction) and causing risk of squeak (secured by exceeding the percentile value in planar direction). Since the mean value is taken for all squeak events, all events factor metric should have the same sign. Therefore it is important that the scaling part $(1 - rel.acc_{planar}/g)$ never becomes negative, because strictly positive values implies no sign changes. g is the gravitational acceleration, $g \approx 9.82$. To ensure that the scaling part $(1 - rel.acc_{planar}/g)$ always is positive, g will be multiplied by a factor of, for example 5. Finding the appropriate multiplication factor, requires consideration of all signals scaling factor individually. By iterating through all the signals and gradually increasing the multiplication factor, eventually a suitable number was found. This number were set with a margin above the minimally required value and could differ depending on the testing environment. In the IP-rig and FP-rig the multiplication factor was set to 5, and for the CAE simulations it was set to 15.

3.5.2 Rattle assessment

Rattle is assessed by calculating the relative normal displacement between the accelerometers in an E-point and comparing that to the measured gap between the part. Rattle occurs when the relative normal displacement is larger than the gap. The gap data were collected from virtual geometrical models. No tolerances have been taken into account. That was not a problem by the same motivation as with the squeak assessment, meaning that tolerances would be important if actual rattle events should be calculated, not just comparing the risk of rattle as was in this project.

The rattle penetration was calculated according to Eq. 3.4, where relative displacement is defined as being positive for widening gaps and negative for closing gaps.

$$Rattle.penetration = nominal.gap + rel.disp_{normal} \tag{3.4}$$

The $Factor_{rattle}$ have been calculated according to Eq. 3.5.

$$Factor_{rattle} = (rel.disp_{normal})(-rel.vel_{normal})(1 - rel.acc_{normal}/g) \tag{3.5}$$

The rattle metric was calculated as the mean value of $Factor_{rattle}$, for all events where both the percentile value were exceeded for normal displacement, and where the relative velocity was negative. This requirement was set since the two components must be in contact to cause rattle (secured by checking percentile value in normal direction) and being in a closing motion (secured by having negative relative velocity).

The same reasoning for calculations of the squeak metric can be applied for the rattle metric. This implies that $Factor_{rattle}$ always will assume negative values. The more negative the value, the greater rattle severity a specific E-Point will have. To ensure solely negative values for $Factor_{rattle}$, a minus sign is needed in the $(-rel.vel_{normal})$ part.

3.6 Shortening Method

This section presents some of the main numerical parameters that needs a decided numerical input when creating a new shorter signal. Testing of different parameter combinations are presented in this section as concepts that are tested in several iterations.

3.6.1 Free parameters

The following five parameters have high significance that someone intending to utilize the developed method from this project should grasp and apply to their specific case. These parameters affect how the method is identifying relevant sections to keep and how it is merging these cut sections. The result varies greatly depending on what parameters are chosen. Plotting the resulting signal is recommended to get a good overview of what is achieved. The factor severity plots of Car A from the IP-rig and the FP-rig measurements can be found in Appendix B and in Appendix C.

Percentile to keep
This parameter decides what percentile of the highest metric value, that time indexes should be kept for further evaluation. Increasing the *percentile to keep* will lower the percentile limit line. Decreasing the *percentile to keep* will raise the percentile limit line, see Figure 3.30. The *percentile to keep* parameter is necessary for sorting out the most important Squeak & Rattle events among the calculated ones. If all events in any E-point were to be considered as important, almost the entire old signal would be kept. This percentile factor is independent of the percentile limit used for assessing Squeak & Rattle occurrences, as described in section 3.5.1.

Max Difference in time
The purpose of this factor is to decide whether Squeak & Rattle events should be in the same cut section, or in a separate one, see Figure 3.31. Practically, it means if it places a ramp-up and a pause between the current section and the next, or if it is merged by keeping the original signal in between these events. It is defined as $(Rampup\ Duration + Pause\ Duration)X$. The factor X is arbitrary and can be edited to fit current needs, 1.1 is a good starting guess. The factor $(Rampup\ Duration + Pause\ Duration)$ is there since it is not possible to cut in shorter distances, if the events occur at shorter than that time twice in a row. This factor also increases the effective new time, which is the value on how much of the new signal is directly copied from the old signal.

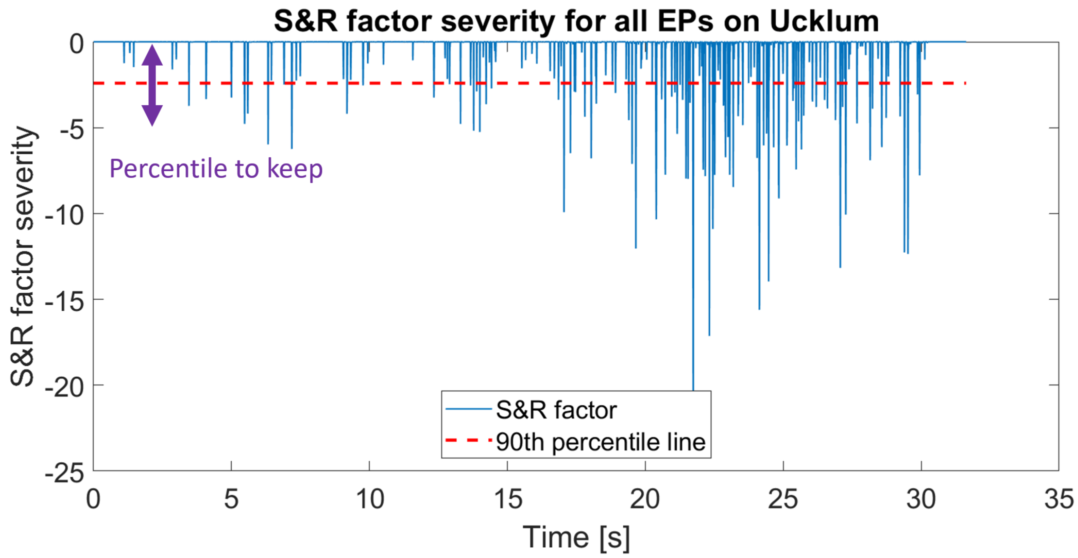

Figure 3.30: Percentile to keep is visualized as the dashed line in red. Increasing the percentile to keep will lower the percentile limit line. Decreasing the percentile to keep will raise the percentile limit line. If the severity of events are crossing this line, then these events are stored as relevant signal parts.

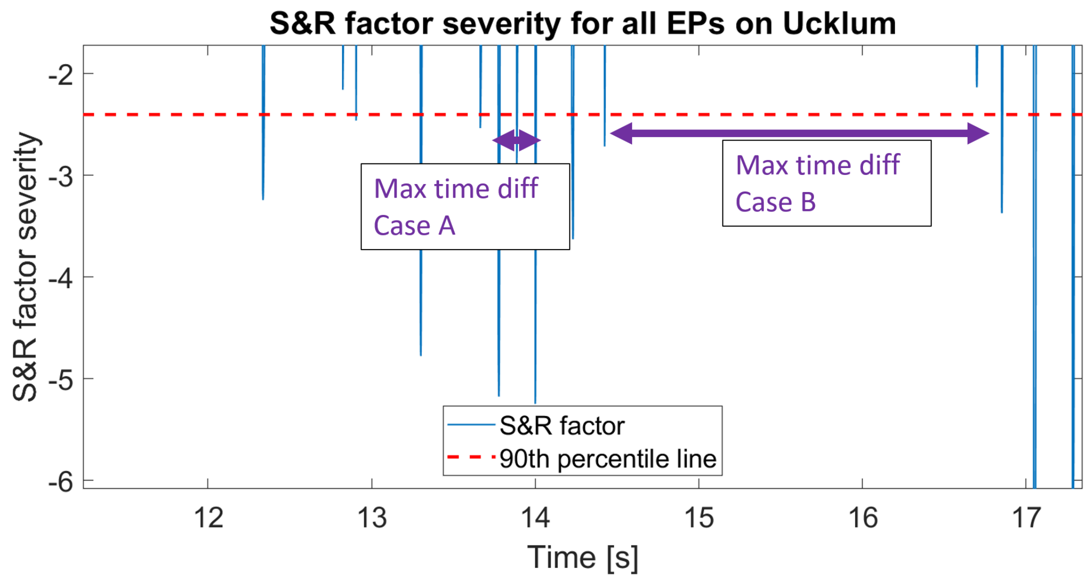

Figure 3.31: Max Difference in time factor visualized. Case A have the events close in time and will be stored as one section. Case B have events with a long time in between, which stores the sections in two separate parts. Thus, this empty space will be discarded.

Pause Duration

When merging the cut signal parts together, a pause is added to let the system rest to reduce the lingering effect from the preceding signal part, see Figure 3.32. The pause duration is simply a zero acceleration string during a certain time duration. The duration is defined as the inverted lowest eigenvalue frequency of the excited part, times a factor. The IP in the CAE simulations has a lowest eigenfrequency of 23 Hz, which gives that the pause is a factor of about 43 ms. A pause factor of one means that the system has rested for at least one period of 23 Hz before a new signal part begins.

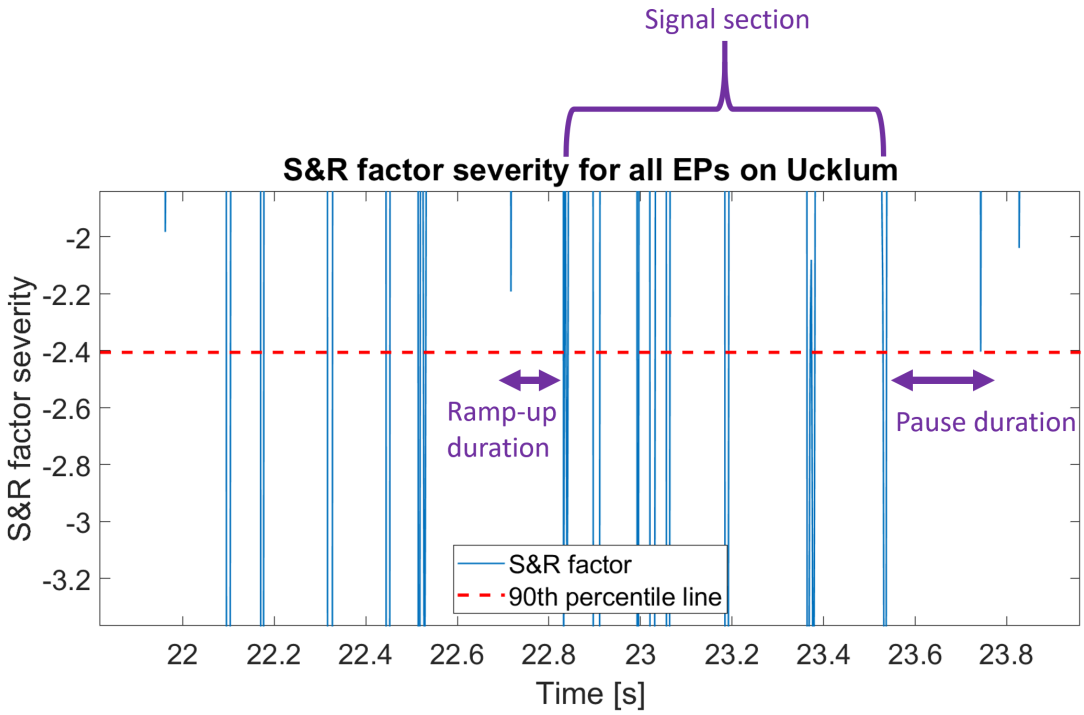

Figure 3.32: For a cut signal section, a ramp-up duration is added before the section to avoid jerks. After this cut section, a pause is added to let the system rest.

Ramp Duration

A time span is added before the interesting signal part to reduce the risk of jerks that may affect the result, see Figure 3.32. This is done by multiplying the amplitude in each time index during this ramp up time, by a quarter of a sine-period ramping from 0 to 1. This means that each new signal part is ramped from 0 to full scale signal amplitude when the desired signal part begins. The duration of this parameter is calculated as Pause Duration divided by a factor.

Minimum time for keeping

This is the minimum time that a squeak or rattle event must be for it to be kept for the new signal, see Figure 3.33. The purpose of this parameter is to avoid a single event with long ramp-up duration and pause duration. Having a lower *Minimum time for keeping*, keeps more events, although decreasing the effective time. Increasing the *Minimum time for keeping*, discards single events far away from other events, thus increasing the effective time. The effective time is analogous to the number of events per time unit in the new signal. The *Minimum time for keeping* parameter is calculated as the *Max Difference in time* divided by a factor, a reasonable initial guess can be three.

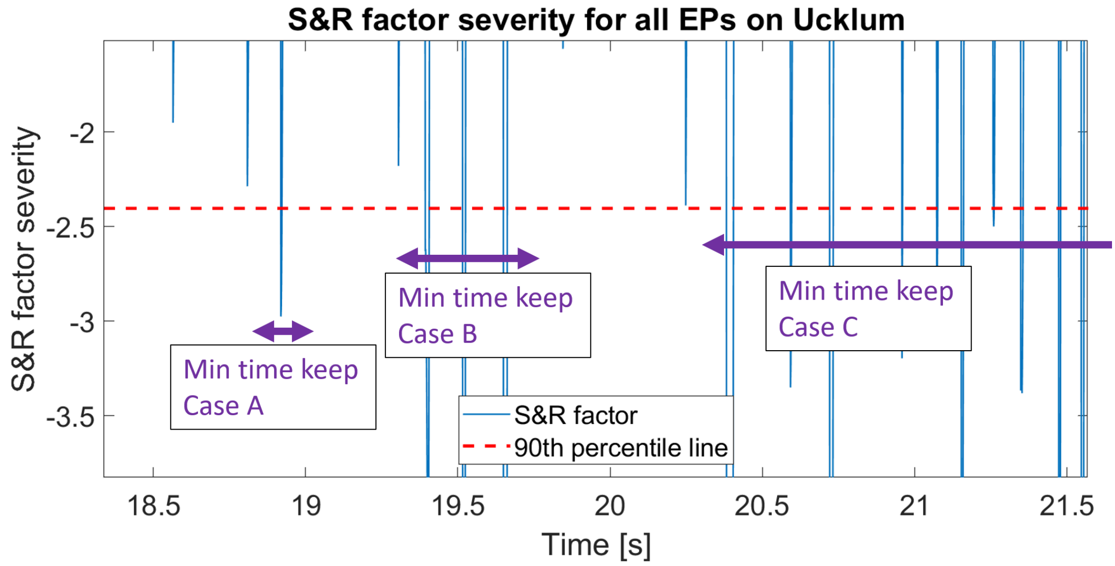

Figure 3.33: *Minimum time for keeping.* Case A will be discarded unless the *Minimum time for keeping* is set particularly low. Case B will likely be stored unless *Minimum time for keeping* is set high. Case C will be stored, unless *Minimum time for keeping* is set extremely high.

3.7 Concepts

The effect of a few parameters, mainly *Pause Duration* and *Ramp-up Duration*, on the result were quite uncertain and some trials were therefore needed to determine a good value for these parameters. It must be noted that extensive statistical trials could be done here to find the absolute optimum, but there was no time for that in this project. Limitations in the number of possible rows in the NASTRAN run files combined with the post-processing of the simulated results incurred further limitations on the number of concepts that could be analysed within the scope of this thesis. For this project, a few experimental concepts was deemed enough for each concept iteration. The excitation signals these parameters result in, are shown in the figures in this section, with the first iteration displayed in Figure 3.34. The first concept is represented by the first section in the signal separated by a long pause from the next concept. These excitation signals are sent to test rigs and the response is measured. The performance of each concept is calculated based on this response.

3.7.1 Requirements and concept performance grading

Desires from engineers at Volvo Cars are presented in this section. They are not weighted against each other more than their relative importance on a high to low scale. The performance of each concept is judged based on their metric value (see Equation 3.5 and 3.3) and their reduction of time. A parameter called *Squeak &*

Rattle to time ratio, mean metric was constructed that weighs the mean metric value to the reduction in time. This parameter is defined as an average of the mean squeak metric ratio and the mean rattle metric ratio, multiplied by time. This is to easier compare the metric values to the reduction in time. It is therefore an important evaluation parameter, where a low value here is desired as on all other evaluation parameters. Furthermore, the new signal should have a comparable count of Squeak & Rattle events. This number proved however to have somewhat linear tendencies with the reduction in time, as there is very many events in one signal and many are disregarded when constructing a new signal. This desire therefore had to be given a lower priority to allow a shorter new signal.

Secondly, their similarity to the original signal in frequency domain is checked. These are the main parameters that concepts should be evaluated against, according to the project objective. The performance of each concept compared to the original signal is presented in result tables such as Table 3.8. Here, the relative importance of each evaluation parameter is presented. The *Squeak & Rattle to time ratio, mean metric* has a higher importance than others as it accounts for both the metric quality and reduction in time. The *99:th percentile metric*, *Mean metric rattle/squeak* and *New signal length factor* is given moderate importance. *Number of events* and *Total event time* is given low importance with the motivation above and input from Volvo Cars. The numerical values of these performance metrics are presented a relative value, and is calculated by comparing the average metric value of each E-point in the new versus old signal response, and then taking the average of that relative value over all E-points and all road tracks.

Based on these performance metrics, it is relatively evident what concept is the best for the first concept iteration. For the final decision from the later iterations, a more thorough investigation has been done under Section 4.1.3.

3.7.2 First Iteration

The first iteration was created by shifting between high and low values for the parameters of interest to find what is optimal. In one experiment, *Min time Keep*, was set to 200ms as a test. Each concept was run in NASTRAN and compared to previous simulations of the original signal to find the difference. The same virtual geometric model of a Car A instrument panel were used in all simulations. The old signals used to create new signals are based on responses from the IP-rig. The new concepts are acceleration signals of the IP's A-pillar attachment points, for the IP-rig as well as the seat rail accelerations. Moreover, this is done for the CAE simulations. In Table 3.5, the tested parameters are presented. In concept C5 the *Min Time Keep* parameter is set to 200ms in hard code, instead of using a factor.

Table 3.5: Concept testing v1

Concept	**C1**	**C2**	**C3**	**C4**	**C5**
Percentile	90	90	90	90	90
Pause Period	5	5	1	10	3
Ramp Up Factor	10	1	1	1	1
Max Diff Time	1.1	1.1	1.1	1.1	1.1
Min Time Keep	3	3	3	3	200ms

In Figure 3.34 the first set of parameters applied to Ucklum can be seen. Starting from left to right is concept one to five, with a pause of zeroes in between each.

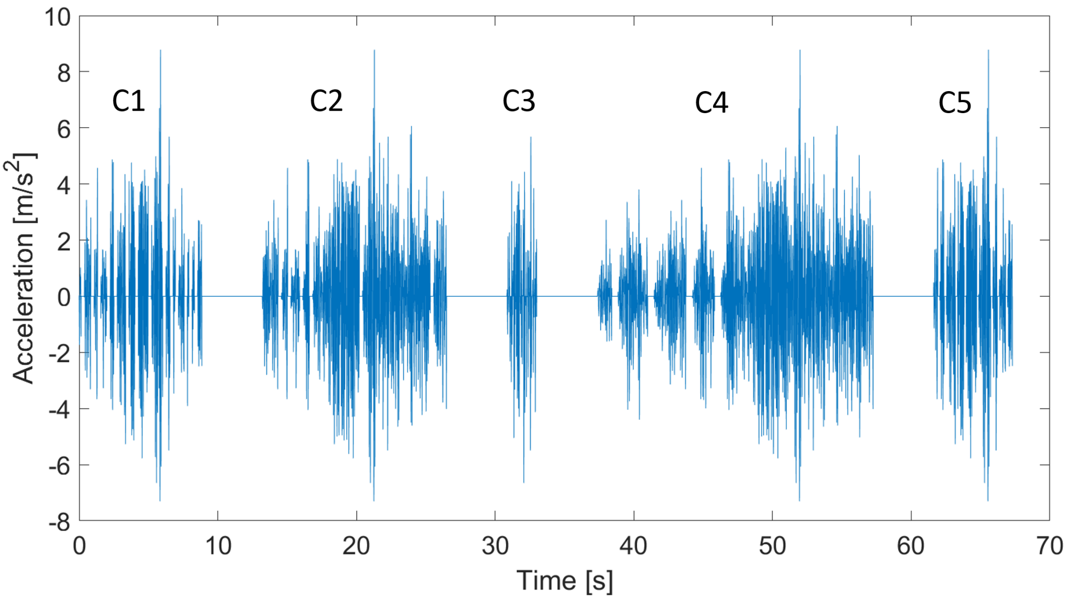

Figure 3.34: First concept iteration visualized, Ucklum signal, A-pillar left excitation, IP-rig.

These new signals was firstly tested in CAE to get an approximate result and see which concept would perform the best. These new concepts were sent to the IP-rig as well, to confirm that the simulations gave a result that could be trusted. The simulations done used a linear model, while the effects of the studied parameters may be in the nonlinear region. This may cause the large difference in results that is observed. The physical testing proved that the CAE result could not be used, as the ranking between concepts was very different in the physical testing, see Table 3.6. It is possible that it may have been possible to use CAE if only the positions that gave a good representation (see Section 3.4) were used. The physical testing in the IP-rig is trusted more than the CAE simulations. Since the IP-rig was available at the time of iterating concepts, the testing after this was done there, while no additional CAE simulations were done.

Table 3.6: Result CAE, first concept iteration, mean metric rattle, Car A

Metric evaluation for rattle (CAE)						
		Concept Value				
Track	Old value	C1	C2	C3	C4	C5
Bardfield	-8.01	-3.28	-4.80	-3.99	-4.80	-3.53
Manhole	-10.11	-3.35	-4.48	-0.79	-3.97	-3.21
Pave DRV	-11.96	-8.70	-7.64	-4.07	-6.33	-9.09
Pave TT	-38.65	-22.03	-18.34	-15.91	-15.51	-21.76
Ucklum	-8.25	-5.01	-5.27	-6.74	-4.20	-6.24
Vienna HPG	-6.41	-4.85	-5.52	-11.79	-5.63	-5.42
Vienna TT	-11.44	-4.21	-4.03	-7.55	-3.87	-4.11
Washboard 1	-0.78	-0.40	-0.44	-0.00	-0.56	-0.41
		New value relative old				
Bardfield		2.21	1.62	1.88	1.63	2.07
Manhole		2.57	2.04	8.48	2.24	2.45
Pave DRV		1.36	1.48	2.55	1.75	1.33
Pave TT		1.81	2.16	2.33	2.48	1.79
Ucklum		1.68	1.55	1.60	1.83	1.49
Vienna HPG		1.43	1.19	2.25	1.15	1.28
Vienna TT		2.46	2.59	1.46	2.66	2.50
Washboard 1		1.86	1.70	10.00	1.42	1.79
Result metric evaluation		1.92	1.79	3.82	1.89	1.84

Table 3.7 presents the test result for the rattle mean metric. The same method is applied to squeak as well. In the upper part of the table the mean metric average over all E-points is presented as a single value for each concept and road track. If a result is *NaN*, the signal does not cause any squeak or rattle. This is not desirable, although acceptable if not occurring on multiple tracks. In rare cases, some ratio might be extremely high, resulting in one track having the possibility to distort the overall concept rating. To mitigate this effect, a limit for the max ratio of one individual track were set slightly above the "naturally" highest values, in Table 3.6 this limit is set to 10. The lower part of the table compiles the relative value of the synthesized signal to the original signal. The relative value is calculated by comparing the average metric value of each E-point in the new versus old signal response, and then taking the average of that relative value over all E-points. This gives a single relative value for each concept and road track, as is seen in the lower part of the table. For the relative values, the numbers are inverted if it is below 1. This implies that a larger number does not mean that the new signal has a higher value, but only presents the factor between them. The purpose of this is if these numbers are used in a formula for evaluation, a concept should not get a good result if it has one high metric and one low that counteracts each others influence on the final grading.

Table 3.7: Result IP-rig, first concept iteration, mean metric rattle, Car A

Metric evaluation for rattle						
		Concept Value				
Track	Old value	C1	C2	C3	C4	C5
Bardfield	-0.59	-0.86	-0.83	-0.88	-0.84	-1.00
Manhole	-0.65	-1.36	-0.99	-0.24	-0.96	-1.53
Pave DRV	-0.68	-1.29	-1.23	-1.42	-1.10	-1.47
Pave TT	-1.17	-1.37	-1.27	-1.11	-1.36	-1.59
Ucklum	-0.70	-1.04	-1.18	-1.08	-1.11	-1.14
Vienna HPG	-0.10	-0.18	-0.19	-0.20	-0.18	-0.20
Vienna TT	-0.27	-0.41	-0.41	-0.37	-0.39	-0.43
Washboard 1	-0.22	-0.21	-0.25	NaN	-0.19	-0.20
Washboard 2	-0.45	-0.64	-0.73	-0.94	-0.66	-0.70
		New value relative old				
Bardfield		2.68	2.96	2.67	3.11	3.13
Manhole		3.09	2.82	1.49	3.14	3.59
Pave DRV		3.49	3.18	3.69	2.71	3.76
Pave TT		3.13	4.38	2.14	4.40	3.52
Ucklum		2.80	3.03	2.95	2.81	3.36
Vienna HPG		4.59	4.28	4.42	4.20	5.77
Vienna TT		3.96	4.92	3.17	4.64	4.24
Washboard 1		1.58	1.61	NaN	1.56	1.53
Washboard 2		3.16	3.29	3.82	3.31	3.15
Result metric evaluation		3.17	3.38	3.04	3.32	3.56

The result from these first concepts are summarized in Table 3.8. All of these numbers display a relative difference factor between the new and old signal. Only the time result is shown as values below one, to in a simple manner show the shortening result in time. Based on the result presented in Table 3.8 concept C3 is selected as a basis for further iterations. This decision is based on that the difference in metric is low compared to the large reduction in time, in the IP-rig result.

Table 3.8: Relative results IP-rig, first concept iteration, rattle evaluation, Car A

	Importance	**Rel. diff. to original**				
Concept	-	C1	C2	C3	C4	C5
Mean metric rattle	Moderate	3.17	3.38	3.04	3.32	3.56
New signal length factor	Moderate	0.36	0.55	0.09	0.70	0.25
S&R to time ratio, mean metric	Higher	1.29	2.06	0.30	2.53	0.99
99:th percentile metric	Moderate	4.07	5.43	3.24	4.98	4.42
Number of events	Lower	2.23	2.12	6.81	2.03	2.66
Total event time	Lower	3.99	3.38	6.91	3.49	3.89

3.7.3 Second iteration

Concept three was kept equal while parameters were tweaked, creating signals similar to concept three. These new parameters are presented in Table 3.9. These signals are also created from IP-rig responses and later concepts were tested in the same rig. The numbering of these concepts continue from number five, as that was the number of concepts in the first iteration, while concept three is kept equal with the same numbering. Notice in the result that concept three is very close in this second iteration to the result in the first, but not exactly the same as physical tests vary slightly each time.

Table 3.9: Concept testing, iteration 2, in IP-rig

Concept	**C6**	**C7**	**C3**	**C8**	**C9**	**C10**
Percentile	80	99	90	90	80	90
Pause Period	1	0	1	0	0	0
Ramp Up Factor	1	1	1	1	1	1
Max Diff Time	1.1	1.1	1.1	97ms*	1.1	200ms
Min Time Keep	3	100	3	32ms*	3	100ms
*Same time duration as in concept three						

In Figure 3.35 the second set of parameters applied to Ucklum can be seen. Starting from left to right is concept six to ten, with a pause of zero acceleration in between each. Concept three is the same as in Figure 3.34.

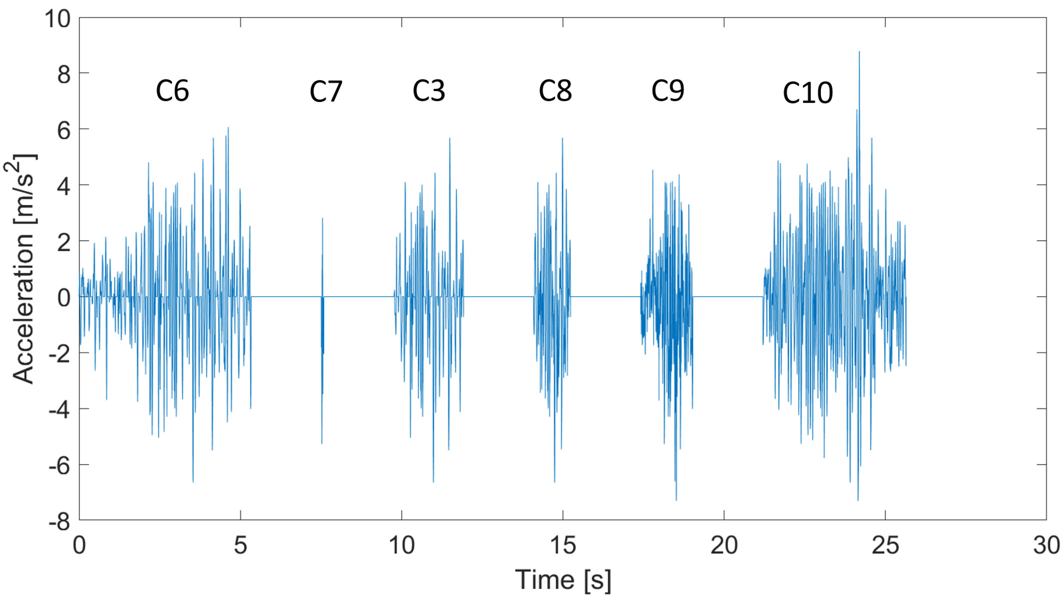

Figure 3.35: Second concept iteration visualized, Ucklum signal, A-pillar left excitation.

In Table 3.10 the mean metric result for rattle is presented. Notice that the performance of concept C3 is very similar here to concept C3 in Table 3.7, as the excitation signal for this concept is the same. Some slight difference is because of IP-rig variances and a slight response randomness.

Table 3.10: Result IP-rig, second concept iteration, mean metric rattle, Car A

Metric evaluation for rattle							
		Concept Value					
Track	Old value	C6	C7	C3	C8	C9	C10
Bardfield	-0.59	-0.74	-0.48	-0.88	-0.86	-0.65	-0.97
Manhole	-0.65	-0.95	NaN	-0.25	-0.66	-1.09	-1.22
Pave DRV	-0.68	-1.17	-0.82	-1.56	-2.60	-1.00	-1.55
Pave TT	-1.17	-1.44	-0.05	-1.17	-1.29	-1.02	-1.51
Ucklum	-0.70	-0.95	-0.03	-1.10	-1.81	-0.93	-1.31
Vienna HPG	-0.10	-0.22	-0.00	-0.20	-0.25	-0.19	-0.23
Vienna TT	-0.27	-0.41	-0.33	-0.37	-0.46	-0.31	-0.50
Washboard 1	-0.22	-0.01	NaN	NaN	NaN	-0.01	-0.19
Washboard 2	-0.45	-0.76	-0.00	-0.95	-0.74	-0.40	-0.75
		New value relative old					
Bardfield		2.49	1.86	2.75	3.64	3.06	3.73
Manhole		2.34	NaN	1.53	2.11	3.54	2.82
Pave DRV		2.39	2.73	3.20	3.89	2.79	3.71
Pave TT		2.61	1.34	2.09	2.17	2.06	2.77
Ucklum		2.61	1.57	3.08	3.46	3.75	3.73
Vienna HPG		5.96	2.58	4.94	6.79	3.42	7.47
Vienna TT		3.64	1.71	3.23	5.07	1.79	5.00
Washboard 1		1.15	NaN	NaN	NaN	1.74	1.89
Washboard 2		3.31	1.65	4.02	4.08	4.93	4.01
Result metric evaluation		2.95	1.92	3.10	3.90	3.01	3.90

Similar to the first results, these second results are presented in a similar way in Table 3.11. Concept C7 has a high value in *number of events* and *total event time* since it is extremely short and has almost no events at all, making this difference factor very large. The average number of events in the original signals are 167 on all tracks and E-points, and in the signals generated by concept C7 that number is 0,52. This means that there is not even one event in many E-points. Due to the extraordinarily few events for concept C7, this concept is not further developed. The reason the mean metric rattle has a low value here at 1,92 may be because there is very few events to calculate an average from. This value may change significantly if the test is repeated.

Table 3.11: Relative results IP-rig, second concept iteration, rattle evaluation, Car A.

	Importance	**Relative difference to original**					
Concept	-	C6	C7	C3	C8	C9	C10
Mean metric rattle	Moderate	2.95	1.92	3.10	3.90	3.01	3.90
New signal length factor	Moderate	0.19	0.00	0.09	0.05	0.05	0.20
S&R to time ratio	Higher	0.63	0.01	0.30	0.23	0.15	0.83
99:th percentile metric	Moderate	3.19	2.72	3.14	3.76	2.90	4.16
Number of events	Lower	7.86	219.03	7.19	10.59	12.96	2.68
Total event time	Lower	31.64	425.82	6.57	9.34	33.94	3.62

From Table 3.11 it is apparent that the most promising concepts are concept C3, C8, and C9, with their low Squeak & Rattle metric to time ratio.

3.7.4 Third iteration

For the final iteration the three best concepts were chosen from the second one. This iteration is the concepts being sent to the FP-rig for verification, with one additional concept. Concept C11, with a larger ramp-up duration factor was introduced as it was uncertain whether there is a delay from exciting the wheels, to a response appears in the instrument panel in the rig. The additional ramp-up duration would also reduce the effect of improperly synchronized time signals. The synchronization time problem is discussed further in Section 5.4. However, this resulted in a significantly longer signal than the other concepts. In this iteration step, new files are being worked with; IP-responses from the FP-rig are used to cut spindle accelerations rather than IP-responses being used to cut IP attachment A-pillar accelerations in the IP-rig as in iteration one and two.

Table 3.12: Concept testing, iteration 3, in FP-rig

Concept	**C11**	**C3**	**C8**	**C9**
Percentile	90	90	90	80
Pause Period	1	1	0	0
Ramp Up Factor	0,1	1	1	1
Max Diff Time	1.1	1.1	97ms*	1.1
Min Time Keep	3	3	32ms*	3
*=Same length as in concept three				

In Figure 3.36, the third set of parameters applied to Ucklum can be seen. Starting from left to right is concept C11, C3, C8 and C9, with a pause of zero acceleration in between each. Concept C3 here is created with the same parameters as before, but for wheel accelerations rather than A-pillar accelerations. It can be seen that the amplitude of the signals is significantly higher in these concepts as they are for the spindle accelerations rather than A-pillar accelerations. This is is essentially because these spindle accelerations is occurring upstream the car suspension.

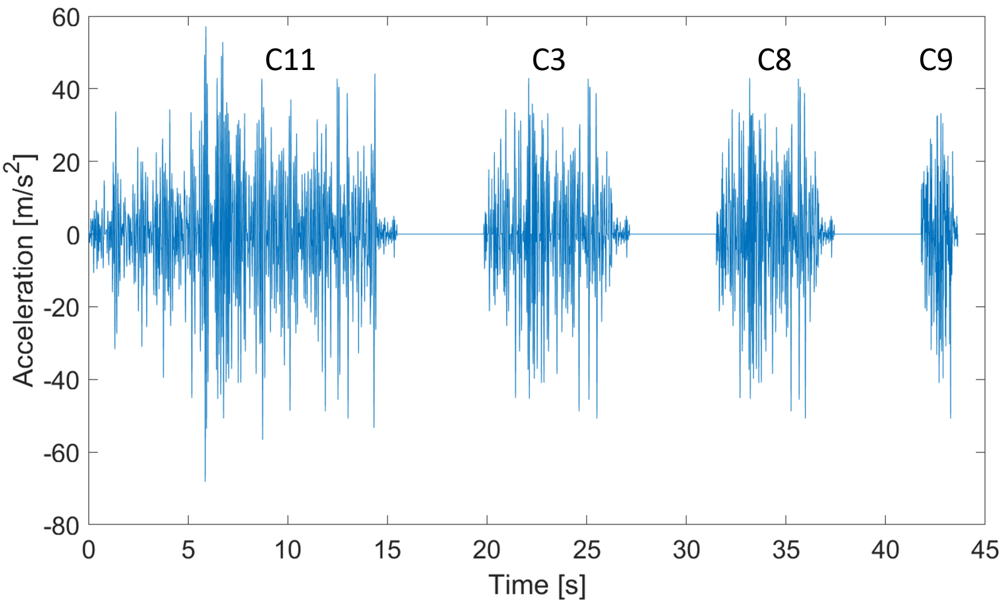

Figure 3.36: Third concept iteration visualized, Ucklum signal, Left front spindle excitation.

The testing of these signals are the last physical measurements done in this project. The result of these are presented in Chapter 4.

3.7.5 Alternative method of shortening the excitation signals

The same metric evaluation method as described for Table 3.7 was done for a method based on frequency domain characteristics of the signal. The previous shortening methodology is based on squeak and rattle events occurring in time domain. The alternative method is in short, transforming the excitation signal from time domain to frequency domain. From the frequency domain, an upper envelope can be formed, that is downsampled by a specified factor. This downsampled upper envelope is thereafter transformed back, into time domain, and the synthesized excitation signal, based on frequency domain characteristics is created. When transforming the signal from frequency domain back to time domain, a random phase was added to the signal. Figure 3.37 displays how an envelope in frequency domain is formed. It is simply formed by constructing a curve tangenting to all the maximal values of the signal. The upper envelope is tangenting to all of the curves higher values, whereas the lower envelope is tangenting to all of the lower values of the signal. Six different concepts were developed for shortening based on frequency domain. Each concept had a specified downsampling factor and were for two of the six concepts repeated in time sequence. For example, concept 1 and 2 have the same total signal length, although concept 1 is downsampled by 9 and repeated twice thereby constituting 3 instances, whereas concept 2 is downsampled by 3 and not repeated. For these concepts with multiple repetitions, the signal was repeated using different phases for the IFFT transformation. The parameters used for these developed concepts is presented in Table 3.13.

The frequency domain method of shortening proved to not work very well since the amplitude got very high with this method. The acceleration amplitude were for some signals exceeding $20m/s^2$ which the IP-rig could not handle. However, in virtual simulation this high amplitude did not pose a problem. When analysing the Squeak & Rattle metric for these shortened signals, the performance was not favourable since these signals were very rough compared to the originally measured signal. It is possible that the method could be improved and further developed until it is possible to use it shorten the signal in frequency domain, but there was insufficient time to investigate it in this project.

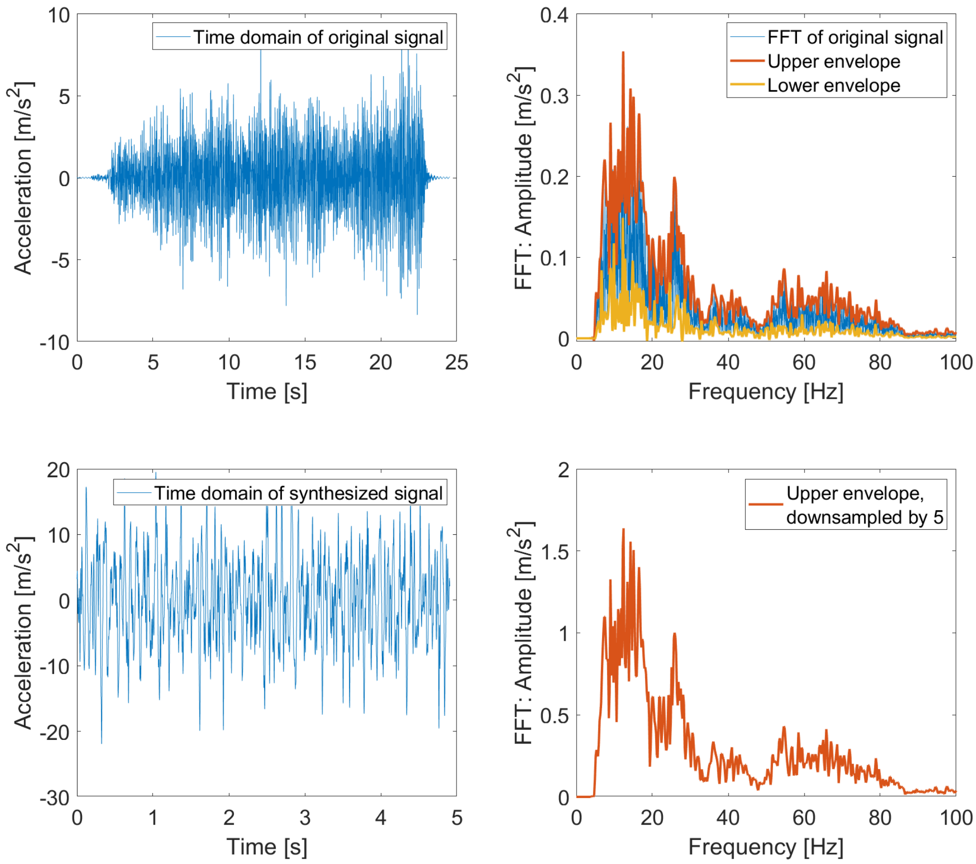

Figure 3.37: Signal synthesizing based on downsampling the envelope in frequency domain.

Table 3.13: Concept testing, based on frequency domain

Concept	**1**	**2**	**3**	**4**	**5**	**6**
Downsampling	9	3	4	2	5	10
Repeated instances	3	1	2	1	1	1

4
Results

The selection of the most optimal concept is based on the physical testing done to the third concept iteration. Part of the results from the testing is presented in Table 4.1, 4.2, 4.4 and 4.3. Here the number of events and mean metric evaluation is presented respectively. All of these tables are presenting and have been developed with averages for all E-points on each track. The method used to generate these tables are the same as for Table 3.7. Table 4.5 and 4.6 present a summary of Table 4.1, 4.2, 4.4 and 4.3, along with other results.

Table 4.1: Result FP-rig, third concept iteration, number of Rattle events, Car A

Number of Rattle events					
		Concept Value			
Track	**Old value**	C11	C3	C8	C9
Bardfield	232.83	182.83	60.33	49.33	12.67
Manhole	31.67	27.33	7.83	4.83	2.00
Pave DRV	108.33	83.67	34.67	28.83	8.33
Ucklum	115.33	70.67	27.33	24.17	8.33
Vienna HPG	145.00	163.50	51.33	46.83	10.67
		New value relative old			
Bardfield		1.65	4.84	6.17	26.42
Manhole		1.30	9.20	5.55	13.17
Pave DRV		1.87	3.68	4.28	17.34
Ucklum		1.95	7.30	6.00	36.13
Vienna HPG		1.72	3.60	3.82	16.07
Result number of events		**1.70**	**5.72**	**5.16**	**21.83**

Table 4.2: Result FP-rig, third concept iteration, metric evaluation Rattle, Car A

Metric evaluation for Rattle					
		Concept Value			
Track	**Old value**	C11	C3	C8	C9
Bardfield	-0.18	-0.26	-0.27	-0.33	-0.25
Manhole	-0.11	-0.13	-0.09	-0.20	-0.19
Pave DRV	-0.16	-0.23	-0.23	-0.26	-0.22
Ucklum	-0.16	-0.26	-0.23	-0.22	-0.32
Vienna HPG	-0.01	-0.02	-0.03	-0.03	-0.02
		New value relative old			
Bardfield		1.74	1.71	2.06	2.39
Manhole		1.72	2.04	1.81	2.10
Pave DRV		1.76	1.68	1.93	1.80
Ucklum		1.78	1.62	1.71	2.19
Vienna HPG		2.19	2.96	2.80	2.81
Result metric evaluation		**1.84**	**2.00**	**2.06**	**2.26**

Table 4.3: Result FP-rig, third concept iteration, number of squeak events, Car A

Number of events squeak					
		Concept Value			
Track	**Old value**	C11	C3	C8	C9
Bardfield	281.00	154.17	50.83	50.00	11.17
Manhole	40.83	23.00	4.83	5.50	2.17
Pave DRV	142.50	69.50	32.00	32.17	6.00
Ucklum	147.33	71.33	23.00	21.50	8.83
Vienna HPG	148.67	112.83	55.50	50.50	13.83
		New value relative old			
Bardfield		6.76	20.91	17.41	12.61
Manhole		10.07	4.87	7.04	10.03
Pave DRV		15.33	3.83	48.28	18.07
Ucklum		26.08	7.38	20.23	36.50
Vienna HPG		4.01	4.94	5.74	17.09
Result number of events		**12.45**	**8.39**	**19.74**	**18.86**

Table 4.4: Result FP-rig, third concept iteration, metric evaluation, Car A

Metric evaluation for squeak					
		Concept Value			
Track	**Old value**	C11	C3	C8	C9
Bardfield	-0.04	-0.05	-0.04	-0.03	-0.00
Manhole	-0.02	-0.02	-0.00	-0.01	-0.03
Pave DRV	-0.03	-0.05	-0.09	-0.07	-0.09
Ucklum	-0.04	-0.03	-0.02	-0.05	-0.04
Vienna HPG	-0.00	-0.00	-0.00	-0.00	-0.00
		New value relative old			
Bardfield		1.51	1.47	3.32	1.44
Manhole		1.48	4.25	1.89	1.82
Pave DRV		1.27	1.56	1.34	1.99
Ucklum		1.91	1.80	1.67	2.72
Vienna HPG		2.45	2.42	2.30	3.38
Result metric evaluation		**1.72**	**2.30**	**2.10**	**2.27**

Some comparisons that are interesting for evaluation purposes are presented in Table 4.5 and Table 4.6. They present general results for squeak and rattle separately. These numbers are developed with the same method, although showing averages for all tracks to further condense the tables. The numbers that are presented are a ratio indicating how different the new signals are compared to the old, on a specific parameter and concept. The construction of the tables are described more in Section 3.7.2.

Table 4.5: Result FP-rig, third concept iteration, rattle evaluation, Car A

	Importance	**Rel. diff. to original**			
Concept	-	C11	C3	C8	C9
Mean metric rattle	Moderate	1.84	2.00	2.06	2.26
New signal length factor	Moderate	0.64	0.24	0.19	0.05
S&R to time ratio, mean metric	Higher	1.14	0.51	0.40	0.12
99:th percentile metric	Moderate	2.71	3.36	2.57	3.20
Number of events	Lower	1.70	5.72	5.16	21.83
Total event time	Lower	2.08	5.70	4.01	15.46

Table 4.6: Result FP-rig, third concept iteration, squeak evaluation, Car A

	Importance	**Rel. diff. to original**			
Concept	-	C11	C3	C8	C9
Mean metric squeak	Moderate	1.72	2.30	2.10	2.27
New signal length factor	Moderate	0.64	0.24	0.19	0.05
S&R to time ratio, mean metric	Higher	1.14	0.51	0.40	0.12
99:th percentile metric	Moderate	2.78	5.73	3.78	5.25
Number of events	Lower	12.45	8.39	19.74	18.86
Total event time	Lower	31.46	9.73	42.36	59.03

From Table 4.5 and 4.6, it can be seen that concept C11, which was concept C3 with longer ramp-up duration, resulted in a signal where the Squeak & Rattle mean metric were better, although the signal length were significantly higher than for other concepts. The Squeak & Rattle to time ratio thus became more than double to that of C3 or C8.

4.1 The optimal concept

The concept with the most favourable performance is presented with motivation why in this section. The performance accounts for both squeak and rattle, more specifically, the mean metric, 99th percentile metric, the tendency to underestimate or overestimate the original signal metric and the number of events for the response signals. The total signal time and frequency domain content of the excitation signals are also included in the performance assessment.

4.1.1 Underestimate and overestimate metric in the FP-rig

The metric evaluation tables are not considering if the synthesized signal is exceeding the metric of the original signal or if it assumes a lower value. To further evaluate the generated concept signals, Table 4.7 presents the occurrence and percentage amount for the metric to exceed the old signal values (referred to as overestimate) or if the the metric is not achieving the same magnitude of the metric as the old signal (referred to as underestimate). The occurrence is calculated as how many of the E-Points get an underestimate/overestimate in relation to the maximally possible. The percentage amount of underestimate/overestimate is calculated as how many percent below or above the metric of synthesized signal is from the original signal. Both the occurrence and percentage amount includes all tracks into the calculations. Besides, the underestimate/overestimate is calculated with the mean of event-factor-vector and the 99th percentile of the event-factor-vector. The event-factor-vector is the vector of event severities, calculated as in Eq. 3.3 and Eq. 3.5. The number of elements in the event-factor-vector is thus the same as the signals sampling rate multiplied by the total signal time. Table 4.8 present similar results for the IP-rig. The reason a concept can result in both underestimation and overestimation is because several tracks and E-Points are assessed. Thus, for a certain road track, two E-Points can show underestimation and three E-Points show overestimation. For another track, it could be one E-Point showing underestimation and four E-Points showing overestimation.

Table 4.7: Underestimate/overestimate for mean of factor and for 99th percentile of factor. All numbers are in percent (%). FP-rig.

	Mean of factor Concept values			**99th perc of factor Concept values**		
Underestimate/Overestimate	C3	C8	C9	C3	C8	C9
Underestimate squeak occurrence	32	40	40	52	52	48
Underestimate squeak percentage	54	47	49	59	62	66
Overestimate squeak occurrence	32	36	24	16	24	16
Overestimate squeak percentage	68	71	122	144	112	95
Underestimate rattle occurrence	40	24	28	44	40	40
Underestimate rattle percentage	37	40	41	57	50	63
Overestimate rattle occurrence	60	72	68	56	56	56
Overestimate rattle percentage	107	117	132	125	156	129

Table 4.8: Underestimate/Overestimate for Mean of factor and for 99th percentile of factor. All numbers are in percent (%). IP-rig.

	Mean of factor Concept values			**99th perc of factor Concept values**		
Underestimate/Overestimate	C3	C8	C9	C3	C8	C9
Underestimate squeak occurrence	4	4	13	18	16	27
Underestimate squeak percentage	35	40	31	33	39	41
Overestimate squeak occurrence	82	84	76	69	73	62
Overestimate squeak percentage	252	378	241	311	413	222
Underestimate rattle occurrence	9	2	7	11	7	13
Underestimate rattle percentage	26	1	14	44	19	28
Overestimate rattle occurrence	80	87	87	76	82	80
Overestimate rattle percentage	227	298	225	232	296	223

4.1.2 Frequency domain comparison of concepts in FP-rig

While the metric used is the primary evaluation tool for selecting the final concept, studying the frequency domain is also important. It can be regarded as a check to ensure that the frequency content is not too different from the original signal. For analysing the difference in frequency content, FFT has been applied to a time domain signal, including all tracks concatenated in sequence, as in Figure 4.1.

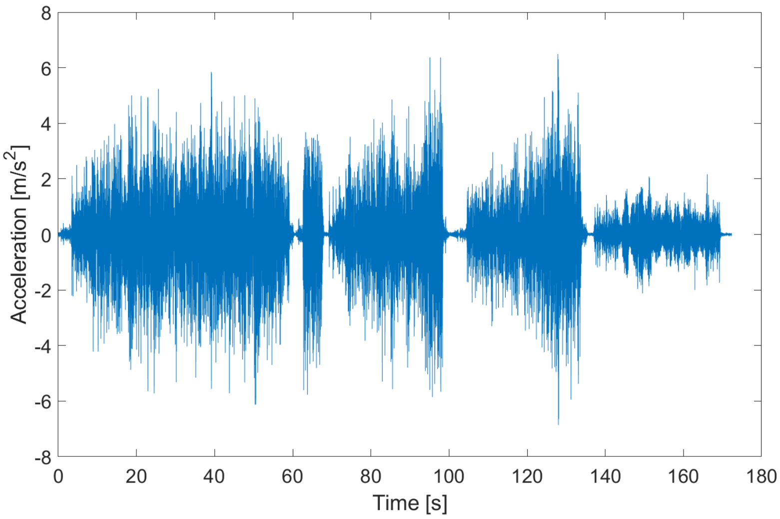

Figure 4.1: All tracks signals is concatenated in sequence. Time domain of IP-A-pillar right in Z-direction of original signal in FP-rig test for Car A.

The original signals frequency content for the IP-attachment on the right side in the FP-rig can be seen in Figure 4.2. Plots for the concepts are presented in Figure 4.3. From these plots, it can be seen that concept C11, C3 and C8 have similar shape to the original signal although the amplitude is higher. C11, C3 and C8 all capture the frequency peaks of around 5 Hz, 13Hz and 18Hz. Concept C9 on the other hand does not get the 18 Hz peak in frequency, while the 5Hz peak is amplified and a peak of around 27 Hz emerges.

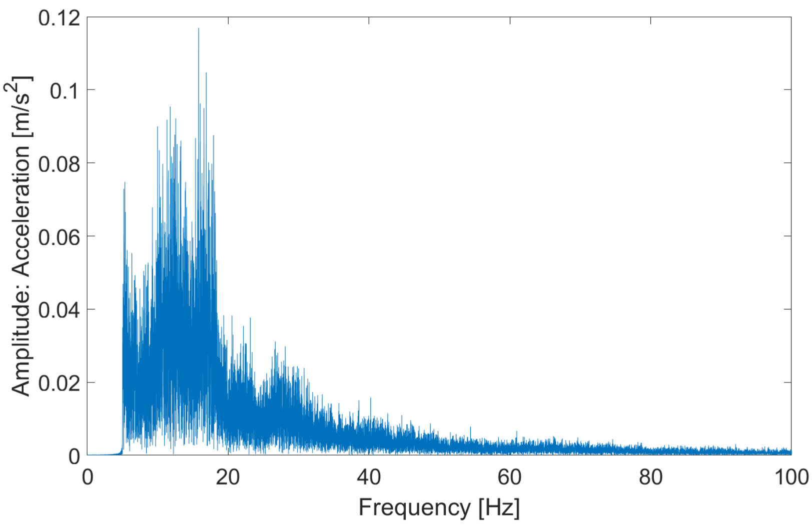

Figure 4.2: Frequency domain of IP-A-pillar right in Z-direction of original signal in FP-rig test for Car A.

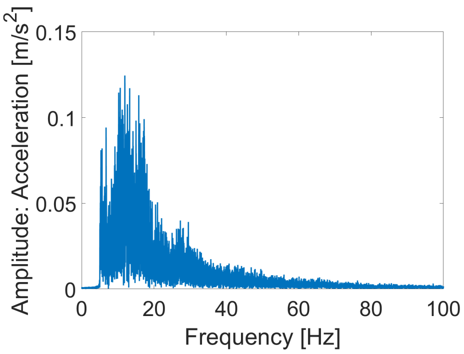

(a) Frequency domain, FP-rig, concept C11

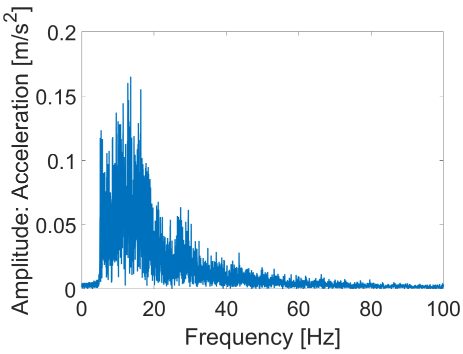

(b) Frequency domain, FP-rig, concept C3

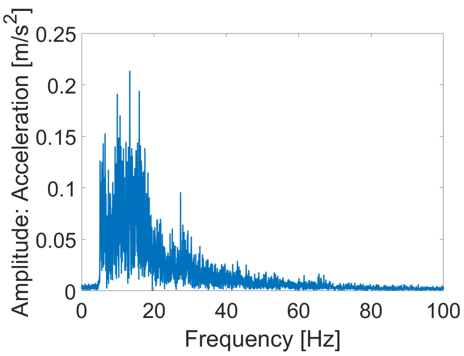

(c) Frequency domain, FP-rig, concept C8

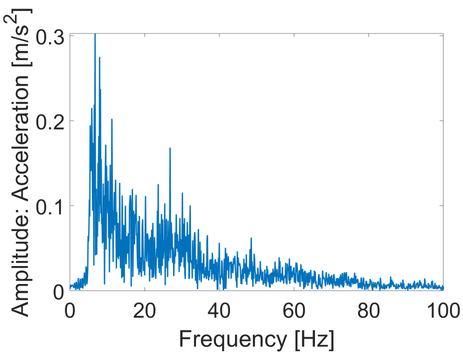

(d) Frequency domain, FP-rig, concept C9

Figure 4.3: Frequency domain content of synthesized acceleration signals, concept C11, C3, C8, and C9. In FP-rig and measured at IP A-pillar attachment in Z-direction.

The same comparison can be done with the excitation signals in the FP-rig, see Figure 4.4 for the original signals excitation signal for right front spindle acceleration. Figure 4.5 shows the the four concepts excitation signal for right front spindle acceleration. As for the IP-attachment on the right side, C11, C3 and C8 have similar frequency content as the original excitation signal, with a peak of around 13 Hz. In contrast, concept C9 achieves a different frequency composition without the clear peak of around 13 Hz.

For comparison in frequency domain content of the excitation signals in the IP-rig, see Appendix D.

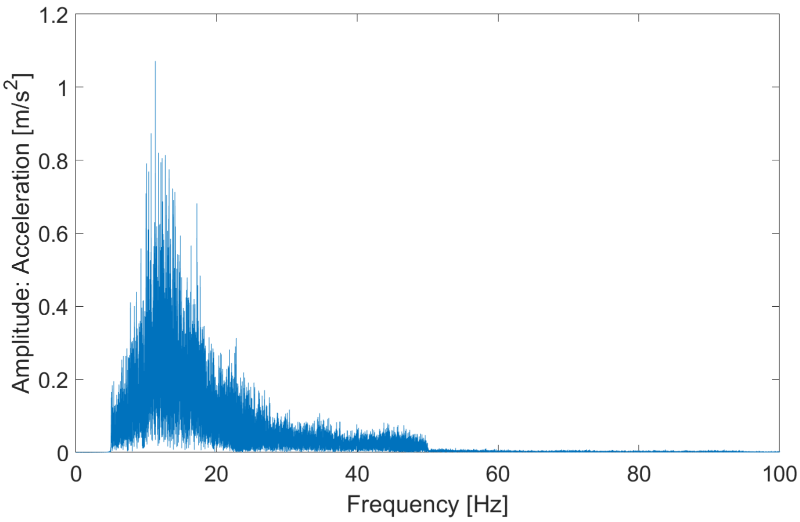

Figure 4.4: Frequency domain of right front wheel spindle in Z-direction of original signal in FP-rig test for Car A.

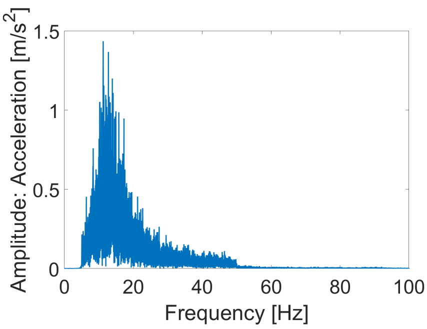

(a) Frequency domain, FP-rig, concept C11

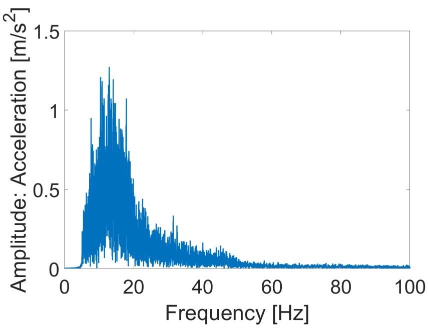

(b) Frequency domain, FP-rig, concept C3

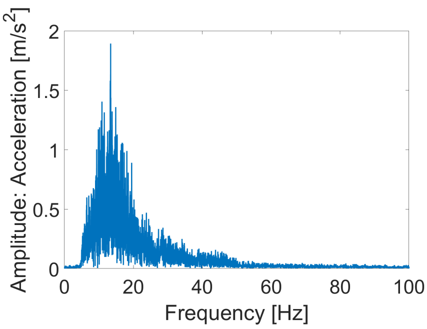

(c) Frequency domain, FP-rig, concept C8

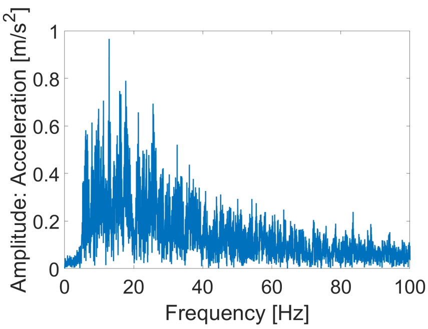

(d) Frequency domain, FP-rig, concept C9

Figure 4.5: Frequency domain content of synthesized acceleration signals, concept C11, C3, C8 and C9. In FP-rig and positioned at right front wheel spindle in Z-direction.

4.1.3 Selection of optimal concept

From Section 3.7.3, based on the IP-rig tests, it was clear that C3, C8 and C9 were most promising due to their low Squeak & Rattle metric to time ratio. By testing the same concepts in the FP-rig, it was assessed that concept C9 did not achieve a sufficiently similar shape in frequency domain, compared to the unshortened excitation signal. If the requirement of similar frequency domain shape would have a very low priority, Concept C9 might be worth to further look into, since the Squeak & Rattle metric to time ratio was remarkably low. Concept C11, which was C3 with longer ramp-up duration, resulted in a signal where the Squeak & Rattle metric were better but the signal length was significantly higher than for other concepts (see Table 4.9). The Squeak & Rattle to time ratio thus became more than double that of C3 or C8 which resulted in disregarding this concept. Therefore, concept C3 and C8 is regarded as the optimal concepts based on the testing done in this project. Additional testing could nevertheless result in even better concepts.

In Table 4.5 and Table 4.6 it can be seen that Concept C3 has in the IP-rig testing better metric values for mean metric, 99th percentile metric, number of events, total time of events for both squeak and rattle evaluation. C8 has shorter total signal time, a reduction of 95% from the original signal length, while concept C3 has a 91% reduction in time. The shorter time for concept C8 leads to a lower Squeak & Rattle metric to time ratio than C3, which favours C8. The frequency content of C3 is however slightly closer the original frequency domain shape, than C8.

By examining the underestimate/overestimate table for IP-rig testing in Table 4.8, C8 has in general more overestimate than C3, both in occurrences and percentiles, while C3 has more underestimate than C8. This difference is not visible in the metric evaluation table. An excitation signal that causes more overestimate is more rough and approaches a worst case scenario, which can be beneficial if not too extreme. The same underestimate/overestimate trend for C3 and C8 is identified in the FP-rig testing, although to a lesser extent (see Table 4.7). Besides, the difference in signal time length is greater in the IP-rig than for the FP-rig.

As a summary, concept C3 is beneficial if a more balanced metric profile and frequency content is prioritized over a greater signal time compression. If a slightly more rough excitation signal, is preferred and higher signal time compression is desired, concept C8 is the optimal choice.

4.1.4 Time domain visualisation of optimal concept

Both concept C3 and C8 have favourable parameter values for the method of shortening long excitation signals. Since the aim is to shorten the signal, concept C8 is proposed as slightly more advantageous, since it results in shorter signals with adequate Squeak & Rattle causing characteristics (see Table 4.5 and 4.6). The optimal concept and developed excitation signal will thus be presented as concept C8. The final step in the method before presenting a final excitation signal is to remove eventual drift by applying Omega Arithmetic as described in Section 2.3. In the physical verification this was done by the engineers at the test rigs.

In Figure 4.6 and 4.7 the time domain representation of the developed excitation signals is displayed for IP-rig and FP-rig.

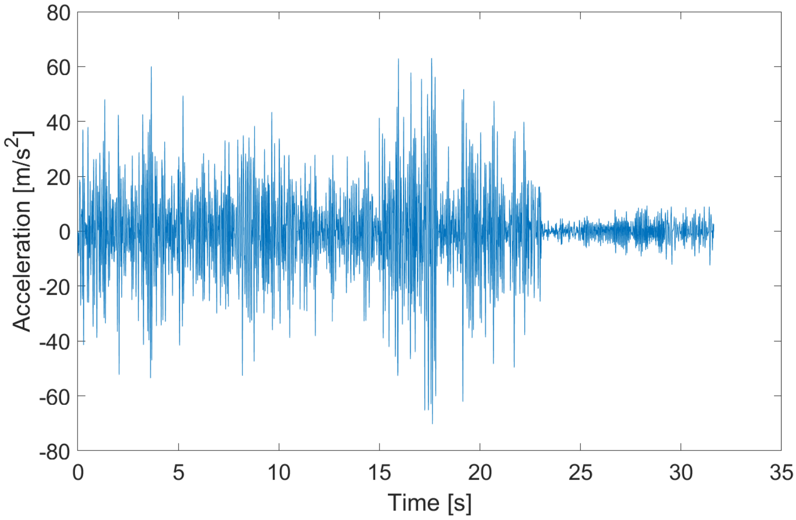

Figure 4.6: Concept C8: Time domain of the optimal excitation signal of right front wheel spindle in FP-rig test for Car A. Five tracks is included.

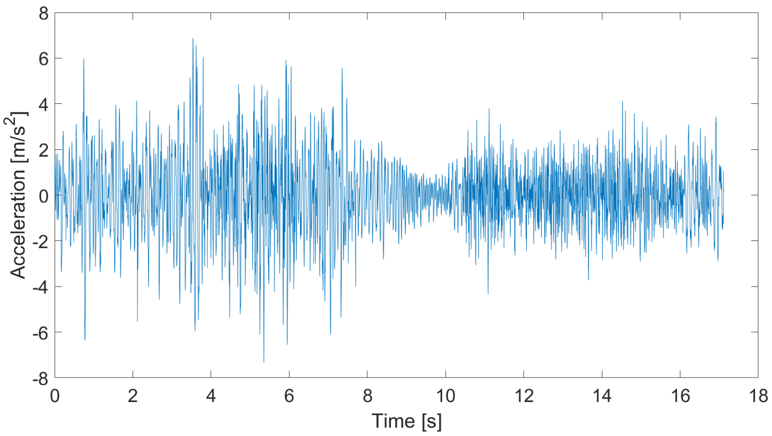

Figure 4.7: Concept C8: Time domain of the optimal excitation signal IP-rig test for Car A. Z-direction of IP A-pillar attachment left. Nine tracks is included.

Table 4.9 presents the new time for each track that is a part of concept C8. For the FP-rig not all tracks are available as previously mentioned.

Table 4.9: New time for each track for concept C8, FP-rig and IP-rig.

		Concept Value	
Track name	**Old time (s)**	**C8 FP-rig (s)**	**C8 IP-rig (s)**
Bardfield	58.44	10.89	2.54
Manhole	7.64	0.97	0.25
Pave DRV	31.62	5.96	0.67
Pave TT	24.54	N.A.	1.23
Ucklum	32.09	5.93	1.14
Vienna HPG	34.54	7.69	2.97
Vienna TT	58.45	N.A.	5.08
Washboard 1	19.06	N.A.	0.03
Washboard 2	21.22	N.A.	1.45
Average time	31.96	6.29	1.71
Average relative	100 %	19 %	5 %

4.2 Statistical data for optimal concept

In section 3.2 several statistical data were calculated in each track case and for certain acceleration directions. The same measurements have been calculated for the new developed concept C8. Since the IP-rig contained all available tracks, the data for this testing rig will be presented in Figure 4.8, 4.9, 4.10 and 4.11. Due to confidentiality the Y-axis of the plots is normalized. X- and Y-direction for the IP attachments were not recorded. Thus, the statistical measurements could not be calculated for IP-magnitude.

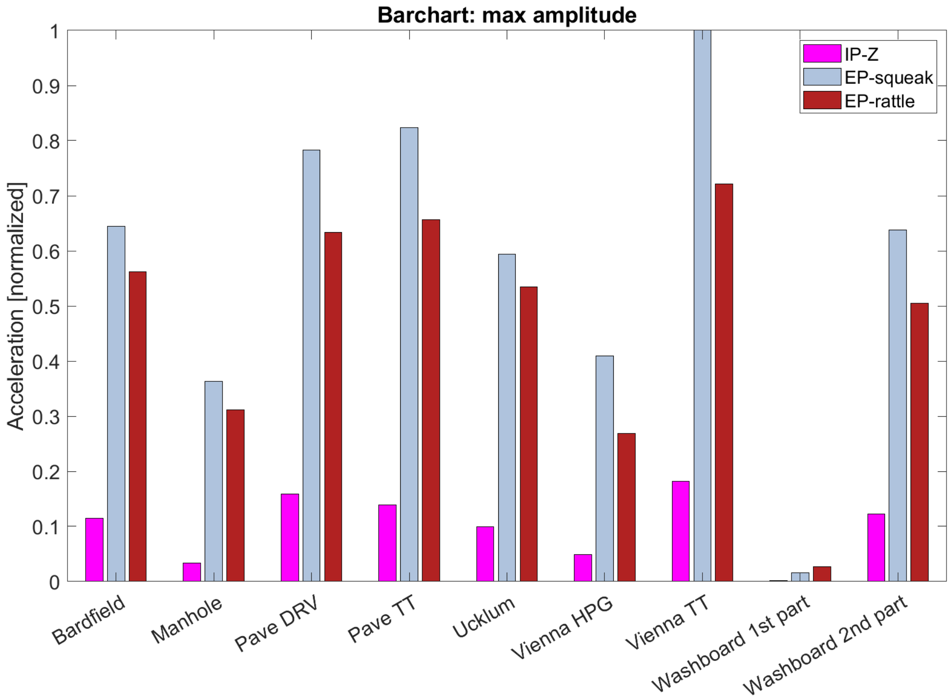

Figure 4.8: Max amplitude for each track in Car A, from IP-rig. Concept C8. Normalized Y-axis.

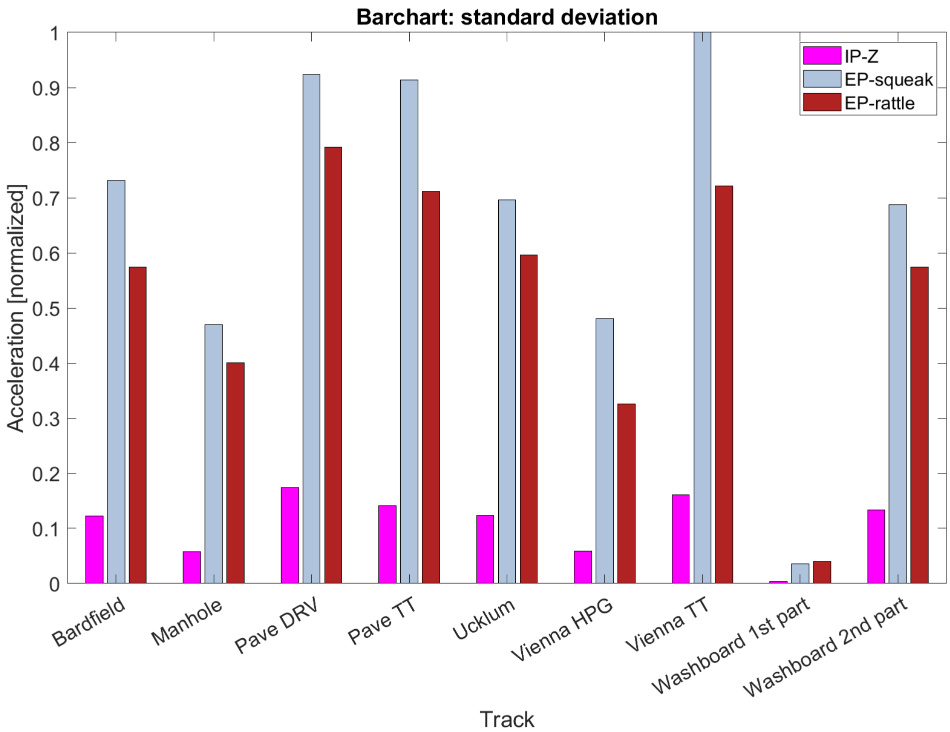

Figure 4.9: Standard deviation for each track in Car A, from IP-rig. Concept C8. Normalized Y-axis.

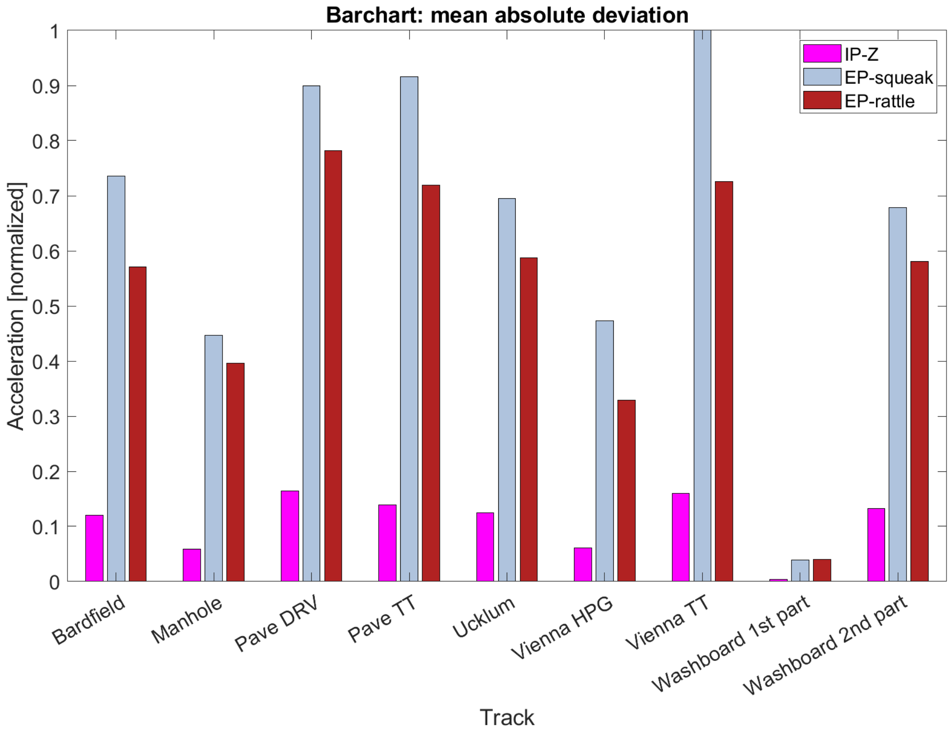

Figure 4.10: Mean absolute deviation for each track in Car A, from IP-rig. Concept C8. Normalized Y-axis.

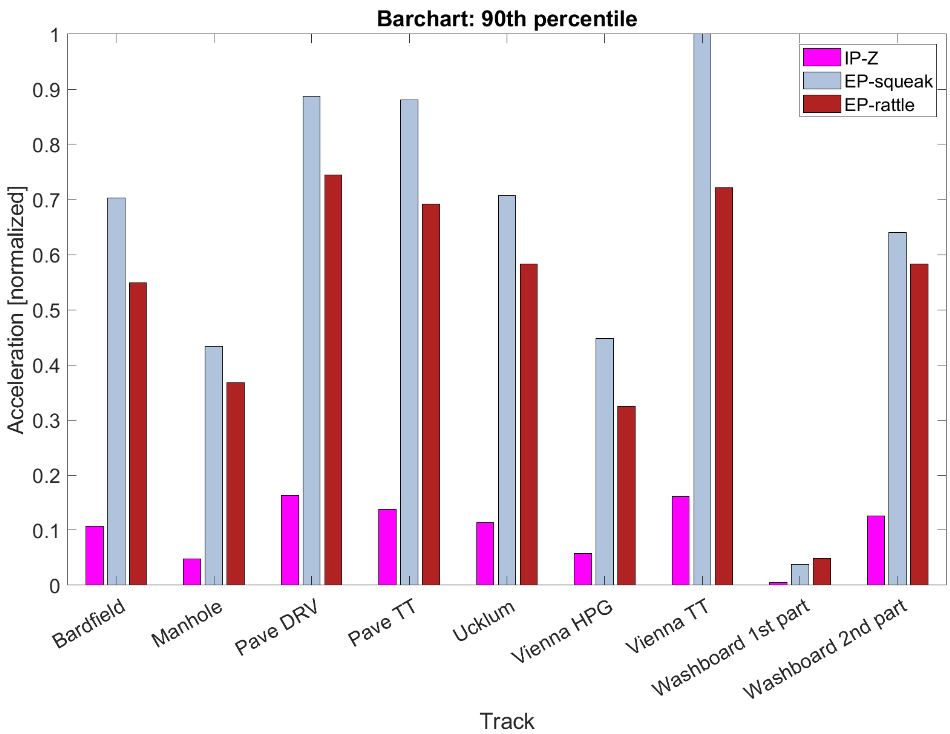

Figure 4.11: 90:th percentile for each track in Car A, from IP-rig. Concept C8. Normalized Y-axis.

5
Discussion

It is obvious that the result show an excitation signal that is shorter in time while keeping a similar curve in frequency domain, and does not have a difference in metric in the same scale as the difference in time. The signal synthesizing is done while the signal is being constructed by parts of an actual recorded test track excitation signal, which means that the signal still should be realistic in some sense. There is however always errors that negatively influence the result to some degree. Some of these errors are presented in this chapter.

During the concept testing phase it was found that pause duration and ramp-up duration might be unnecessary factors, as concept C8 was chosen as the most optimal one in this project based on the desires that was given. It is however possible that both pause duration and ramp-up duration may be needed if the requirements of the synthesised signal is changed in the future, and it may be valuable to have this factor then. It was also valuable to investigate this to make sure these were not critical factors.

5.1 Difference in factor severity FP-rig and IP-rig

By comparing the factor severity plots in Appendix B and Appendix C, it is apparent that the IP-rig in general have significantly higher factor severity than in the FP-rig, sometimes up to 10 times greater. The cause of this is thought to be that the instrument panel used in the IP-rig were an older variant with certain components such as the glove box being more loose than in the car used in the FP-rig. The FP-rigs IP was from a newer car with notably less loose components. Since the IP-rigs IP had looser parts, they were more prone to high relative translation in the E-Point interfaces, hence a more severe factor severity, as this factor is highly dependent on the degree of relative displacement, relative velocity and relative acceleration.

5.2 Different synthesized signal time length in FP-rig compared to IP-rig

Concept C3, C8 and C9 are the only concepts tested in both the FP-rig and the IP-rig. The signal time shortening is as summarized in table 5.1. It is notable that C3 and C8 have different signal time shortenings depending on what rig it is tested in. In the FP-rig it is more than double the signal length than in the IP-rig. The synthesized signals are based upon the responses from the IP vibrations. The IP in the IP-rig was an older variant than the IP in the FP-rig. This variation in instrument panels have therefore resulted in a different spread of events in time domain. The hypothesis is that the IP-rig responses cause a slightly more clustered event distribution than in the FP-rig, see Appendix C for plots of the event distribution and severity. The less event-clustered responses will thus be more affected by the parameter *Max Diff Time*. Since the parameter *Max Diff Time* extends the time of the selected sections to nearby events if occurring close enough, it will eventually result in a longer total synthesized signal time. The exception to this phenomenon is if the time interval to nearby events is longer than *Max Diff Time* and the event-section-time is shorter than the *Min Time Keep*, resulting in a shorter total synthesized signal time, as occurred for track *Washboard 1st part* for certain concepts.

Table 5.1: Comparison of signal time shortening in FP-rig compared to IP-rig. For example, a signal length factor of 0.05 means that it is 95% shorter in time than the original signal.

	Relative difference to original		
Test-rig	C3	C8	C9
IP-rig: New signal length factor	0.09	0.05	0.05
FP-rig: New signal length factor	0.24	0.19	0.05

Concept C9 had the same synthesized signal time length in both the IP-rig and the FP-rig. This is also the only concept where the *Max Diff Time* is zero. For concept C3 and C8, *Max Diff Time* is above zero. With zero *Max Diff Time*, the effect of differently event-clustered responses are practically nonexistent, since the event-sections can not extend to nearby event-sections. Concept C9 did not have any ramp-up or pause duration either, which made the synthesized signal time length the same for the IP-rig and FP-rig. However, if C9 would have ramp-up or pause duration, then differently event-clustered responses could result in variations of synthesized signal time length, although to a lesser degree than the parameter *Max Diff Time*.

5.3 Metric ratio in context

By comparing the concepts performance metric to the unshortened signals performance metric, a ratio is provided as in Table 4.5, Table 4.5 and Table 3.11. A metric ratio of for example two or three might not be particularly telling, whether that is a reasonable value after signal shortening or not. One way to give perspective on this number is to compare the unshortened response signals in the IP-rig to the unshortened response signals in the FP-rig. This will highlight how the variation of different IPs and test rigs can affect the metric, despite testing on the same road track and having the same signal length. Consequently, a comparison of metrics in IP-rig compared to FP-rig for squeak and rattle is presented in Table 5.2 and Table 5.3.

Table 5.2: Comparison of metric in IP-rig compared to FP-rig, rattle metrics.

Metric value for Rattle				
	Mean metric		**99th perc metric**	
Track	**FP-rig**	**IP-rig**	**FP-rig**	**IP-rig**
Bardfield	-0.18	-0.59	-0.75	-2.22
Manhole	-0.11	-0.65	-0.45	-2.22
Pave DRV	-0.16	-0.68	-0.73	-2.75
Ucklum	-0.16	-0.71	-0.63	-3.11
Vienna HPG	-0.01	-0.10	-0.06	-0.45
IP-rig metric value relative FP-rig (Rattle)				
	Mean metric		**99th perc metric**	
Track	**FP-rig**	**IP-rig**	**FP-rig**	**IP-rig**
Bardfield	1	7.61	1	6.95
Manhole	1	7.88	1	7.94
Pave DRV	1	4.57	1	3.27
Ucklum	1	7.05	1	8.05
Vienna HPG	1	14.13	1	12.98
Result metric evaluation	**1**	**8.25**	**1**	**7.84**

Table 5.3: Comparison of metric in IP-rig compared to FP-rig, squeak metrics.

Metric value for Squeak				
	Mean metric		**99th perc metric**	
Track	**FP-rig**	**IP-rig**	**FP-rig**	**IP-rig**
Bardfield	-0.04	-0.05	-0.18	-0.20
Manhole	-0.02	-0.05	-0.07	-0.23
Pave DRV	-0.03	-0.13	-0.17	-0.92
Ucklum	-0.04	-0.07	-0.21	-0.46
Vienna HPG	-0.00	-0.00	-0.01	-0.01
IP-rig metric value relative FP-rig (Squeak)				
	Mean metric		**99th perc metric**	
Track	**FP-rig**	**IP-rig**	**FP-rig**	**IP-rig**
Bardfield	1	9.38	1	12.58
Manhole	1	9.01	1	10.72
Pave DRV	1	5.62	1	5.02
Ucklum	1	8.85	1	10.72
Vienna HPG	1	17.90	1	17.13
Result metric evaluation	**1**	**10.15**	**1**	**11.23**

Since the metric ratio for squeak and rattle is ranging from 7.84 to 11.23, it reveals that smaller changes in either the test rig or variations of the IP can have a great impact in the resulting metric evaluation. This finding furthermore shows that the metric ratio is indeed very sensitive and responds highly to variations of any parameter in the testing. Consequently, it should be emphasized that the synthesized signal metrics ratios of around two or three is not a particularly high number. Whereas the synthesized signals does have a different squeak and rattle characteristics than the unshortened signals, it does not indicate of having substandard quality of producing squeak and rattle events as an excitation signal.

5.4 Potential errors sources

There is a substantial amount of testing done in this project which always introduces some kind of errors. The events that have been identified that may affect the result are mainly human-error-based, nevertheless deemed rather small. This section only describes some of the known parameters that might contribute to a less qualitative result, given a perfect method. It does not describe any flaws that the method may introduce, since that is subjective depending on what the desired result is. It is also possible that there is some unknown errors that have not been considered. One of the error factors is the accuracy of how the accelerometers were positioned when doing measurements. Another is the calibration of the accelerometers that had to be done before each test. A third is about the synchronisation between the measured response in the FP-rig and the excitation signal. A fourth error source is the small random differences in responses from identical excitations and eventual tolerance errors in the test rigs.

5.4.1 Positioning of accelerometers

The accelerometers were mounted manually in the car in approximately the correct direction, aligned with the global coordinate system of the car. Alternatively, they were placed in an direction that clearly did not match the local Squeak & Rattle direction. The signals would instead later be corrected using a MATLAB script for rotational transformation. The approximate angles between the accelerometer coordinate system and the global coordinate system were found by measuring in ANSA. This was done by finding an approximate position on the virtual model while comparing with pictures taken during the physical measurements, and measuring the angle from there. It is estimated that all accelerometers were aligned or corrected for misalignment to within an accuracy of around 10°.

5.4.2 Calibration

Before each test, the accelerometers needed to be calibrated in order to give accurate readings in the amplitude span of interest. This was done by auto-ranging the SQuadriga accelerometers for eight seconds while performing the most extreme of the road tracks, with high amplitudes. It is difficult to do this exactly the same each time, and any eventual difference in calibration may have caused may have induced errors of reasonably low severity.

The IPEtronix accelerometers were reset while the car was standing still before the testing was done. They did however still output non-stationary readings ranging from negative 0,5 m/s^2 to positive 0,5 m/s^2, when it ideally should be 0 m/s^2.

5.4.3 Synchronisation

The response of the test was measured in the instrument panel and was considered the result of the test. Based on this result time intervals are calculated that should be kept for the new signal. These intervals needed to be cut from the excitation signal and merged into a new excitation signal. The issue was that the excitation signal and the response signals had different starting times. That means that they needed to be synchronized manually, so that the first excitation accelerations matches the first response accelerations. In Figure 5.1, the synchronization of track Bardfield can be seen. Similar figures for the other excitation signals can be found in Appendix A.

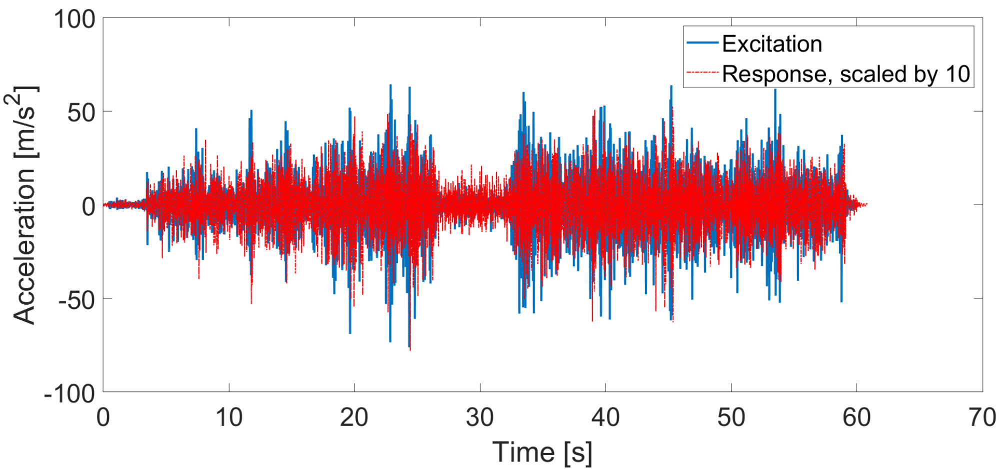

Figure 5.1: Graph used for synchronizing responses with excitation. The amplitude of the response signals were of significantly lower amplitude than the excitation signals. Therefore, the response signals were temporarily scaled by a factor 10 for easier synchronization.

5.4.4 Response differences

As with all physical devices, the test rigs have some error in how well it can replicate the signals exactly the same each time. There is also uncertainty in how different the response of the car would be, given an identical signal. To test this effect on the result, the grading parameters in the following tables were calculated for the response in the FP-rig and the IP-rig for the same excitation signal, run twice in a row. The comparison is done as a relation between the differences in the result. These relative differences is presented in Table 5.4 and 5.5 for the FP-rig. Differences for the IP-rig is presented in Appendix E in Table E.1, E.2, E.3, and E.4. As this was realized post-testing this result is done with what was available, resulting in that only two tracks for the FP-rig was tested, while all tracks was tested in the IP-rig. Unshortened signals were used.

Table 5.4: Rattle evaluation, FP-rig error.

	Relative difference in FP-rig, rattle		
Track	Manhole Car B	Ucklum Car B	Manhole Car A
Mean metric rattle	1,044	1,018	1,099
99:th percentile metric	1,038	1,049	1,380
Number of events	1,044	1,050	1,103
Total event time	1,037	1,063	1,064

Table 5.5: Squeak evaluation, FP-rig error.

	Relative difference in FP-rig, squeak		
Track	Manhole Car B	Ucklum Car B	Manhole Car A
Mean metric squeak	1,025	1,027	1,076
99:th percentile metric	1,073	1,079	1,085
Number of events	1,036	1,023	1,066
Total event time	1,022	1,039	1,087

5.5 Signal shortening methodology - summary and discussion

The method for shortening the signal can be described as a careful copy and paste of interesting time intervals. Firstly, the time intervals that are of interest in a Squeak & Rattle point of view, are identified. This is done by finding where in time, Squeak & Rattle events occur, by comparing relative displacements to the gaps or inverse impulse rates. The squeak and rattle criteria proved to give very few events in some cases, and therefore a percentile value was chosen instead that would represent squeak. After finding these time indexes their event severity is calculated by using Equation 3.5 and 3.3. If all these time indexes would be saved then almost the entire original signal would be saved (if using ramp-up and pause duration). Therefore a percentile value of these metric values were selected and saved for the next step. The 90th percentile proved to be a suitable limit for this purpose. If this exclusively would be done prior to merging the cut signal parts, then the number of signal fragments kept would be particularly high. That would make merging them in an appropriate way difficult and the new signal quality may contain a lot of unwanted acceleration jerks. Therefore a *max difference time* parameter is introduced that decide the difference in time two events can be while in the same cut signal part. If this time is exceeded then the new time index ends up in another separate signal part. If two events are within this time limit, then the original signal is kept in between these time indexes, and a longer signal part is saved. In the chosen concept, C8, this value was set as the same time as in concept C3.

There were uncertainties whether a previous signal part would affect the response of a following part in the synthesised signal. Therefore a pause duration factor was added that adds rest duration between the cut signal parts when they are merged. This was in retrospect unnecessary, as the chosen concept did not have any pauses. Furthermore, there were uncertainties whether immediately starting a signal part as it was cut, would cause unfavorable jerks. A ramp-up duration was added to ensure a smooth start of each section, with the same length as the pause duration. However, this ramp-up duration was not necessary according to the results of the chosen concept.

Finally a parameter that decides if a cut signal part is too short in time or not to be stored for the synthesised signal was introduced. If this is at zero milliseconds, then there is a high probability that there is a large number of short signal bursts in the synthesised signal, which may reduce the effective new time. According to Table 3.35 this value is about 32 milliseconds in concept C8. It must again be noted that the chosen concept is not a calculated absolute optimum, rather an iterated solution that is expected to fulfill the given desires on the new signal. It is possible that for example the *minimum time for keeping* can be zero in an even better concept.

All of this development of a synthesised signals was first done for each road track separately and tested separately. When concept C8 was chosen as the overall best one, the different road tracks were merged into one final signal.

5.6 Final remarks for the shortened signal

There is a difference of result from the FP-rig compared to the IP-rig as can be seen in Section 4.1. Therefore the resulting response data is presented here for both these excitation signals, for concept C8. The main objective was to reduce the excitation signal in time domain. This has been done and the new signal is about 19% of the length of the original signal in the FP-rig signal, and 5% in IP-rig signal. Some additional relevant numbers are presented in Table 5.6, all numbers are averages for all road tracks.

Table 5.6: Evaluation parameters for concept C8

	Relative difference to original, concept C8			
	Rattle FP	Squeak FP	Rattle IP	Squeak IP
Mean Metric	2.06	2.10	3.90	4.65
New signal length factor	0.19	0.19	0.05	0.05
S&R to time ratio, mean metric	0.40	0.40	0.23	0.23
99:th percentile metric	2.57	3.78	3.76	4.72
Number of events	5.16	19.74	10.59	7.80
Total event time	4.01	42.36	9.34	6.27

6
Conclusion

The activities in this project can be divided into several parts for an overview. The first part of this project have been centered around recording acceleration signals on test tracks and in test rigs. These acceleration signals have thereafter been processed, structured and analysed in the second part of the project. The third project part could be defined as synthesizing new, shortened excitation signals. The fourth and final part is verifying the developed excitation signals by additional testing in the test rigs and analysing these results.

Two approaches have been done for shortening recorded signals, either based on the response signals output in time domain or in frequency domain. The frequency domain shortening method proved to be unsuccessful, while the time domain shortening method proved to be effective in generating Squeak & Rattle causing excitation signals. The time domain methodology of generating shortened excitation signals is based on a few equations for finding critical Squeak & Rattle events in time domain. Five parameters are used for selecting relevant signal sections and merging them together into a synthesized excitation signal. A multitude of metrics can be calculated for comparison with the unshortened excitation signal. The Squeak & Rattle metric to time ratios are regarded as the most important parameter for evaluating various concepts in effectiveness, as this parameter contains both Squeak & Rattle performance and shortening of time. Additionally, the number of events and frequency composition of the developed excitation signals is compared to the original excitation signals as a part of the evaluation process.

As the criteria for what is the best new concept were not strictly defined, rather a developed method, partly formulated in software scripts is considered a large part of the final product. This method allow engineers to tweak parameters to get the type of signals they require for a certain need, rather than having just one signal that has been decided by this project. Nonetheless, a developed signal is part of the main product that is developed in this project and it proved to be concept eight from concept iteration two. The signal time compression for the optimal concept were ranging from 81% to 95% depending on which test rig the responses were gathered from. The developed excitation signals metrics were measured to be slightly more rough than the recorded excitation signals. However, this can be regarded as an advantage, if a somewhat *worst-case* excitation signal is desired for future Squeak & Rattle simulations.

6.1 Future Work

Throughout the project, several areas that may be subject to actions to improve the quality of the result have been identified. There has not been enough time to do several of these and if a better result than what is reached in this project is desired, the following suggestions for future work may be investigated.

It would be valuable if the developed method would be tested for other cars within the same platform, and for cars in other platforms to further confirm its functionality. An overview of what has been done in this project compared to what was desired is presented in Figure 6.1. For platform two, the tracks were recorded at the TT-track and in the FP-rig as a preparation for eventual future work.

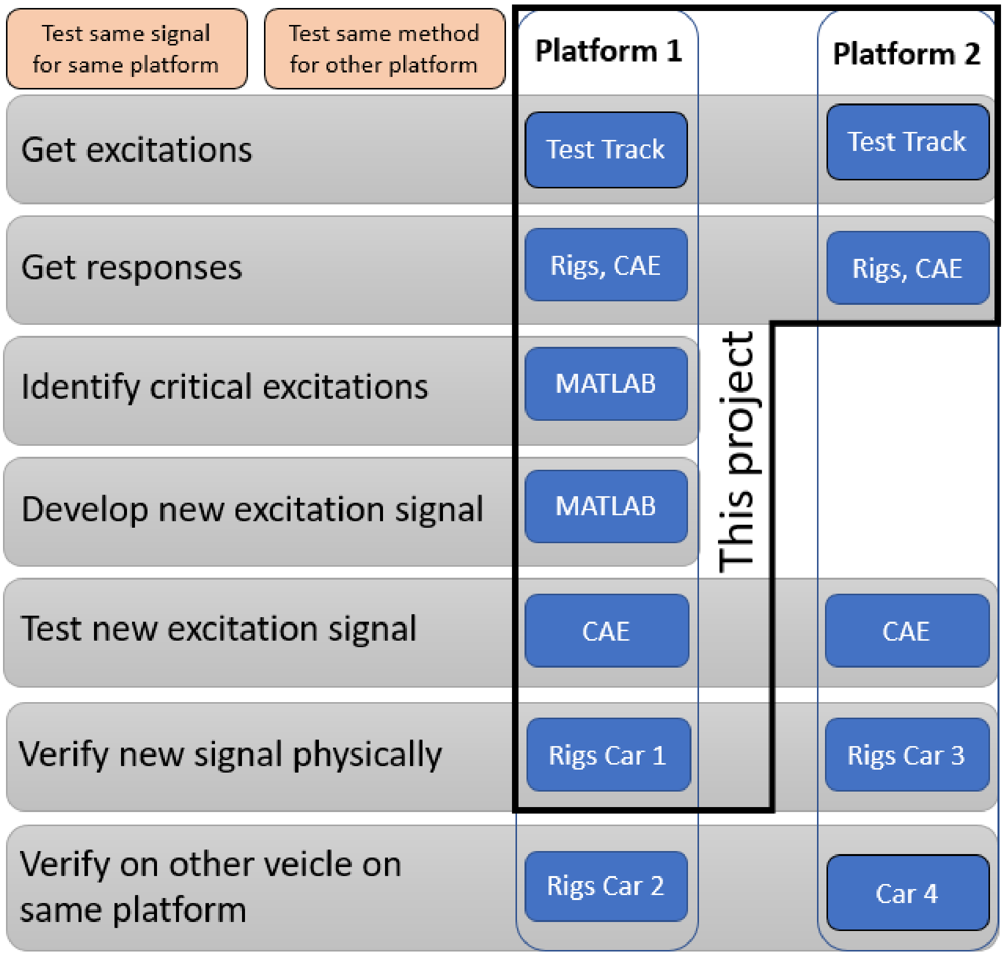

Figure 6.1: Rough description of this project and how it could be further verified.

From the concept study, it can be seen that a short pause and ramp-up duration is better than long durations. This holds when comparing the Squeak & Rattle metric to time ratio. An additional parameter that may be of value when assessing the new signal is effective new time. This is the actual relative time in the new signal that is copied from the original signal. Depending on what parameters is chosen the effective new time may be low. This happens for example if the pause duration is too long which just adds time to the new signal without adding any real value. If everything else is the same, a signal with a high value in effective new time is desired rather than a signal with a low value. However, for a more precise mapping of which parameters affect each metric and to what degree, a more rigorous study must be done. It may also be relevant to relate rattle to squeak, weighing them to each other to get a less subjective selection of concepts based on the metric results.

A better estimate of the gaps between the parts in an E-point would give a better estimate of how much rattle is actually occurring. This has not been a high priority in this project as it has been sufficient to merely obtain a rough estimate to assess the risk of rattle, rather than actual rattle events. Moreover, it is possible to greatly increase the accuracy of the squeak assessment if better test data and measurements for stick and slip is collected for the exact materials used in the E-points.

Another detail that may very well increase the quality of the result would be to have close discussions with the engineers that will be using the developed signals, and using their input to tweak the parameters and eventually edit segments of the method. They might request more detailed requirements on the synthesized signal, rather than solely similar metrics and similar profile in frequency domain, while shorter in time. The ideal would probably be if they could use the signal and give feedback as a part of an iteration loop. This has been attempted to replicate in this project by the CAE simulations and iterations in the test rigs, nonetheless, without their specific needs as input. It must however be kept in mind that this thesis was framed by engineers and researchers that would later use the product, and these broad requirements is what they wanted fulfilled.

An additional option that may give a better result is to introduce different shortening parameters for different road tracks or excitation signals. It is possible that their variation result in different optimal parameter configurations, depending on their specific characteristics. Lastly it may be highly beneficial to utilize multidisciplinary optimization methods when choosing parameter values. An example of this can be to create a surrogate model based on extensive physical testing or simulated results, and then being able to predict the theoretically optimal parameter values.

References

BETA CAE. (2020a). *Ansa pre-processor - beta cae systems.* Retrieved 2020-06-08, from https://www.beta-cae.com/ansa.htm

BETA CAE. (2020b). *Meta post-processor - beta cae systems.* Retrieved 2020-06-08, from https://www.beta-cae.com/meta.htm

Cooley, J. W., & Tukey, J. W. (1965). An algorithm for the machine calculation of complex fourier series. *Mathematics of computation*, *19*(90), 297–301.

Cortinhas, C., & Black, K. (2012). *Statistics for business and economics.* Chichester: Wiley.

Evans, P. R. (2001). Rotations and rotation matrices. *Acta Crystallographica Section D: Biological Crystallography*, *57*(10), 1355–1359.

Feng, J., & Hobelsberger, J. (1999). Detection and scaling of squeak & rattle sounds. *SAE transactions*, 2685–2694.

Ling., W. K. (2007). *Nonlinear digital filters: Analysis and applications [elektronisk resurs].* Academic Press.

Mercer, C. (2006). *Acceleration, velocity and displacement spectra – omega arithmetic.* Retrieved 2020-04-24, from http://prosig.com/wp-content/uploads/pdf/blogArticles/OmegaArithmetic.pdf

MSC Software. (2020). *Msc nastran - multidisciplinary structural analysis.* Retrieved 2020-06-08, from https://www.mscsoftware.com/product/msc-nastran

Sundararajan, D. (2001). *The discrete fourier transform : theory, algorithms and applications.* Singapore: World Scientific.

Weber, J., Sabiniarz, P., Wickman, C., Lindkvist, L., & Söderberg, R. (2013). Squeak&rattle simulation at volvo car corporation using the e-line™ method. In *5th ansa & μeta international conference.*

ZIEGLER-Instruments. (2016). SSP-04 Stick-Slip Test Bench manual..

A

Synchronisation Graphs

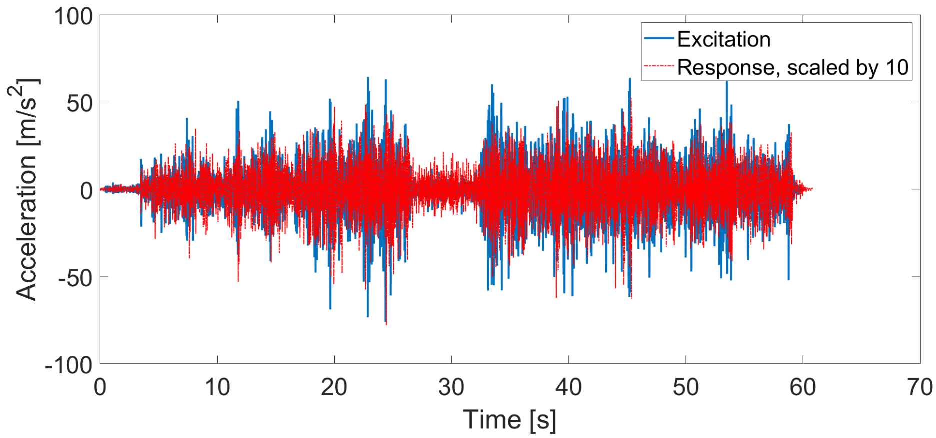

(a) Bardfield Synchronisation Graph

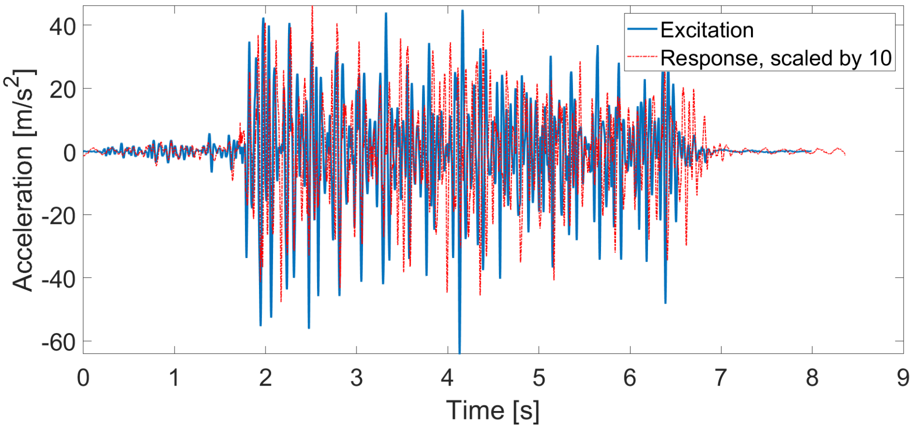

(b) Manhole Synchronisation Graph

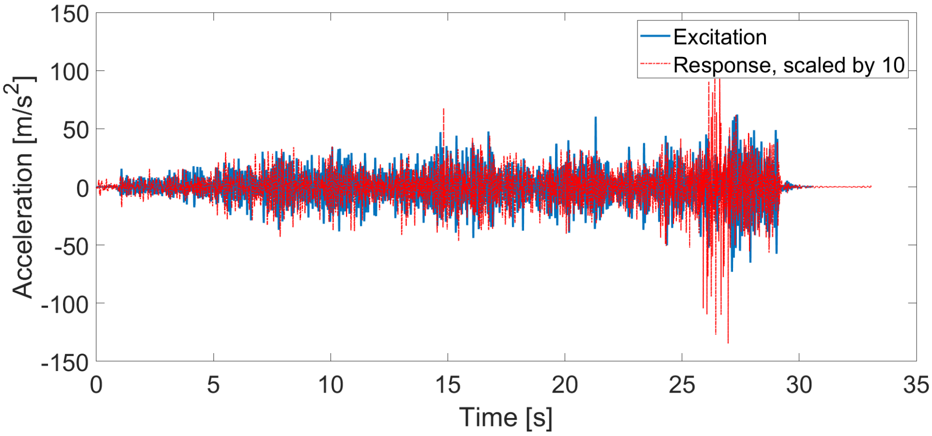

(c) Pave DRV Synchronisation Graph

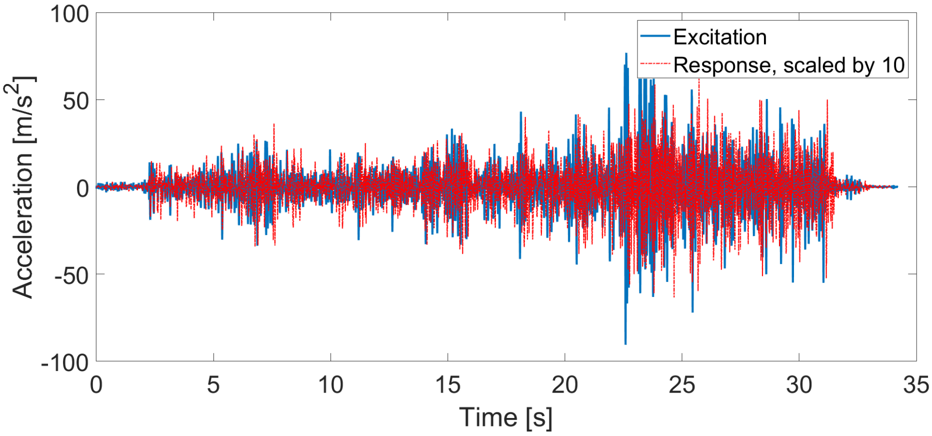

(d) Ucklum Synchronisation Graph

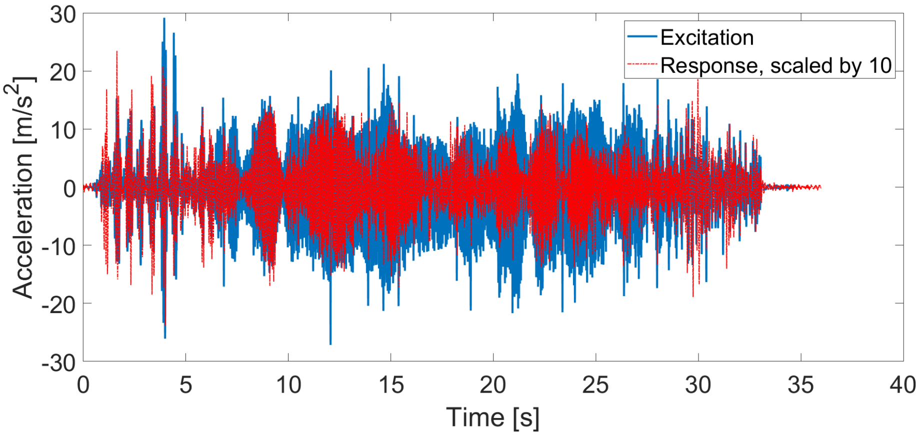

(e) Vienna Synchronisation Graph

Figure A.1: Graphs used for synchronisation of drive files for four poster rig, IP-responses compared to spindle accelerations.

B

Factor severity plots, IP-rig

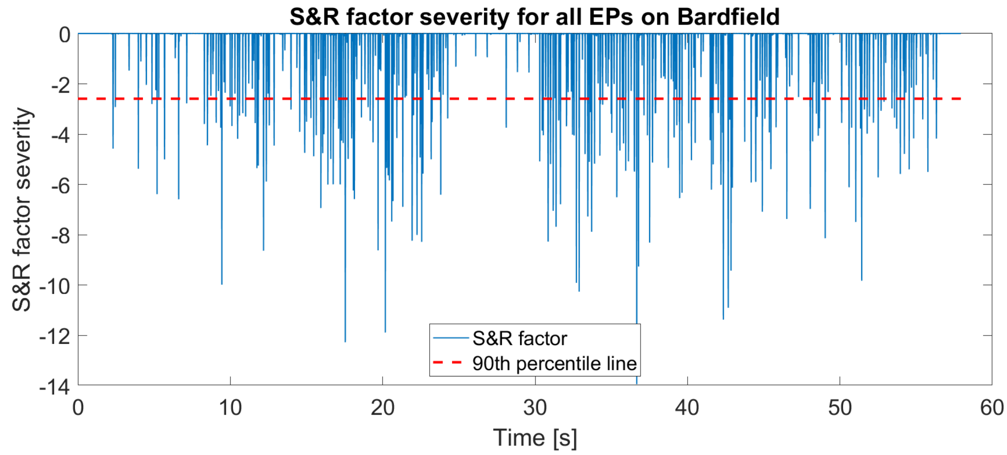

(a) Bardfield factor severity plot

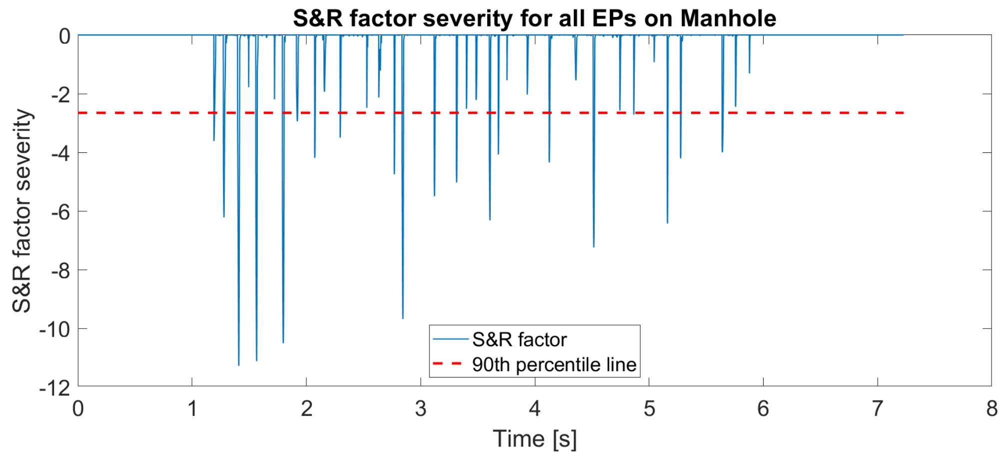

(b) Manhole factor severity plot

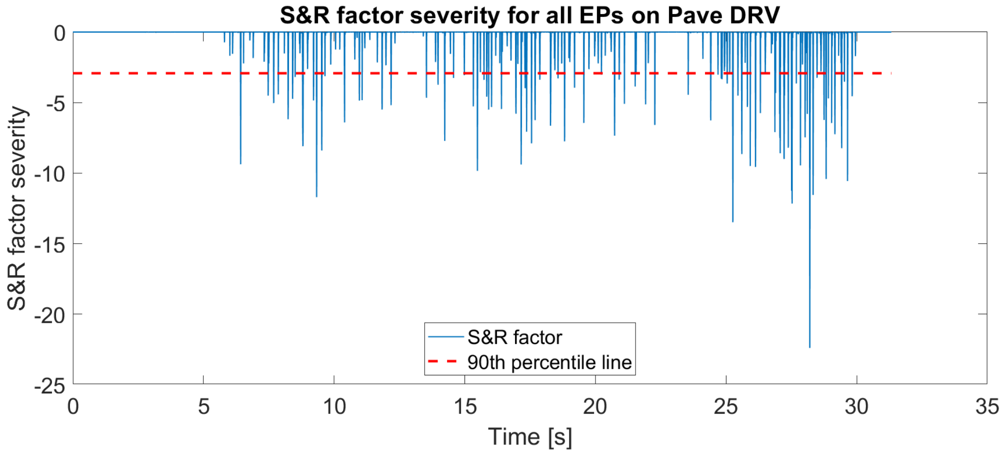

(c) Pave DRV factor severity plot

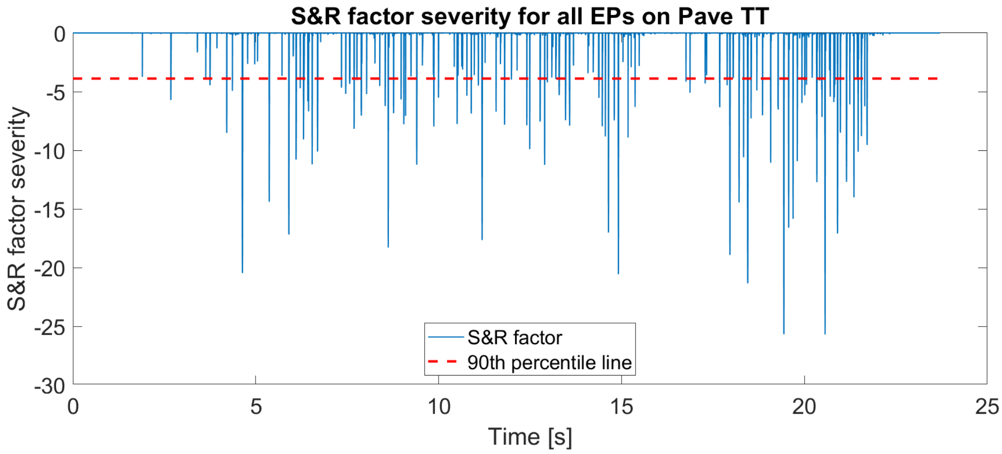

(d) Pave TT factor severity plot

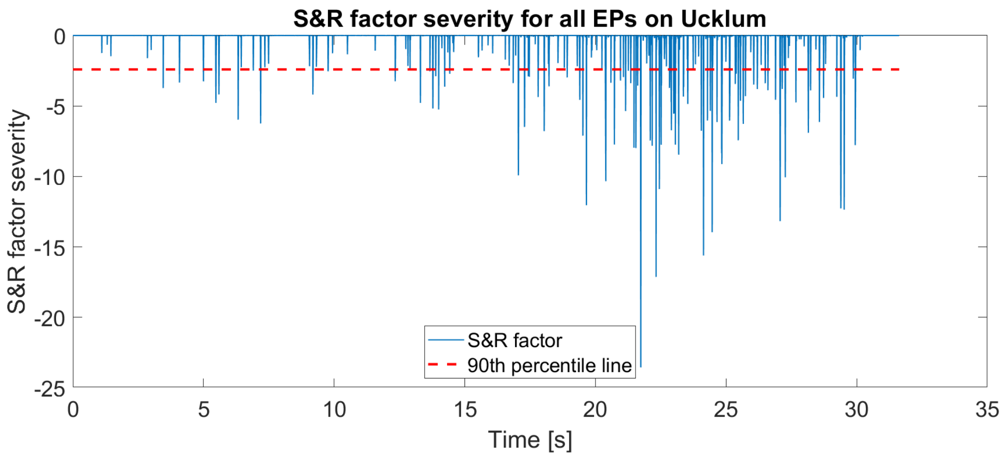

(e) Ucklum factor severity plot

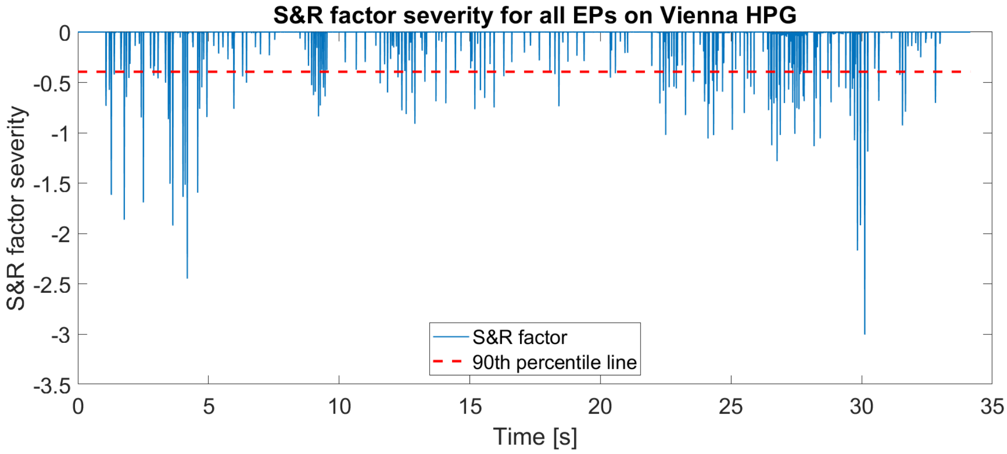

(f) Vienna HPG factor severity plot

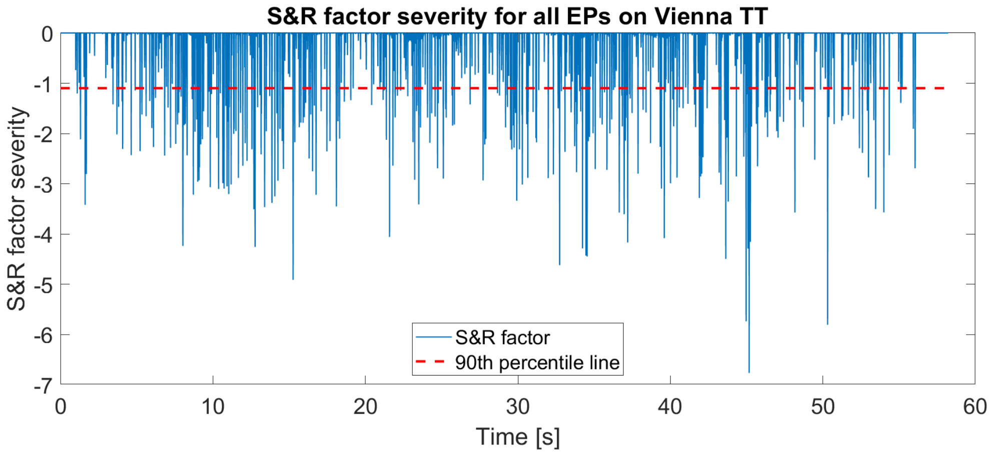

(g) Vienna TT factor severity plot

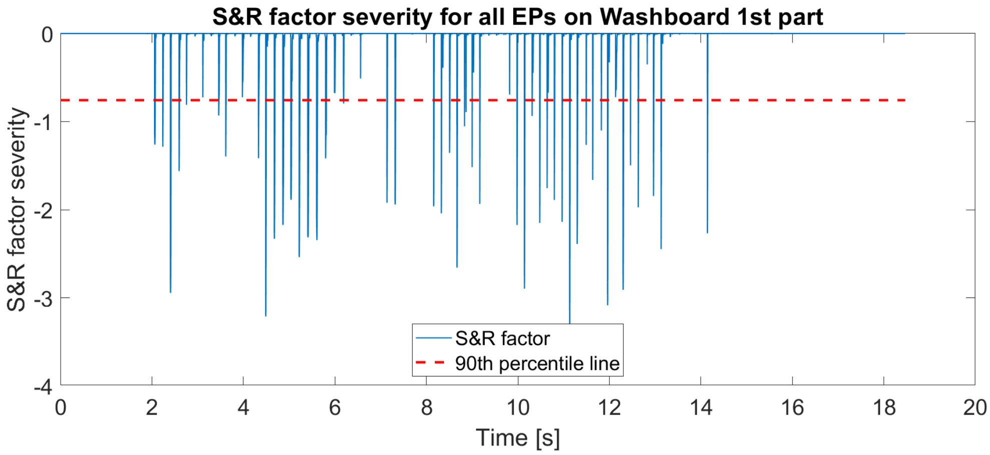

(h) Washboard 1st part factor severity plot

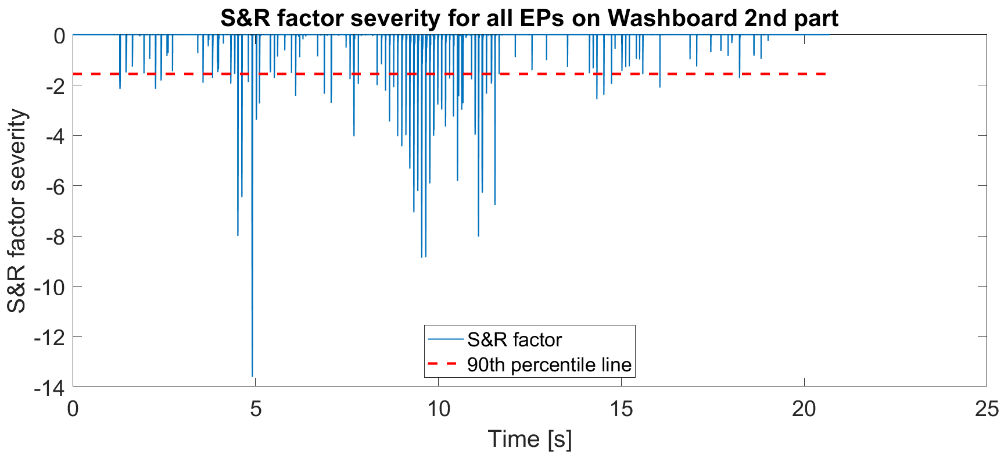

(i) Washboard 2nd part factor severity plot

Figure B.-2: Factor severity plots used for selecting relevant parts in the unshortened signal. Factor severity is calculated based on responses from the IP-rig

C

Factor severity plots, FP-rig

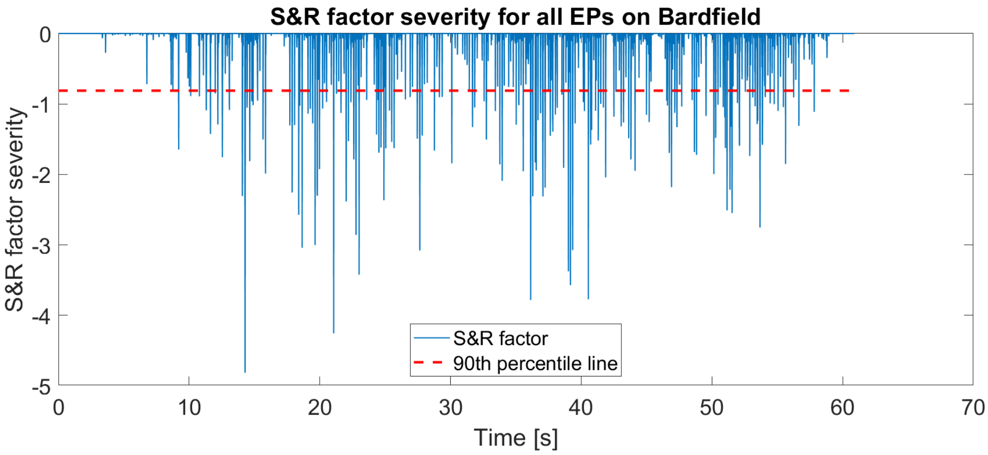

(a) Bardfield factor severity plot

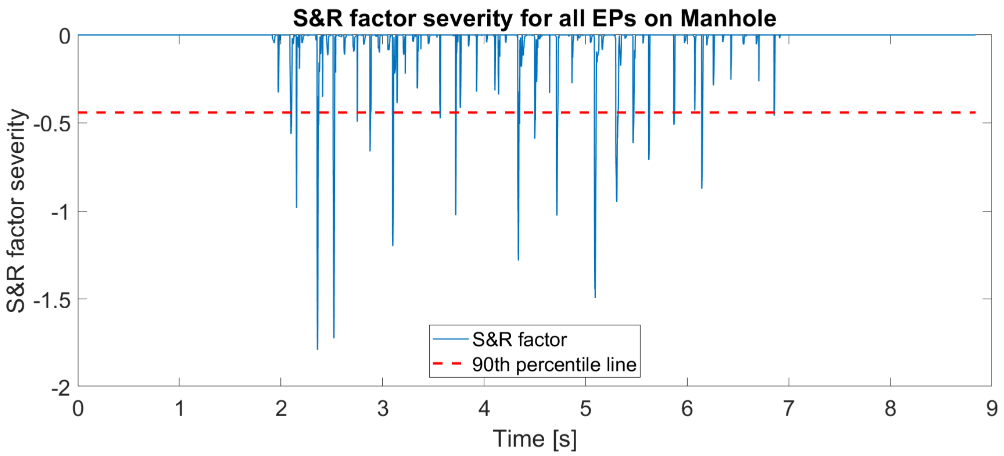

(b) Manhole factor severity plot

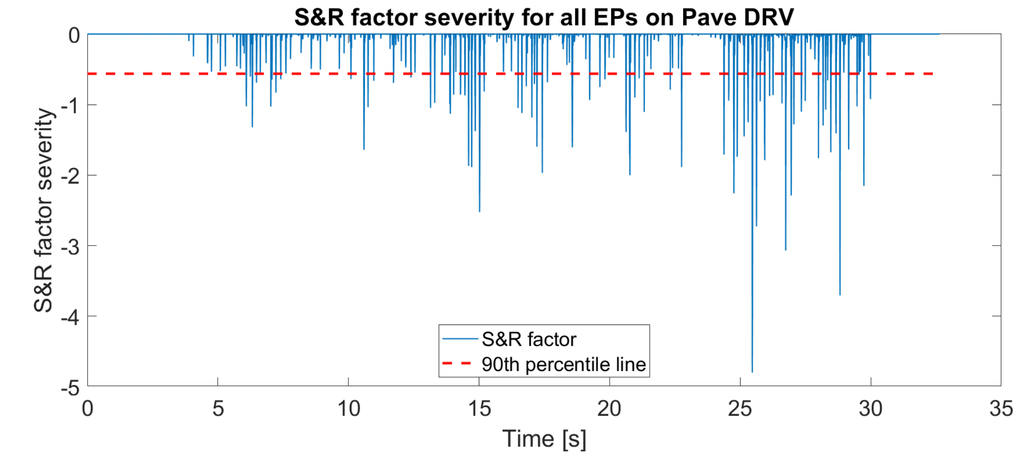

(c) Pave DRV factor severity plot

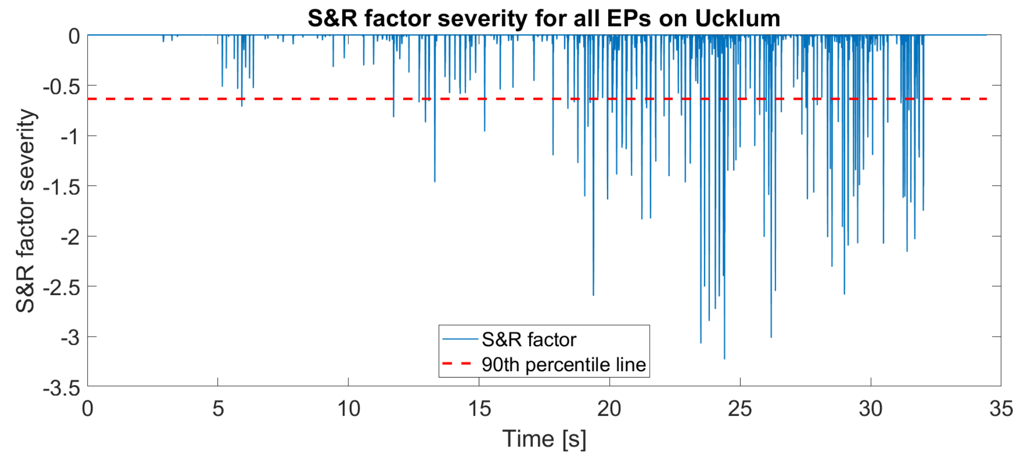

(d) Ucklum factor severity plot

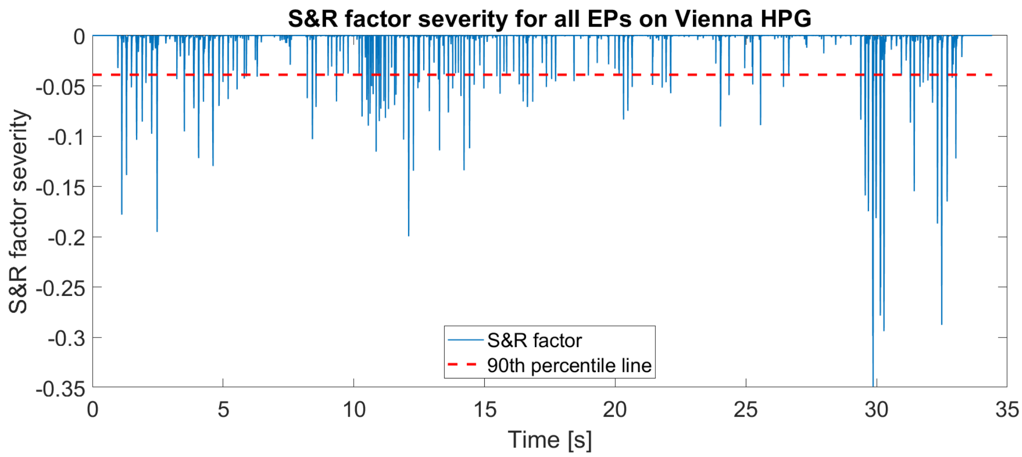

(e) Vienna HPG factor severity plot

Figure C.0: Factor severity plots used for selecting relevant parts in the unshortened signal. Factor severity is calculated based on responses from the FP-rig

D

Frequency domain comparison, IP rig, second iteration concepts

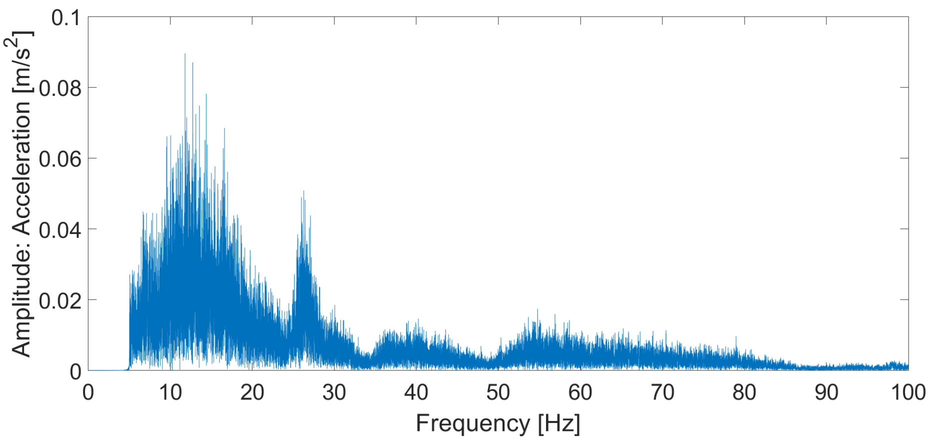

(a) Frequency domain composition of original signal

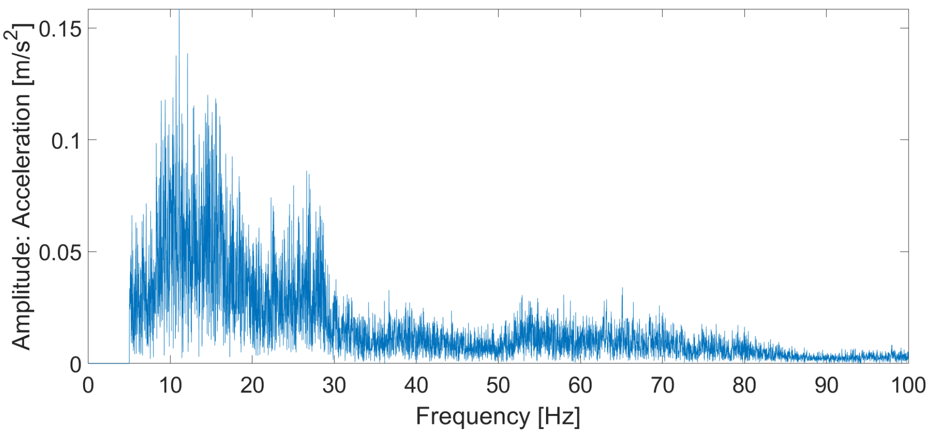

(b) Frequency domain composition of concept C6 signal

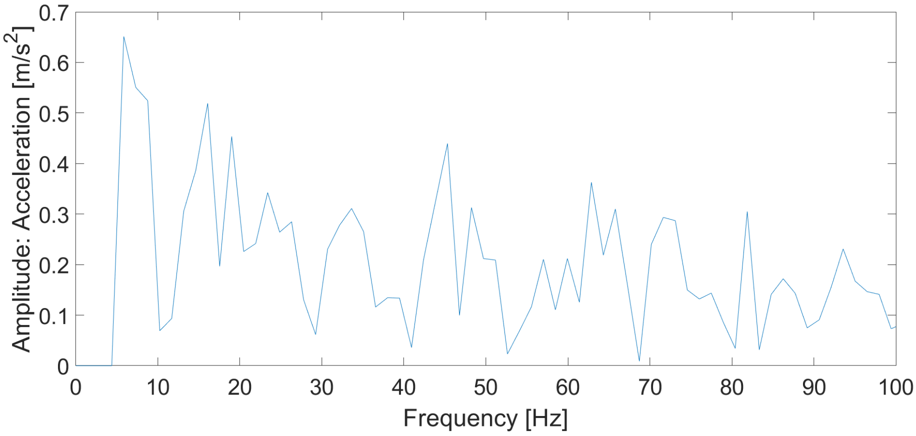

(c) Frequency domain composition of concept C7 signal

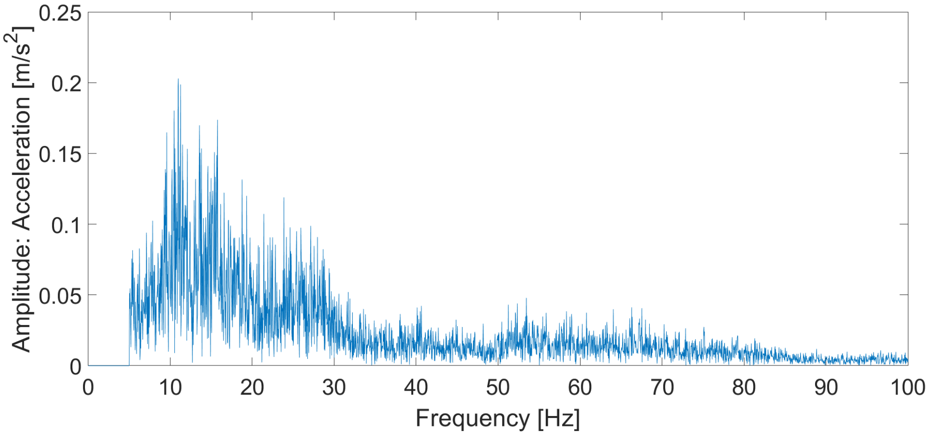

(d) Frequency domain composition of concept C3 signal

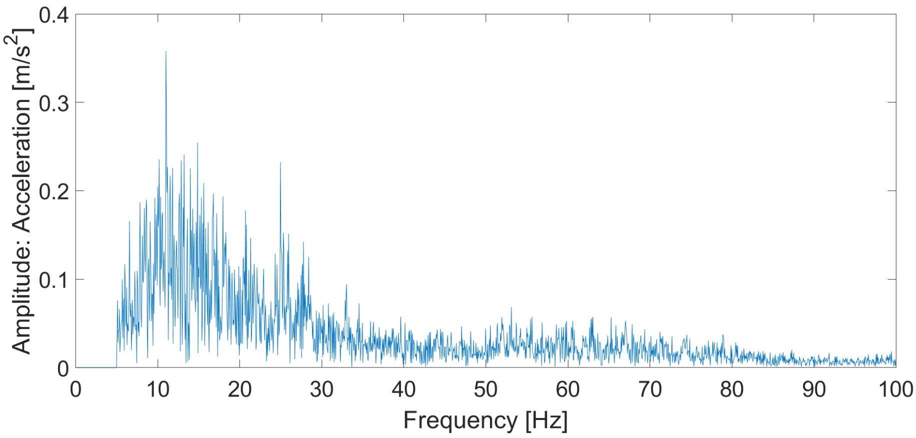

(e) Frequency domain composition of concept C8 signal

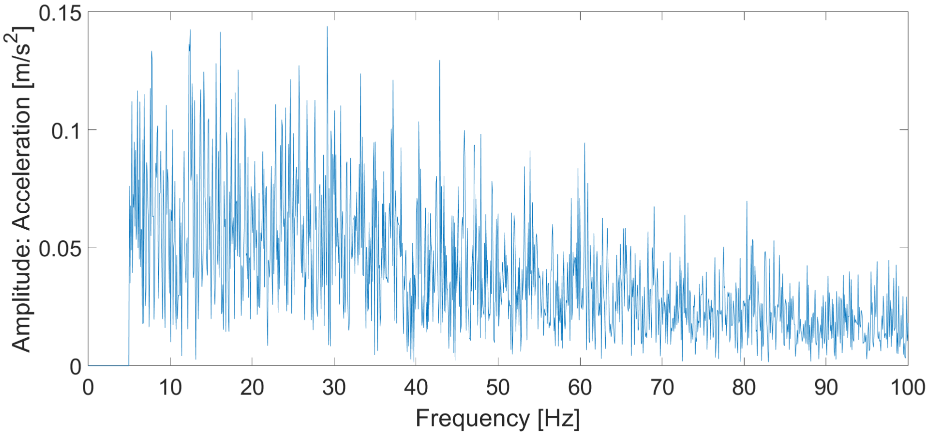

(f) Frequency domain composition of concept C9 signal

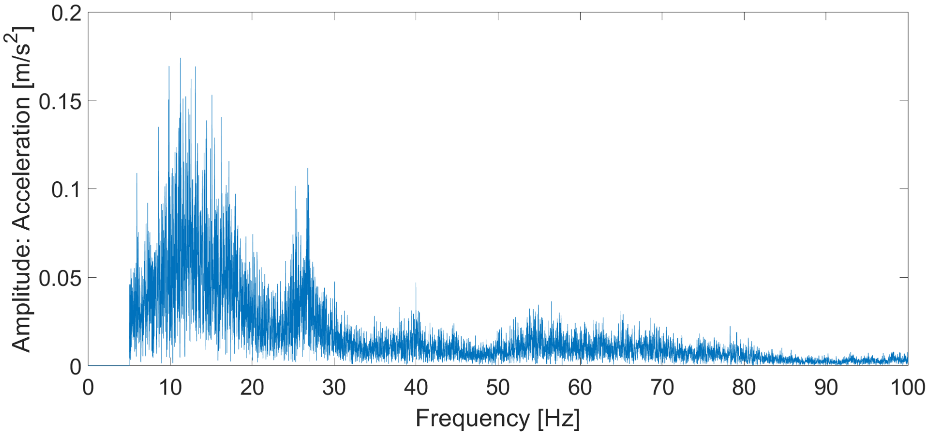

(g) Frequency domain composition of concept C10 signal

Figure D.-1: Frequency domain comparison of concept C6-C10 and C3 signals to the original signal. The concepts are from the second concept iteration from the IP-rig. The frequency content is from all nine tracks excitation signals concatenated sequentially.

E

Relative metric differences between consecutive recordings for same signal, IP-rig

Table E.1: Rattle evaluation, IP-rig error. Road tracks Bardfield - Ucklum.

	Relative difference in IP-rig, rattle				
Track	Bardfield	Manhole	Pave DRV	Pave TT	Ucklum
Mean metric rattle	1,007	1,021	1,006	1,010	1,007
99:th percentile metric	1,010	1,043	1,012	1,008	1,019
Number of events	1,007	1,009	1,009	1,007	1,008
Total event time	1,008	1,007	1,009	1,010	1,012

Table E.2: Rattle evaluation, IP-rig error. Road tracks Vienna HPG - Washboard 2nd part.

	Relative difference in IP-rig, rattle			
Track	Vienna HPG	Vienna TT	Washboard 1	Washboard 2
Mean metric rattle	1,019	1,009	1,074	1,006
99:th percentile metric	1,029	1,019	1,091	1,028
Number of events	1,014	1,011	1,078	1,017
Total event time	1,012	1,012	1,099	1,009

Table E.3: Squeak evaluation, IP-rig error. Road tracks Bardfield - Ucklum.

	Relative difference in IP-rig, squeak				
Track	Bardfield	Manhole	Pave DRV	Pave TT	Ucklum
Mean metric squeak	1,010	1,034	1,005	1,007	1,018
99:th percentile metric	1,019	1,025	1,020	1,030	1,033
Number of events	1,015	1,024	1,013	1,013	1,017
Total event time	1,014	1,012	1,013	1,009	1,014

Table E.4: Squeak evaluation, IP-rig error. Road tracks Vienna HPG - Washboard 2nd part.

	Relative difference in IP-rig, squeak			
Track	Vienna HPG	Vienna TT	Washboard 1	Washboard 2
Mean metric squeak	1,026	1,010	1,075	1,011
99:th percentile metric	1,057	1,016	1,167	1,017
Number of events	1,009	1,022	1,141	1,033
Total event time	1,009	1,019	1,198	1,028